CHALMERS

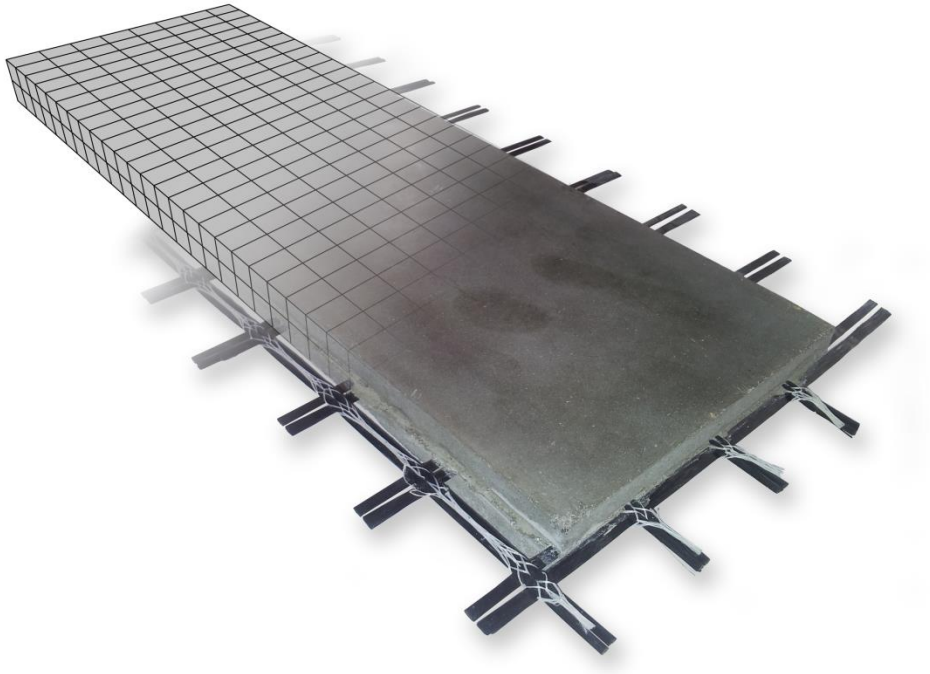

FE-modelling of Textile Reinforced Concrete Façade Elements

Master of Science Thesis in the Master's Programme
Structural Engineering and Building Technology

MARTIN PETTERSSON
PATRIK THORSSON

Department of Civil and Environmental Engineering
Division of Structural Engineering
Concrete Structures
CHALMERS UNIVERSITY OF TECHNOLOGY
Gothenburg, Sweden 2014

Master's Thesis 2014:61

MASTER'S THESIS 2014:61

FE-modelling of Textile Reinforced Concrete Façade Elements

Master of Science Thesis in the Master's Programme
Structural Engineering and Building Technology

MARTIN PETTERSSON

PATRIK THORSSON

Department of Civil and Environmental Engineering
Division of Division of Structural Engineering
Concrete Structures
CHALMERS UNIVERSITY OF TECHNOLOGY
Gothenburg, Sweden 2014

FE-modelling of Textile Reinforced Concrete Façade Elements
Master of Science Thesis in the Master's Programme

Structural Engineering and Building Technology
MARTIN PETTERSSON
PATRIK THORSSON

Examensarbete / Institutionen för bygg- och miljöteknik,
Chalmers tekniska högskola 2014:61

Department of Civil and Environmental Engineering
Division of Division of *Structural Engineering*
Concrete Structures
Chalmers University of Technology
SE-412 96 Göteborg
Sweden
Telephone: + 46 (0)31-772 1000

Cover:
Illustrative picture of FE-modelling of textile reinforced concrete. Photo is taken from a pull out-test specimen.

Chalmers Repro Service / Department of Civil and Environmental Engineering
Gothenburg, Sweden 2014

FE-modelling of Textile Reinforced Concrete Façade Elements

Master of Science Thesis in the Master's Programme
Structural Engineering and Building Technology

MARTIN PETTERSSON
PATRIK THORSSON
Department of Civil and Environmental Engineering
Division of Division of *Structural Engineering*
Concrete Structures
Chalmers University of Technology

ABSTRACT

Awareness of the environmental impact of the building industry is increasing. Steel reinforced concrete is the most commonly used construction material and also a material with a high energy consumption and carbon dioxide footprint. Large environmental gains could arise if an alternative to steel reinforced concrete is developed. In this context, textile reinforced concrete (TRC) is shown to be a promising alternative with advantages as lower energy consumption and reduced carbon dioxide footprint. Predictions also imply that TRC elements could have other benefits as an increased service life and lower need for maintenance due to the non-corrosive reinforcement.

The aim of this thesis was to validate FE-modelling as a reliable analysis method and to identify difficulties and uncertainties in FE-modelling of textile reinforced concrete. A 2D FE-model was developed and verified by comparison to a 4-point bending test conducted prior to this thesis. Discrepancies were then used to understand the behaviour and the effects of different key parameters. Results from the modelling indicate that bond failure was the determining failure mechanism in the experiments. Emphasis on finding solutions to enhance bond for a high tensile strength-low bond material such as the carbon fibre reinforcement could increase material utilization. The current tensile strength-bond ratio also shows promising ductile behaviour which would allow for moment redistribution in statically indeterminate structures.

Furthermore, this model was used to analyse different façade element designs according to requirements and recommendations found in design codes. Besides the FE-modelling, critical details in TRC façade elements are discussed and compared to steel reinforced solutions.

Key words: TRC, FE-modelling, concrete, textile reinforcement, façade elements, bond stress-slip, non-linear analysis, failure

FE-modellering av textilarmerade betongfasadelement

Examensarbete inom Structural Engineering and Building Technology

MARTIN PETTERSSON

PATRIK THORSSON

Institutionen för bygg- och miljöteknik

Avdelningen för konstruktionsteknik

Betongbyggnad

Chalmers tekniska högskola

SAMMANFATTNING

Byggsektorns miljöpåverkan får mer och mer uppmärksamhet. Konventionellt armerad betong är det mest använda byggnadsmaterialet och samtidigt ett material som kräver mycket energi och ger höga koldioxidutsläpp vid framställning. Vid utveckling av alternativ till konventionellt armerad betong kan stora miljömässiga vinster uppstå. I denna kontext visar sig Textil-armerad betong (TRC) vara ett lovande alternativ med möjligheter till betydligt lägre energibehov och koldioxidutsläpp. Förhoppningar finns även att TRC kan ha fördelar som längre livslängd och minskat underhållsbehov tack vare dess icke-korrosiva armering. Osäkerheter kvarstår kring dessa faktorer och det ligger utanför omfattningen av det här arbetet.

Målsättningen med det här arbetet är att validera FE-modellering som en pålitlig analysmetod och att identifiera svårigheter och osäkerheter kring FE-modellering av textilarmerad betong. En 2D FE-model utvecklades och kontrollerades genom jämförelse med försök belastade i 4-punktsböjning som hade utförts innan detta arbete. Avvikelser användes sedan för att förstå verkningssättet och olika nyckelparametrars effekter. Resultat från modelleringen indikerade att vidhäftningsbrott var den avgörande brottmekanismen i experimenten. Metoder att förbättra vidhäftning för ett material med hög draghållfasthet och låg vidhäftning kan leda till förbättrad utnyttjandegrad av materialen. Ett material med motsvarande förhållande mellan draghållfasthet och vidhäftning visar lovande plastiskt beteende. Detta kan användas för att omlagra spänningar och moment i statiskt obestämda strukturer.

Vidare användes den utvecklade modellen för att analysera fasadelement med varierande parametrar i enlighet med krav och rekommendationer funna i aktuella standarder och normer. I tillägg till FE-modellering diskuteras kritiska detaljer i TRC-fasadelement, vilka jämförs med stålarmerade lösningar.

Nyckelord: TRC, FE-modellering, betong, textilarmering, fasadelement, vidhäftning-glidning, icke-linjär analys, brott

Contents

Preface

The work presented in this thesis was performed between January and June 2014 at the Division of Structural Engineering, Concrete Structures, Chalmers University of Technology, Sweden.

This study is based on work performed by Natalie Williams Portal, Lic.Eng., in a research project involving the investigation of using textile reinforced concrete (TRC) in future buildings.

We would like to thank our supervisor Natalie Williams Portal and examiner Professor Karin Lundgren for their guidance and helpful critique throughout this work. We would also like to thank all other members of the department of Structural Engineering that has provided answers to our questions.

Gothenburg, June 2014

Martin Pettersson Patrik Thorsson

1 Introduction

Concrete is today the world's most used construction material but at the same time, it is being increasingly questioned because of its high usage of resources and energy consumption (Naik, 2008). To address this issue, numerous research projects are currently ongoing on the subject to reach more sustainable solutions. Among others, textile reinforced concrete (TRC) is a promising composition that has lately attracted attention. Substitution of steel reinforcement with textile fibre meshes of e. g. carbon, alkali resistant glass or basalt fibres may lead to more slender, resource effective and less energy demanding structures (Williams Portal, 2013).

Along with computational development, ideas for new types of design and materials allowing for light-weight and free-form structures are heavily requested by today's designers. To support this development, innovative materials are needed. With a flexible and easily shaped reinforcement as textile reinforcement mesh, the requests may be answered.

1.1 Background

Ever since concrete appeared amongst other building materials, its low tensile strength has been an issue to solve. Heavy-weight, compressive structures were the only solution until the reinforced concrete was invented in 1867 (Marsh, 1904). This composite material made it possible to use concrete for numerous structural members e.g. beams, slabs and plates. Today, these are conventional products for structural engineers and the old problems are replaced by new. Corrosive steel needs protection and the most common way is to cover the reinforcement bars with a concrete layer up to 60 mm thick depending on the surrounding conditions. This cover layer, in a cracked section, has barely any influence on the load bearing capacity and is, in traditional façade elements, a large part of the total mass. Accordingly, TRC, including non-corrosive textile reinforcement, is a very suitable composite material for façade elements.

1.2 Objectives

The main aim of this Master's thesis project was to develop a non-linear 2D FE-model to identify difficulties and uncertainties in TRC FE-modelling. Another aim was to give design suggestions for TRC façade elements regarding geometry and to identify critical details.

1.3 Method

In the first stage of the work, input parameters for materials and other properties were collected from material producers and results from experimental work. The collected data was used to produce a preliminary 2D FE-model which was compared to members tested in 4-point bending tests. The results were verified and all parameters calibrated to match the composite behaviour. When all properties were determined they were used in the design phase. In this second stage, two types of façade elements were modelled in 2D with a common geometry and realistic load conditions at a prescribed location. Since the model was in 2D it incorporates only one-way action.

The results, e.g. stresses, deflections and cracking, were compared to requirements and recommendations (Eurocode 2, ACI) pertaining to façade elements and according to an iterative process an optimized geometry was obtained. Since the deflection was the toughest requirement, a 3D model only considering the linear-elastic behaviour of materials was created to verify the deflections in two-way action. One can refer to the detailed flowchart of the method depicted in Figure 1-1 for further details.

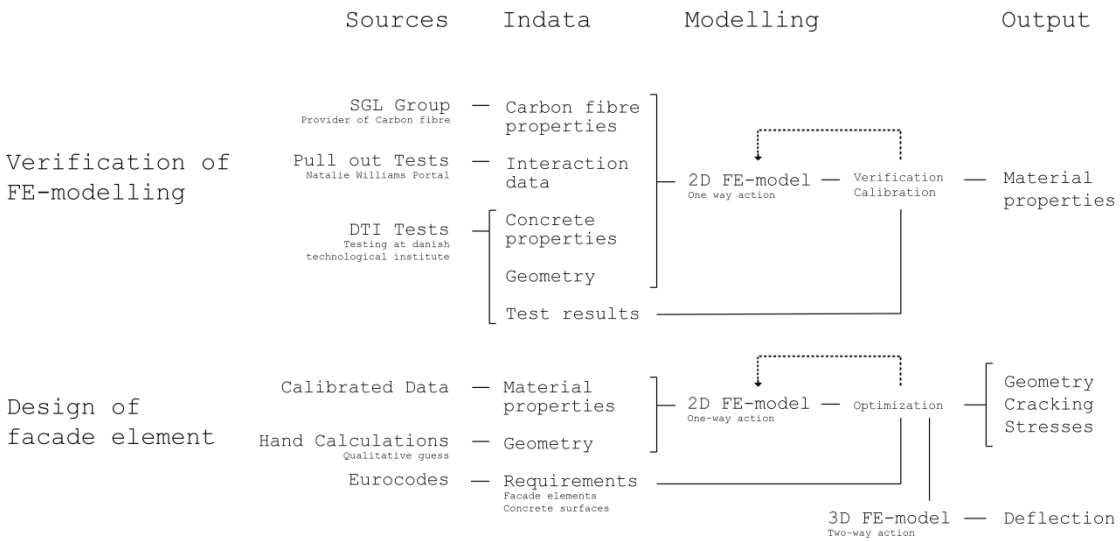

Figure 1-1 Method flowchart

1.4 Limitations

All models are based on testing of certain materials and the results presented in this thesis are valid for those explicit material combinations only. Other textile materials such as AR-glass or basalt, as well as other concrete properties are not regarded. Likewise is the interaction properties based on pull-out tests of one specific carbon fibre yarn and no other yarn or textile mesh are regarded.

Effects from creep and shrinkage are not included in the FE-modelling. Material testing was performed at a concrete age of 99 days and all analysis in this work is based on properties obtained from those experiments.

Furthermore, for façade elements, only non-load bearing elements are considered. As such, the load that was included was wind load, implying that some loads were ignored e.g. self-weight, temperature, moisture and accidental loads, shrinkage and movements of load-bearing structure.

Loss in stiffness due to creep is not regarded in analysis of façade elements. This simplification was considered reasonable since the only long-term load acting on a non-load bearing façade element is self-weight and as this is acting perpendicular to the main load.

Properties for reinforcement loaded in shear were not available at the time of this work and thus this failure mode was not included in the analysis. However, by analysing the stress pattern obtained in the analyses no major shear loaded sections of the reinforcement were found and the results are therefore assumed to be reliable.

Effects of cyclic loading of façade elements were not analysed. It was assumed that the number of loading cycles to levels where this was important to be included was limited during the life-span of a façade element and that more frequent loading cycles were at a level where they would not significantly influence the behaviour of the structure.

All FE-analyses were performed using DIANA. Verification with other FEM-software was not included in the scope of this work.

1.5 Tools

Finite Element Analyses

For finite element analysis the software DIANA (DIsplacement ANAlyser) was used. Since the late 1980's DIANA has been used to analyse reinforced concrete structures. The reinforced concrete models in DIANA are based on exact geometry definition of reinforcement and concrete while describing explicitly the material failure and bond behaviour (TNO Diana, 2011).

Pre-processor

The geometry and topology input data for DIANA was created in Midas FX+ which is a pre-processor able to receive both geometrical and analysis data. However, material properties and analysis data is added manually to the input and command files (.dat and .dcf).

Post-processor

Midas FX+ was used to view stress distribution, displacements, crack positions and extract data. Microsoft Excel was used for data processing and graphs.

Calculations

To verify results, calculate loads and material properties as well as to make estimations for e.g. geometries, PTC Mathcad was used. Iterative processes were implemented and solved in MATLAB.

2 Textile Reinforced Concrete

There are many alternative ways to reinforce concrete using fibres. The most developed solution to this date is by mixing short fibres with concrete. This solution gives a composite with higher tensile capacity than concrete without fibres. Due to the random arrangement of fibres, the utilization of individual fibres varies to a large extent. Part of the fibres becomes positioned perpendicular to the load direction and other parts end up in low stressed sections as shown in Figure 2-1. To address this, the possibility of using textile meshes to arrange fibres in a more ordered manner has been researched and evaluated for over a decade by collaborative research centres 532 and 528 at RWTH Aachen University and Dresden University of Technology (Orlowsky and Raupach, 2011). Other major research efforts were made in Brazil, the USA and Israel (Mobasher, 2012). This solution has been shown to lead to higher load-bearing capacity of the member with the same amount of reinforcement or to a reduction of the required reinforcement for the same load-bearing capacity.

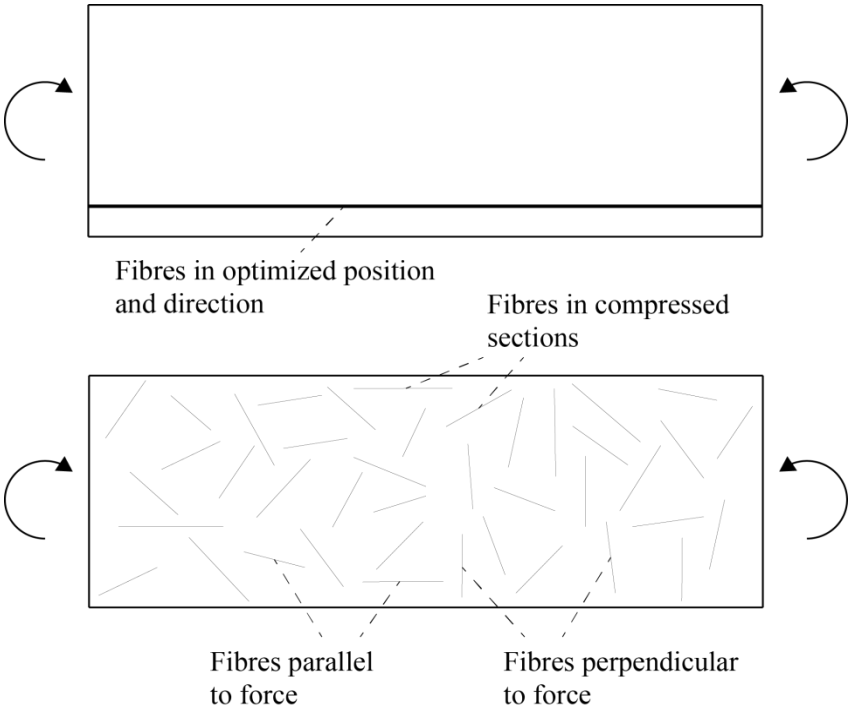

Figure 2-1 Arrangement of fibres

2.1 Concrete

Requirements and limitations of the concrete may vary depending on the textile mesh geometry and properties. Aggregate sizes are often limited by the size of the mesh and cover layer. Limited maximum size of aggregates leads to an increase of cement paste in the concrete mixture and an increase of energy consumption. If adequate penetration of the mesh and enclosure of reinforcement can be ensured, larger aggregates could potentially be used. Further research and development to address this issue is needed. Alternatively, admixtures and supplementary cementing materials

(SCM) can be implemented as to replace large quantities of cement in a concrete mix (Remezanianpour, 2014).

2.2 Textile

Textile meshes applicable as reinforcement exists in a large number of variations. Many different materials can be used such as carbon fibres, glass fibres or basalt as depicted in Figure 2-2. A textile yarn consists of numerous single fibres in a range from typically 800 (glass fibres) to 24000 (carbon fibres) (Brameshuber, 2006). A yarn can vary in cross-section area, shape and circumference and can either be simply packed together or, in a sizing process using adhesives e.g. epoxy, made into one cooperative cross-section. These yarns can then be arranged in meshes of different types and sizes; 2D or 3D, sparse or dense, woven, glued together or held together using additional threads. The way the meshes are arranged can affect principally the tensile capacity and the bond behaviour (Brameshuber, 2006).

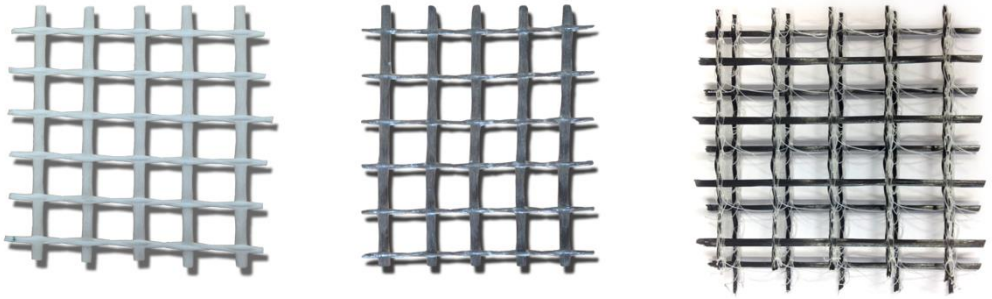

Figure 2-2 Textile mesh types (left to right: glass, basalt, carbon)

2.3 Interaction

The interaction between textile reinforcement and concrete is an important parameter regarding crack distance, crack width and, if the bond strength is the determining factor, the ultimate capacity. With a lower bond capacity, cracks grow to a larger extent and the distance to transfer tensile stresses to the concrete, hence the crack distance, becomes longer. When steel reinforcement bars are used the stress distribution over the cross-section is assumed to be constant because of the high shear stiffness of steel. Since a textile reinforcement yarn is not homogenous and the ability to transfer longitudinal shear stresses is limited, the stress distribution may vary over the cross-section (see Figure 2-3). This may not significantly affect the behaviour in early stages but can influence the ultimate capacity. The longitudinal shear stiffness of a yarn can however be increased by e.g. epoxy impregnation.

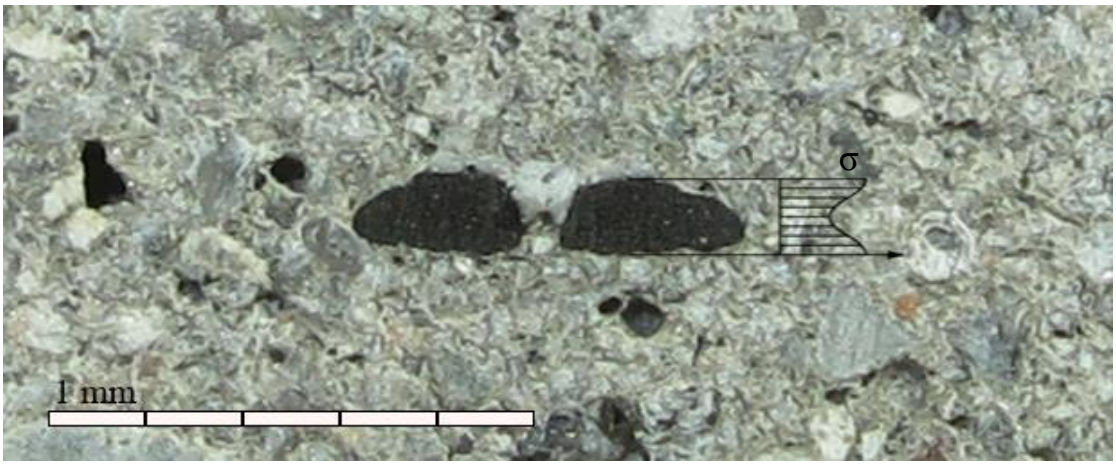

Figure 2-3 Pull-out test specimen, assumed stress distribution

2.4 Advantages of TRC

The most pronounced advantage of TRC is the possibility to minimize the amount of concrete. Since Portland cement is one of the most used binder and also one of the most pollutant and energy consuming materials in the building industry (Graham, 2002), this minimization contributes a lot to reduce the usages of natural resources.

Besides the environmental advantages, textile reinforcement also offers possibilities for lightweight and free-form design where the textile can be used both as form work and reinforcement. In 2009, the architectural workshop Concrete Flesh was held at Chalmers University of Technology to experimentally study different ways to design with concrete. The conventional way of casting in boxes was replaced by casting with textile or plastic as forms. This is one of many initiatives that show on an increasing interest in free-form concrete design and with a high strength textiles this experiments could become actual members in buildings.

3 Requirements for Concrete Façade Elements

Requirements for a concrete façade element, as for all structural members, consist of two groups, functional and aesthetic requirements. The functional requirements ensure the safety and comfort of the people using the structure. Those requirements are mandated at an international (Eurocodes) and national level (EKS–national application of Eurocodes), or alternatively by various design codes (fib Model Code, ACI-American Concrete Institute). Aesthetic requirements are not regulated but can be set if a certain architectural quality is wanted which is commonly determined by the client. Since a façade panel is more often visually experienced than other structural parts, those requirements can be set quite high in certain cases.

According to Eurocode 2 (EC2), SS-EN 1992-1-1:2005, a structure is required to undergo an analysis to determine that the structure can withstand the loads it is exposed to, both mechanical and chemical. This includes external loads e.g. wind and snow loads, internal loads e.g. self-weight and shrinkage and environmental loads. The main loads acting on a non-loadbearing façade element are wind loads, self-weight and chloride penetration. Depending on the design, the panels can also be exposed to e.g. rhombic distortion from deflections in the main structure or impact from vehicles. Other minor loads are temperature loads and stresses from shrinkage.

3.1 Deformation

Functional requirements for deflections in façade elements are not specifically regulated in the Eurocodes. However, L/250 is mentioned as a guideline for deflections in structural members in general (EC2). This suggested value regards quasi-permanent loads and since the main loads on façade elements resulting in deformations are short-term loads, it is not completely applicable. Consequently, all elements must be designed according to the client's requirements for the specific elements.

Since deformations not only cause an unsafe expression or a non-comfortable experience but also a non-attractive appearance, it can also be considered an aesthetic requirement. Depending on the client's demands, the final requirement can even be tougher. In Figure 3-1, sets of façade elements are shown with different mid-point deflections to give an idea of how the deflection affects the aesthetic appearance. The elements are modelled with pinned edges which creates sharp shadow effects. A similar deflection for a fixed element creates a more smooth shadow and a less obvious deflection. Definite limits for acceptable deflections are difficult both to define in the design of an element but also to measure and verify after construction. Further investigations in this field could lead to altered recommendations and guidelines.

Also, other undesired effects e.g. vibrations should be considered in design. For structural members there are recommendations in Eurocodes for both acceleration and amplitude, but again this applies for members in contact with people such as floors rather than wall elements. Those recommendations could be used for the façade element design if the client does not have any special requests.

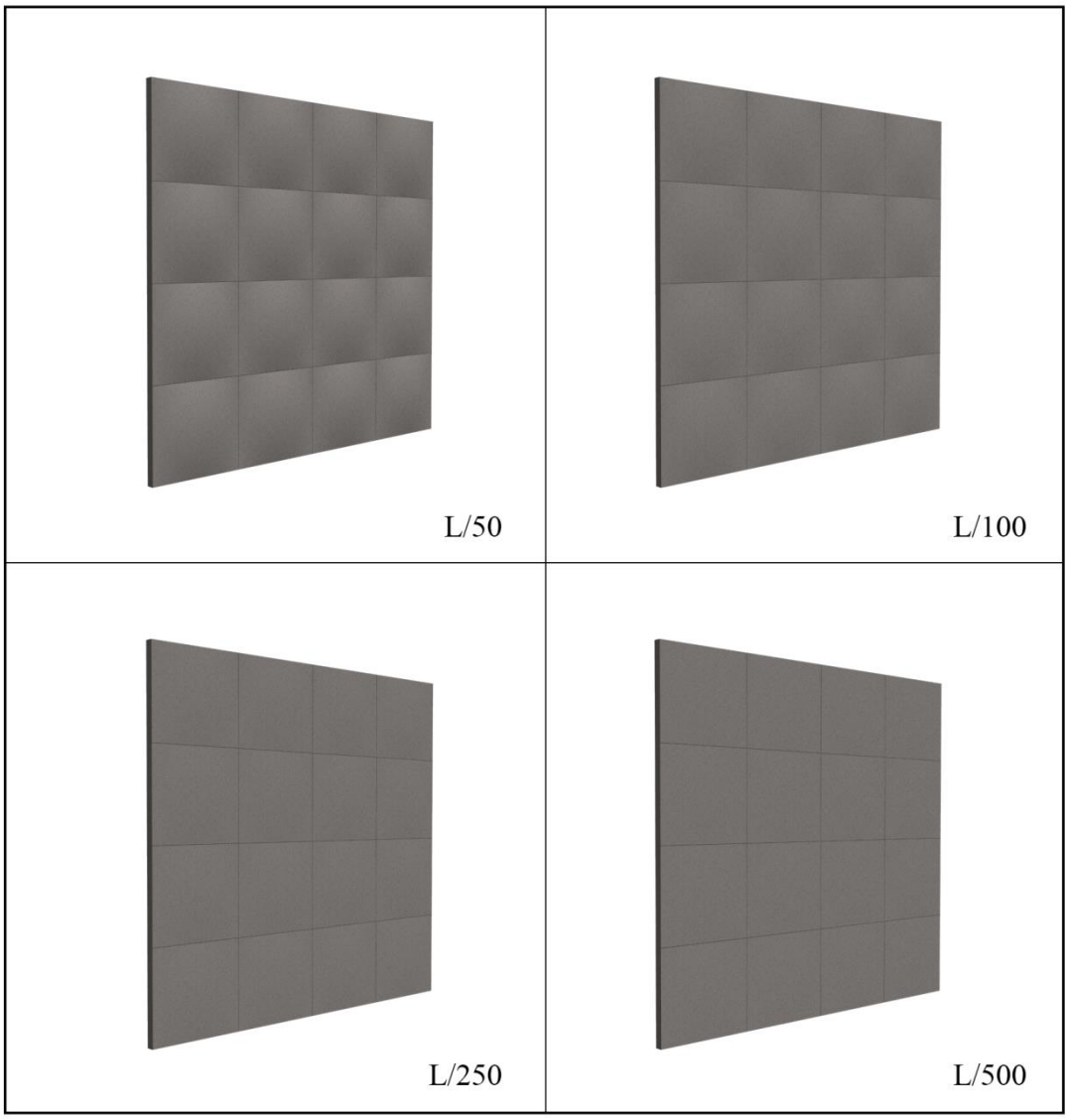

Figure 3-1 Visual effects on façade elements from deformation of different magnitudes

3.2 Reinforcement

According to EC2, SS-EN 1992-1-1(2005) Section 7.3.2, minimum reinforcement is required if there is a need to limit crack widths in tensile loaded regions. For concrete reinforced with carbon-fibre textiles this may be required to avoid brittle failure of the element and to ensure serviceability of the member if cracking were to occur due to secondary effects e.g. shrinkage, restraining effects, temperature loads or settlements. Minimum reinforcement can be calculated according to Equation 3-1.

$$A_{s,min}\sigma_s = k_c k\, f_{ct,eff} A_{ct} \qquad \text{Eq. 3-1}$$

Where:

$A_{s,min}$ is the cross-section area of the minimum reinforcement in the tensile zone. The tensile zone is defined here as the part of the cross-section with tensile stress just before formation of the first crack

A_{ct} is the concrete cross-section area in the tensile zone.

σ_s is the absolute value of the maximum allowed stress in the reinforcement immediately after crack-formation. For steel the latter can be chosen as yield stress of the reinforcement (f_{yk} for regular steel reinforcement and $f_{0,2k}$ for cold-worked steel) or lower to limit crack widths. For other materials such as textile reinforcement recommendations are not yet available. Since there are large uncertainties regarding properties for textile reinforcement the value of σ_s should be chosen carefully and conservatively.

k_c is a coefficient accounting for the stress distribution immediately before crack formation.

k is a correcting factor accounting for non-linear Eigen-stresses before crack formation.

$f_{ct,eff}$ is the mean value of the tensile capacity of the concrete at the age when the first crack is assumed to occur.

Model Code 2010 does not suggest any changes regarding the calculation of minimum reinforcement in EC2. Limits for reinforcement cross-section area can be determined according to Clauses 9.2.1.1(1) and (3)

$$A_{s,min} = 0.26 f_{ct,m}/f_{yk} b_t d \quad < 0.0013 b_t d \qquad \text{Eq. 3-2}$$

$$A_{s,max} = 0.04 A_c \qquad \text{Eq. 3-3}$$

Where:

d is the effective depth of the section

b_t is the average width of the tension zone of the cross-section

f_{ctm} is the average tensile concrete strength

f_{yk} is the characteristic value yield strength of the reinforcement

A_c is the gross concrete cross-sectional area.

Secondary, transverse reinforcement with an area of at least 20% of the main reinforcement should be put into a one way slab.

According to SS-EN 14992 (2012), there is a need for minimum reinforcement in precast concrete panels as a function of the panel thickness:

- Thickness ≤ 120 mm: One layer of reinforcement placed in centre of panel
- Thickness > 120 mm: Two layers of reinforcement distributed between two faces of panel.

Additionally, non-metallic reinforcement is discussed in FIB Model Code 2010 and is described as "*Reinforcing elements consisting of a high number of continuous, directionalized, organic or inorganic fibres, typically embedded in a polymeric matrix.*" Furthermore, it describes how non-metallic reinforcement should be quantified and how different properties needs to be determined. However, specific guidance of how calculations could be performed is not presented.

3.3 Cracking

In conventional reinforced concrete, limits for cracking are mainly established to prevent corrosion. When using non-corrosive reinforcement such as carbon fibre textiles, those limits no longer apply. However, depending on the client, requirements for crack widths can be set for aesthetic purposes and those can sometimes exceed the requirements for corrosion resistance. For exterior façades with a rough surface, a crack width of 0.25 mm can be accepted (ACI committee 533, 1993). For surfaces with higher architectural importance such as smooth interior surfaces the crack width should not exceed 0.10 mm or for polished surfaces not appear at all.

3.4 Cover Layer

In EC2, a couple of variables such as exposure class, water-cement ratio and reinforcement diameter determine the cover layer thickness. This is to ensure sufficient adhesion and corrosion resistance. When non-corrosive materials are used the variable for corrosion resistance can be ignored and the cover layer thickness reduced from 50 mm for elements exposed to tough conditions down to 1 mm (Yin et al. 2013) if only bond properties are regarded. However, to achieve a reasonable production procedure, a cover layer thickness of approximately 5 mm is assumed to be sufficient.

3.5 Summary of Requirements

In Table 3-1, examples of requirements for façade elements are collected and presented. Steel and textile reinforced concrete are compared for functional and aesthetic requirements.

Table 3-1 Example of requirements

	Functional Requirements		Aesthetic Requirements
Reinforcement	Steel	Textile	Steel/Textile
Deflection [-]	-	-	L/250
Crack width [mm]	0.25	-	0.10
Cover Layer [mm]	40	6	-
Minimum Reinforcement	See Chapter 3.2	-	-

4 FE-Modelling of TRC One-Way Slab

The first FE-model in this work was developed and verified using results from experiments performed by the Danish Technological Institute (DTI). More specifically, the experimental results ant the numerical results are presented and compared in this section. Different key parameters in the model were calibrated based on the comparison.

4.1 Experimental Work

The experimental work included in this report was conducted by DTI; more details can be found in references (Williams Portal, 2013). TRC test specimens reinforced by a carbon-fibre mesh have been subjected to bending in a 4-point bending test, where a force has been applied in steps at two symmetrically located points (see Figure 4-1). The applied force and the mid-point deflection have been plotted in a load-to-deflection-curve. This curve, together with cracking behaviour such as number of cracks and time of appearance were in this work used for comparison with the FE-model.

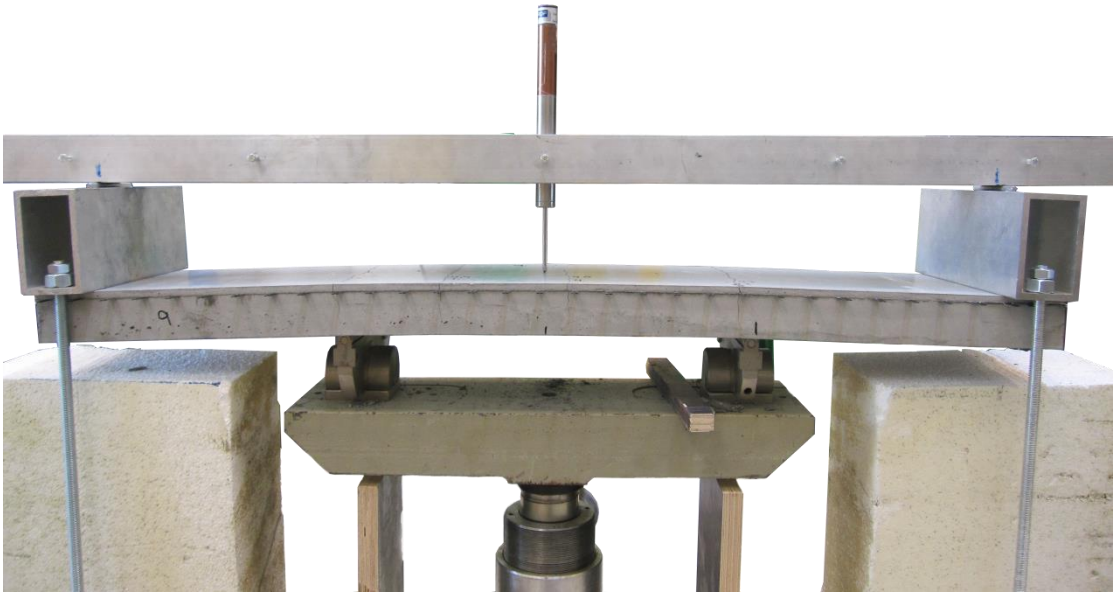

Figure 4-1 4-point bending test

4.1.1 Geometry

The test specimens were 1000 x 200 x 50 mm (L x W x H) and were reinforced by one layer of carbon fibre mesh placed 7.5 mm from the top edge. The supports were situated 30 mm from the edge and the loads 200 mm from the centre.

4.1.2 Concrete

The concrete mix composition (w/c = 0.42, w/c_{eq} = 0.33) used to cast all specimens can be found in references (Williams Portal, 2013). The mean concrete cylinder compressive strength corresponding to 28 days, f_{cm}, was derived from material test

results to be 53.6 MPa. Based on f_{cm}, the mean modulus of elasticity, E_{cm}, was estimated to be 36.4 GPa using EC2. Lastly, the mean value of the tensile splitting strength tests was found to be 4.7 MPa.

4.1.3 Carbon Fibre

The carbon fibre mesh used in the test is Sigratex grid 300 produced by SGL Group (Germany). The mesh is made up of a yarn called Sigrafil C30 T050 which, in turn, consists of two threads. The threads are made of 25000 filaments impregnated with epoxy. These definitions for mesh, yarn, threads and filaments are used in the report. The properties are presented in Table 4-1.

Table 4-1 Properties of carbon fibre textile mesh

Property	Provided by manufacturer	Calculated
Filament properties		
Density [kg/m^3]	1800	
Tensile strength [MPa]	4000	
Young´s modulus [Gpa]	240	
Ultimate strain [-]	0.017	
Yarn properties		
Fineness [tex]	3300	
Number of filaments	50 000	
Perimeter [mm]		4.73*
Cross-section area per yarn [mm^2]		1.83
Mesh properties		
Weft [mm]	30	
Warp [mm]	30	

*Perimeter can be defined in different ways (Brameshuber, 2006). The perimeter stated here is the one used to determine the bond stress-slip properties.

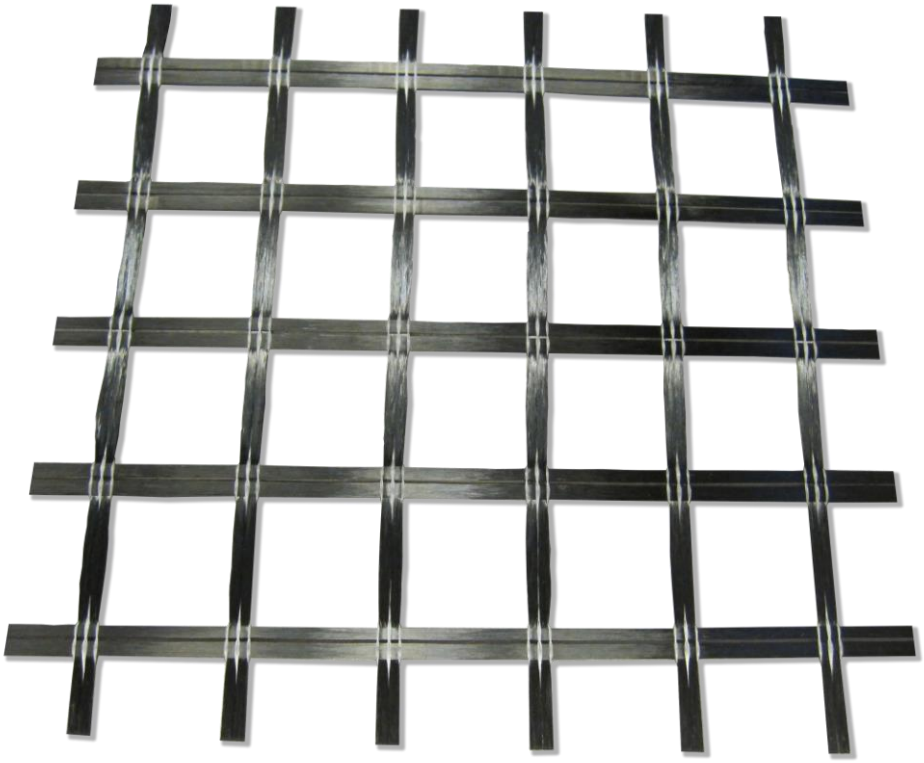

Figure 4-2 Carbone fibre textile grid used in experiment

4.1.4 Experimental Results

The three tests show similar behaviour regarding both maximum load bearing capacity, cracking load, number of cracks and deflection. Initially in the uncracked state, they all follow a linear curve until approximately 4.4 kN where first cracking and loss of stiffness occurs. In next state, four to six cracks develop and grow until the specimen can be seen as fully cracked at a mid-point displacement of 5-10 mm and a load of slightly more than 4.3 kN. In the last state, the load and displacement increases almost linearly until failure at a load of approximately 8.5 kN.

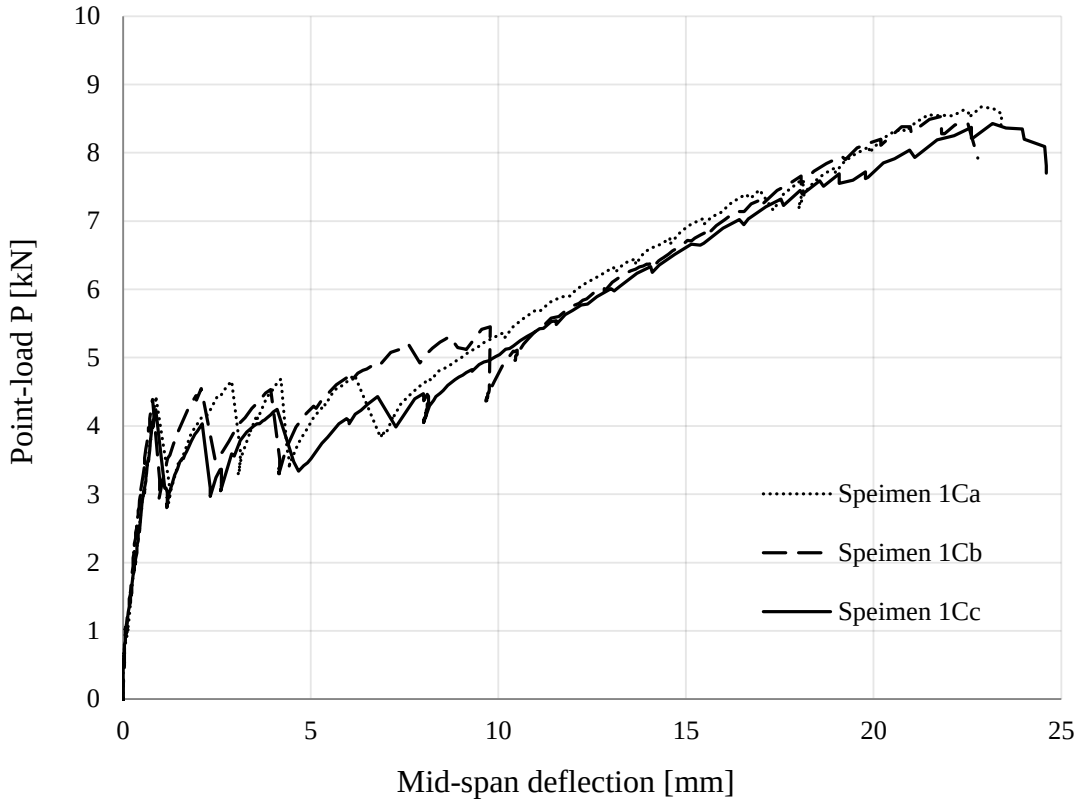

Figure 4-3 Experimental results, mid-span deflection to load-curve

By studying the test specimen after failure it is seen that the bond slip is very large and that tensile failure occurred to some extent in the yarns. An explanation can be that, due to the heterogeneous structure of the yarn, the stress distribution is uneven. A stress concentration occurs at the outer most fibres which fail before the mean tensile strength is reached. This is assumed to be followed by a bond failure. Another possibility is that a pure bond failure occurs, followed by rupture of some filaments due to tensile and shear stresses.

Figure 4-4 Experiment specimen after failure

4.2 FE-modelling

The FE-model that was verified by comparison with the experimental results is created in the FE-program DIANA. The aforementioned material properties and geometry from the experiments were used as input data in the model

To reduce the required computational time, the symmetry of the test was used. By doing so, the behaviour of the FE-model is expected to differ slightly from the experiments due to the fact that cracks in the experiment did not occur identically on both sides of the symmetry axis. Also, it is important to note that the FE-model is upside down compared to the experimental setup.

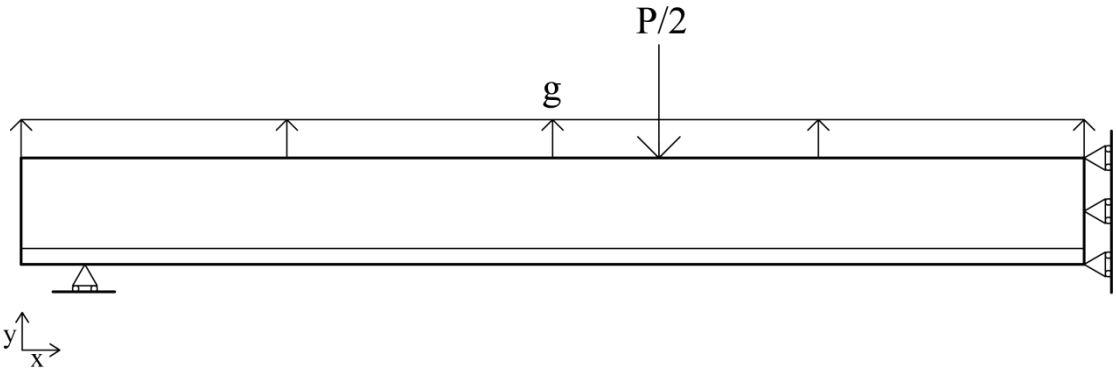

Figure 4-5 FE-model overview

4.2.1 Material Properties

The 4-point bending tests were conducted at a concrete age of 94-99 days and the corresponding concrete compressive strength was extrapolated to be 84.7 MPa from material tests. Remaining properties needed as input were calculated according to fib model code for concrete structures. The calculations resulted in the properties presented in Table 4-2.

Table 4-2 Concrete properties

Compressive strength	f_{cm}	84.7 MPa
Tensile strength	f_{ctm}	4.7 MPa
Young´s modulus	E_{cm}	41.8 MPa
Fracture energy	G_F	162 N/m

The tensile response of the concrete was taken into account by using the Hordijk model (TNO Diana, 2011) and the compressive response according to a modified Thorenfeldt curve (see Figure 4-6). The original Thorenfeldt curve has been defined after measurements of compressive tests on 300 mm long specimen. As such, when assuming that crushing will occur in one element row, the Thorenfeldt curve is modified for the applied element size of 2.5 mm (Zandi Hanjari, 2008).

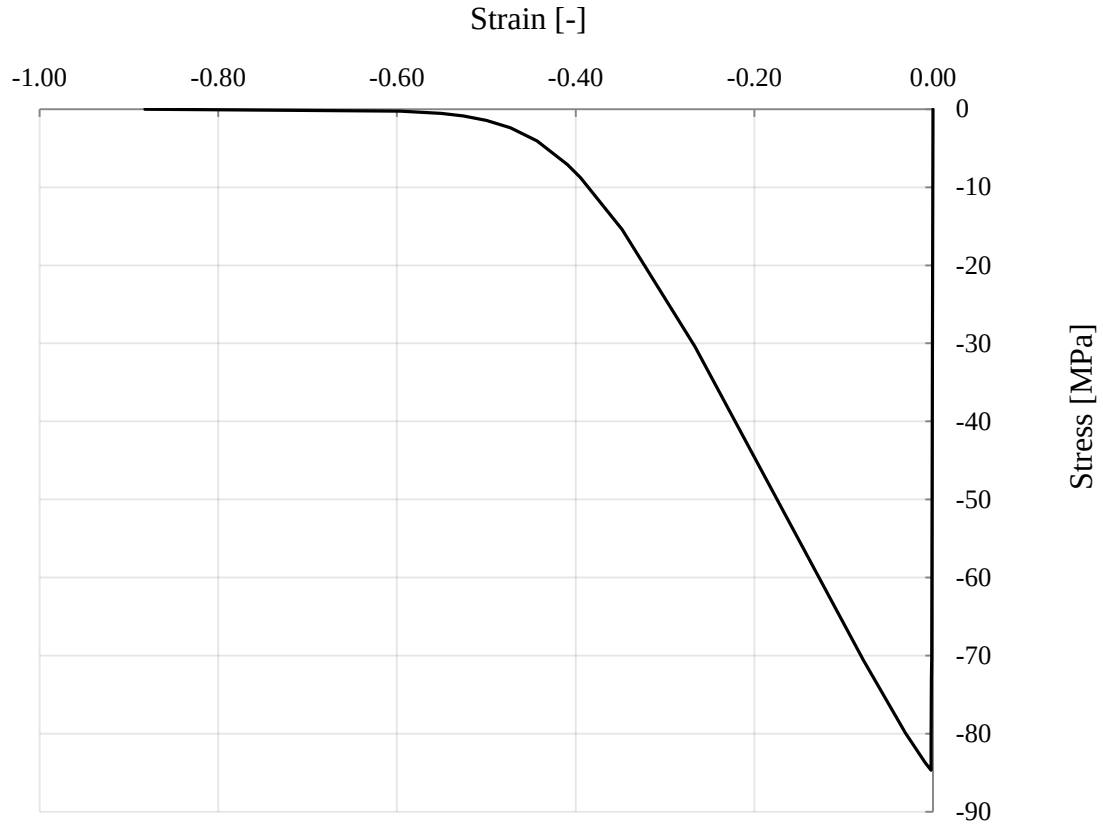

Figure 4-6 Modified Thorenfeldt curve

The cracking properties for concrete were modelled using the rotating crack model and crack band width was chosen equal to element size which is recommended in TNO Diana user's manual.

The carbon fibre properties were provided from the manufacturer; those properties were used in the FE-model, that is, a tensile strength of 4000 MPa and an elastic modulus of 240 GPa (as shown in Table 4-1). The material was modelled linearly which means that tensile failure in the reinforcement textile cannot be captured in the model.

4.2.2 Mesh and Element Types

The mesh size of 2.5 x 2.5 mm was chosen to fit a few element rows below the reinforcement and at the same time make sure that the reinforcement was placed at a row of nodes. The element type used for the concrete elements was a four node quadrilateral isoparametric plane stress element, named Q8MEM in DIANA. Default integration was used; i.e. 2x2 integration points and Gauss integration. The elements have two translation degrees of freedom (DOF) in every node, thus no rotation DOF. For the textile reinforcement, L2TRU element was used which is a two node truss element. The element has two DOF in each node and one integration point. To include the bond slip relationship, the reinforcement cannot be modelled in the same nodes as the concrete. Instead, specific nodes were created for those elements, at the same coordinates. The nodes were linked together by the interface elements called L8IF where the bond-slip properties were applied. Those elements translate stresses and strains from the concrete to the reinforcement.

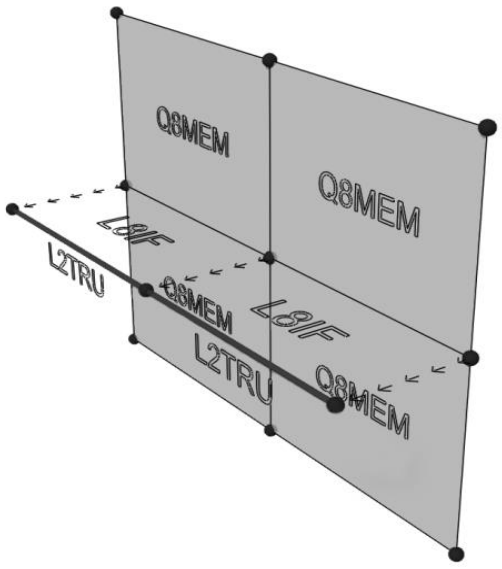

Figure 4-7 Element types

The bond-slip relationship between textile reinforcement and concrete is a very important parameter for the behaviour of the structure, both regarding cracking and ultimate capacity. The input data was obtained from a pull-out test presented in (Williams Portal et al., 2014) where the slip of a single yarn from a textile reinforcement mesh has been measured for a short embedment length. From the results a bond stress/slip curve has been calculated using the pulling force, length and perimeter (see Figure 4.8). It was however presumed that the bond slip behaviour of a

single yarn in the pull-out test may differ greatly from that of a mesh in a member exposed to bending. Possible variables that can affect the behaviour are described in Chapter 4.3. If a different geometry or material was used for the textile reinforcement mesh, for instance, the bond-slip input has to be reconsidered due to e.g. perimeter to cross-sectional area ratio.

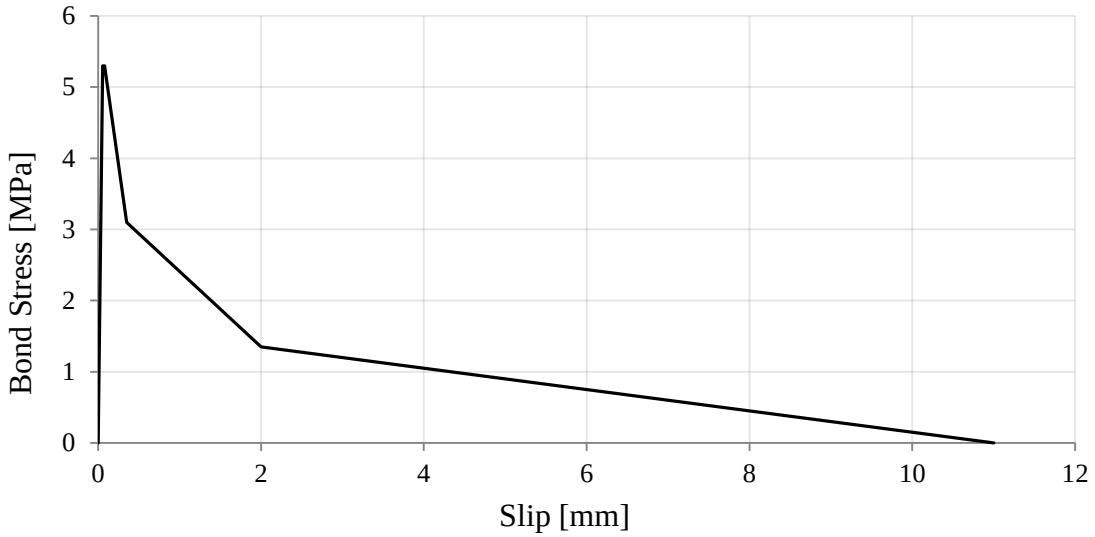

Figure 4-8 Bond slip relationship for textile in concrete (Williams Portal et al. 2014)

4.2.3 Boundary Conditions

To save computational time, the symmetry of the structure was used in the model. Half of the beam was modelled and all nodes at the centre are prevented to move in x-direction which also leads to prevented rotation around the z-axis, as previously shown in Figure 4-5. The end support was modelled as prevention in y-direction. To get rid of possible singularities and stress concentration, the surrounding nodes were modelled as slave nodes to the support node, that is, the node in the centre of the support. To make this possible, rotational DOF was created in those nodes using a dummy beam with zero stiffness of the element type L6BEN as illustrated in Figure 4-9.

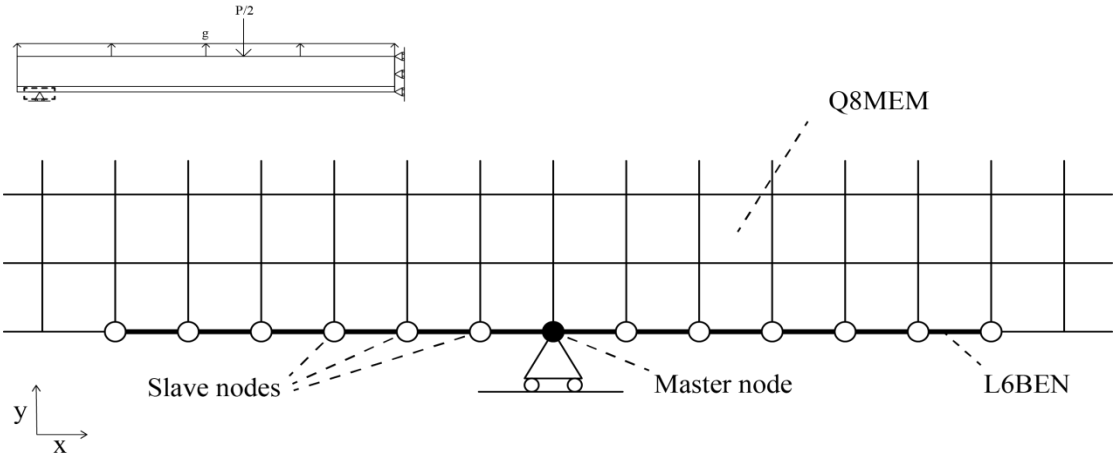

Figure 4-9 Detail of support modelling

4.2.4 Loads and Analysis Method

A two phased analysis was used to apply load in the model. In the first phase, the self-weight was added as an evenly distributed load in all elements. The output from phase one was transferred to phase two where the point load was applied. Together the two phases resulted in a moment distribution as shown in Figure 4-10.

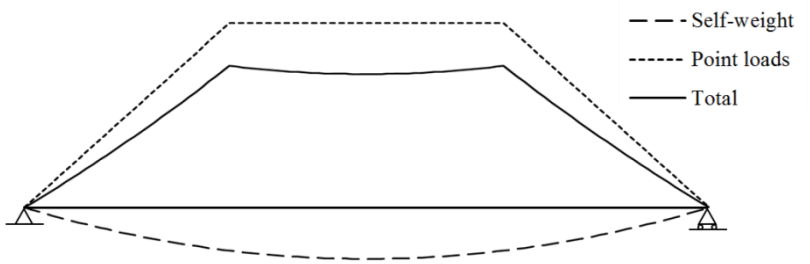

Figure 4-10 Resulting moment

The point loads were applied as a fixed deformation with a step size of 1 μm. In each step, equilibrium was found with secant tangent iterations which yielded the most stable solution. This deformation controlled loading means that the behaviour, especially during the cracking state, can be followed more accurately and that the results can more easily be compared to the test results. Tolerances used are energy (0.001), displacement (0.01) and force (0.01). A solution within those tolerances is considered adequate and the analysis continues to the next load step. If the tolerances are not reached after a maximum number of iterations, the analysis can still continue as long as convergence occurs. As a result, slight discrepancies can appear in the solution. In the case of divergence, the analysis terminates.

Since the point loads were applied on one single node, local crushing of the concrete must be prevented. Therefore, the loaded node was tied to the neighbouring nodes which lie within the loaded zone indicated in Figure 4-11. This method is identical to that used at the end supports described in Chapter 4.2.3.

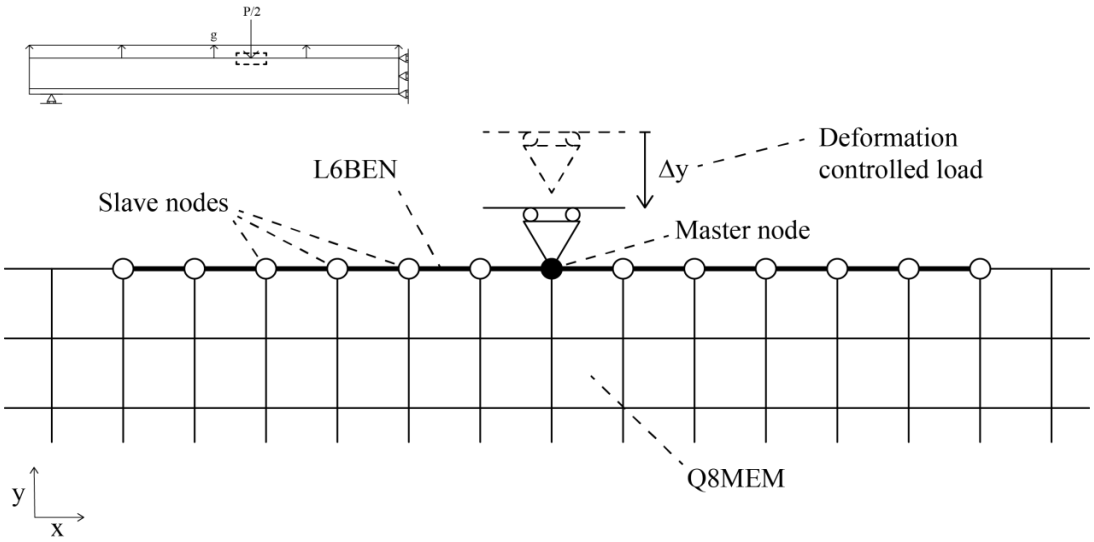

Figure 4-11 Detail of load modelling

4.2.5 FE-results

The load to mid-span deflection diagram (Figure 4-12) resulting from the numerical analysis shows that the first crack occurs at approximately 4.8 kN and that the member fails at approximately 10.0 kN. Furthermore, two early cracks occur which actually corresponds to three to four cracks considering the symmetry. The stresses in different stages, namely pre-cracking, first-cracking, crack formation, ultimate capacity and failure are shown in Figures 4-13 to 4-17.

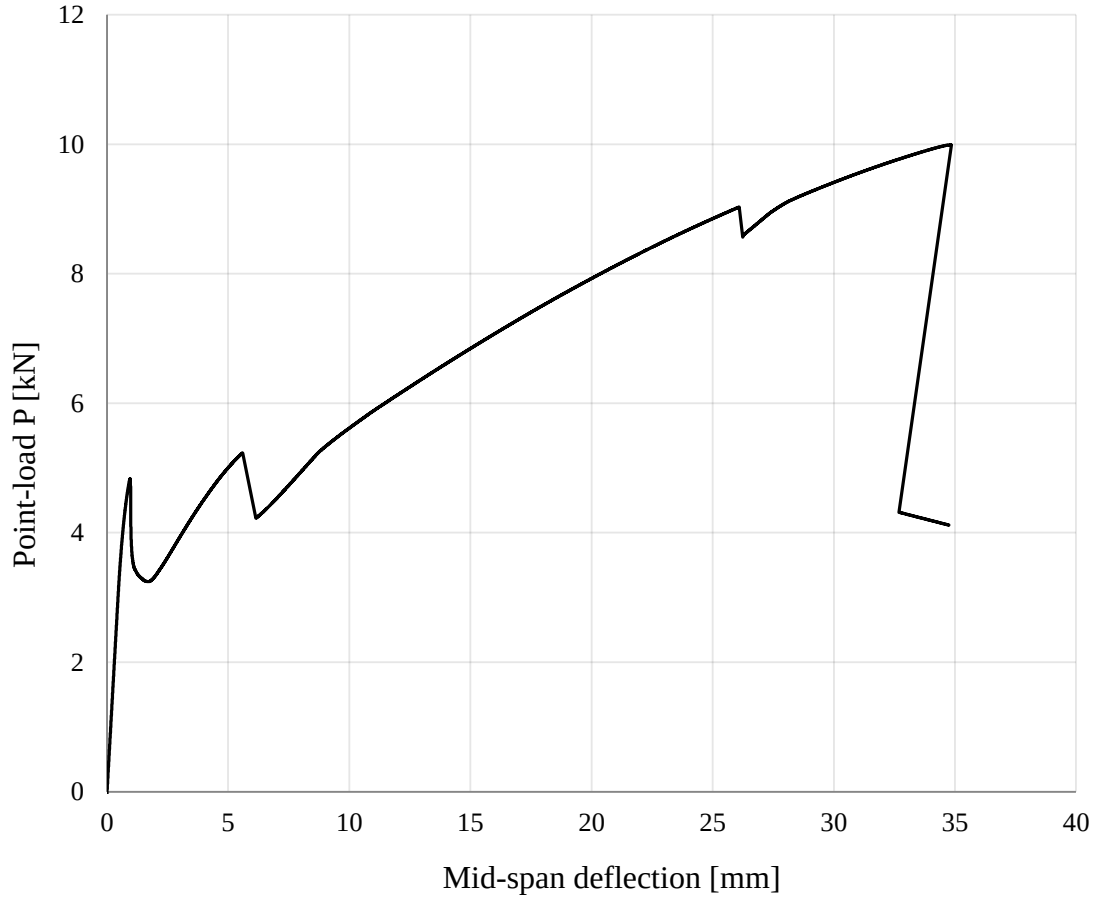

Figure 4-12 FE-results, mid-span deflection to load-curve

In the uncracked state, the member has an almost linear behaviour which matches the expectations. The two materials show a continuous stress pattern and the bond between them is still intact (Figure 4-13). At a load of 4.7 kN tensile stresses are localizing in the concrete (Figure 4-14) and results in the first crack at 4.8 kN. At this point, stresses in the concrete around the crack are released and the stresses in the textile increased (Figure 4-15). In addition, the bond stresses are increased and some slip occurs. Stresses continue to localize in the same way as for the first crack which results in further crack formation (Figure 4-16). In the load step before failure, the bond stress peak has reached the edge which means that the bond is about to release as can be seen from Figure 4-17.

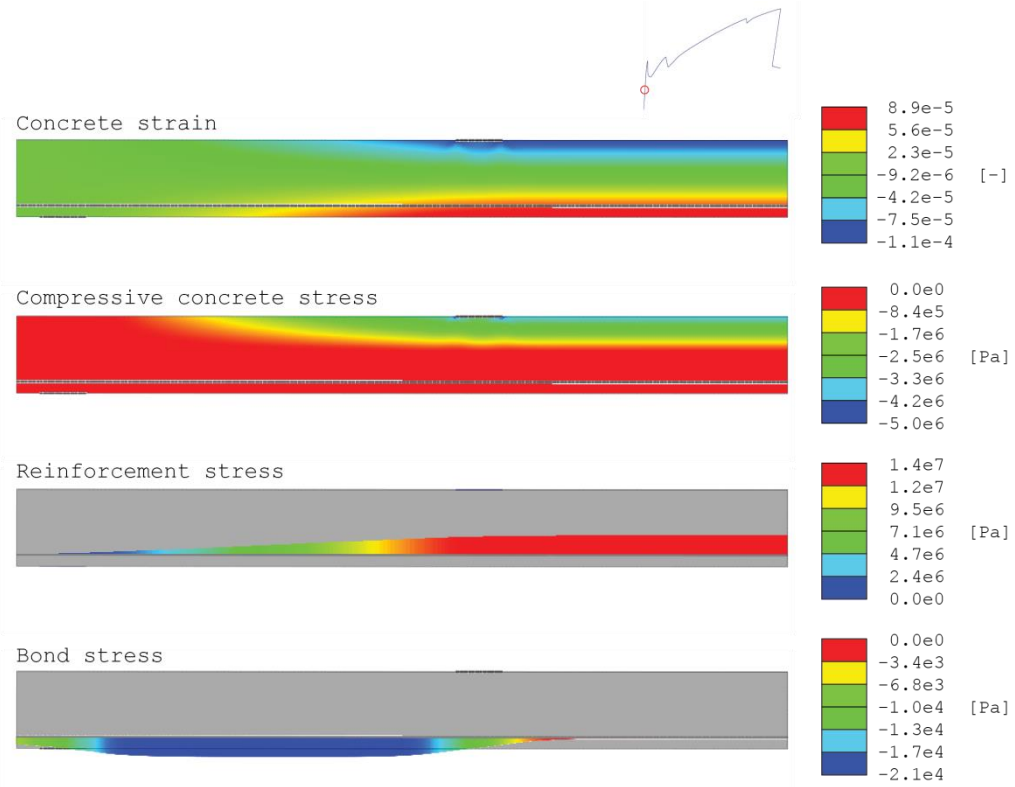

Figure 4-13 FE-results, initial state

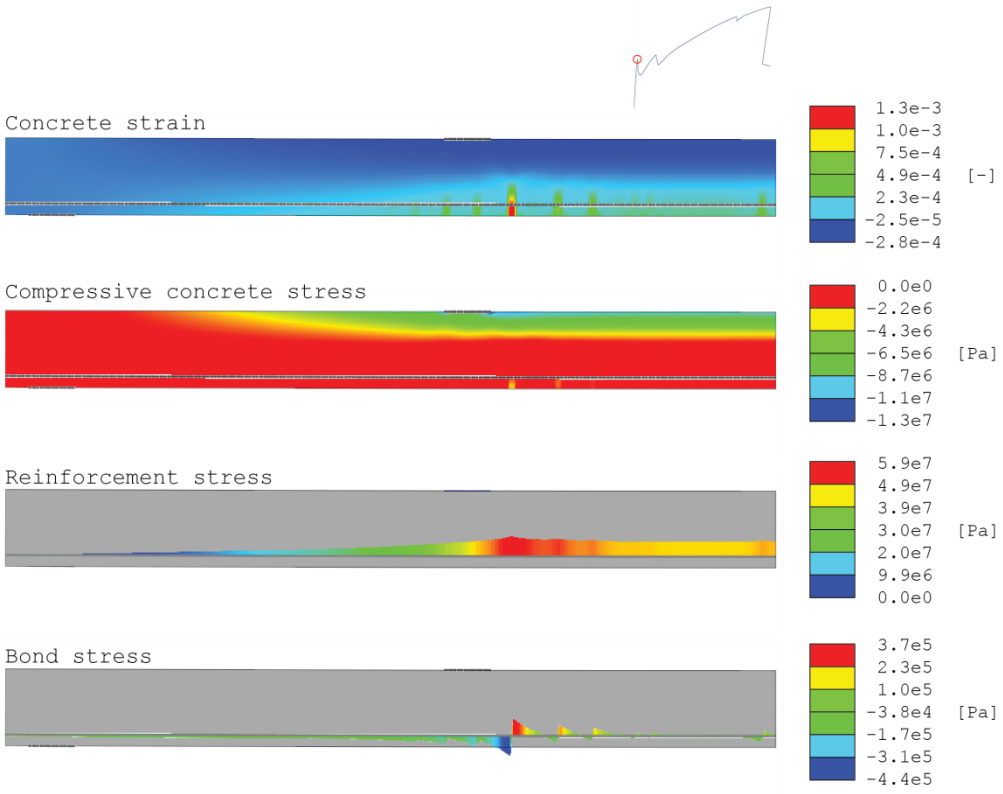

Figure 4-14 FE-results, before first crack

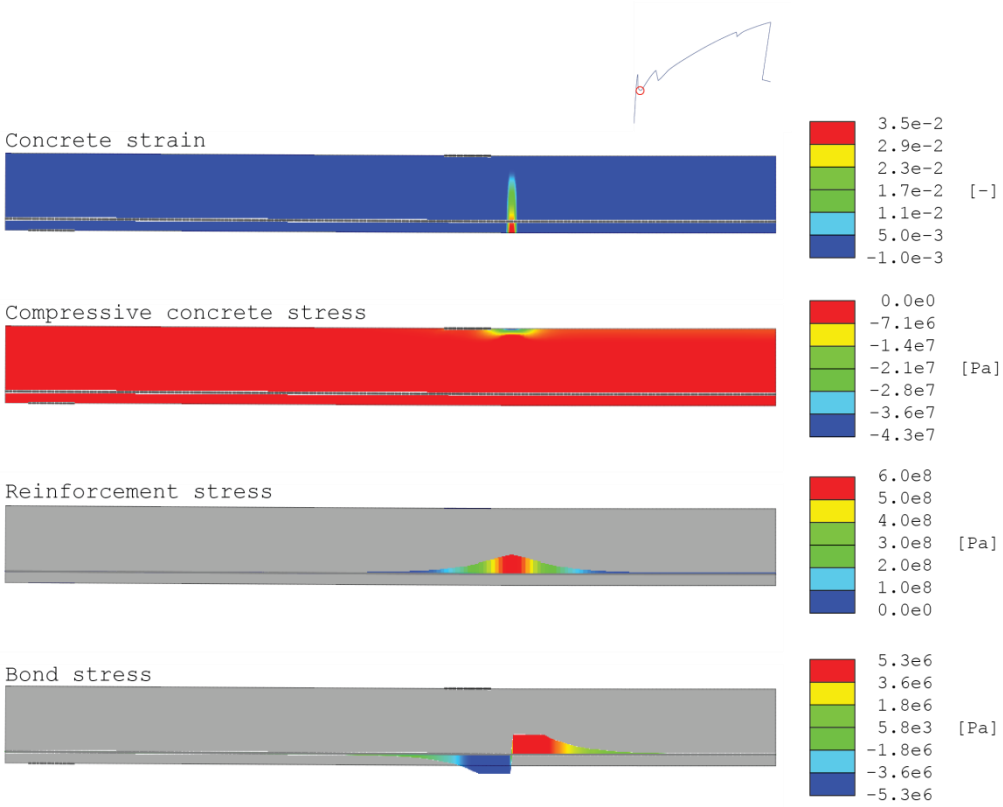

Figure 4-15 FE-results, after first crack

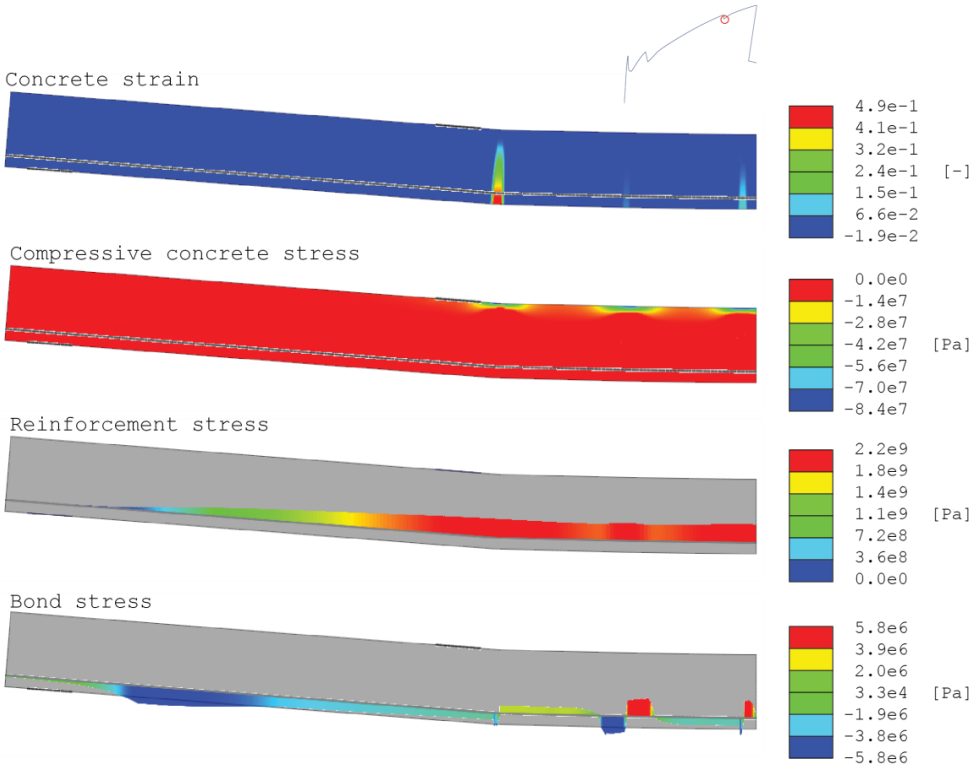

Figure 4-16 FE-results, third crack

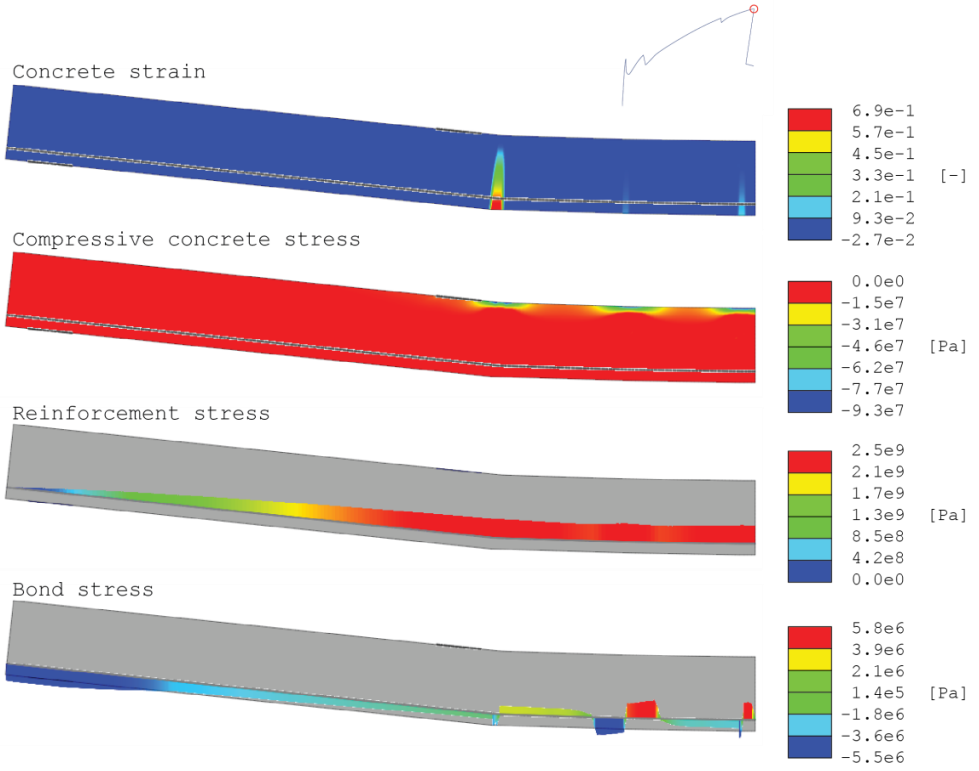

Figure 4-17 FE-results, ultimate capacity

At a mid-point deflection of 35 mm and a load of 10 kN, bond failure occurs. At this point, the concrete compressive stress is 93 MPa (utilization of 110%) and reinforcement tensile stress is 2500 MPa (utilization of 63%). The high compressive stress is concentrated in a single node. When looking at the mean stress on each element (see Appendix A) the maximum stress is approximately 66 MPa (utilization of 78 %). This means that a better anchoring of the textile can increase the capacity of the member. In Figure 4-18, the development of the bond stress can be followed. After cracking the bond stress in that point reaches its peak value. With increased load the area where this peak value is reached grows until failure when it reaches the end of the member. Figure 4-19 shows the corresponding slip.

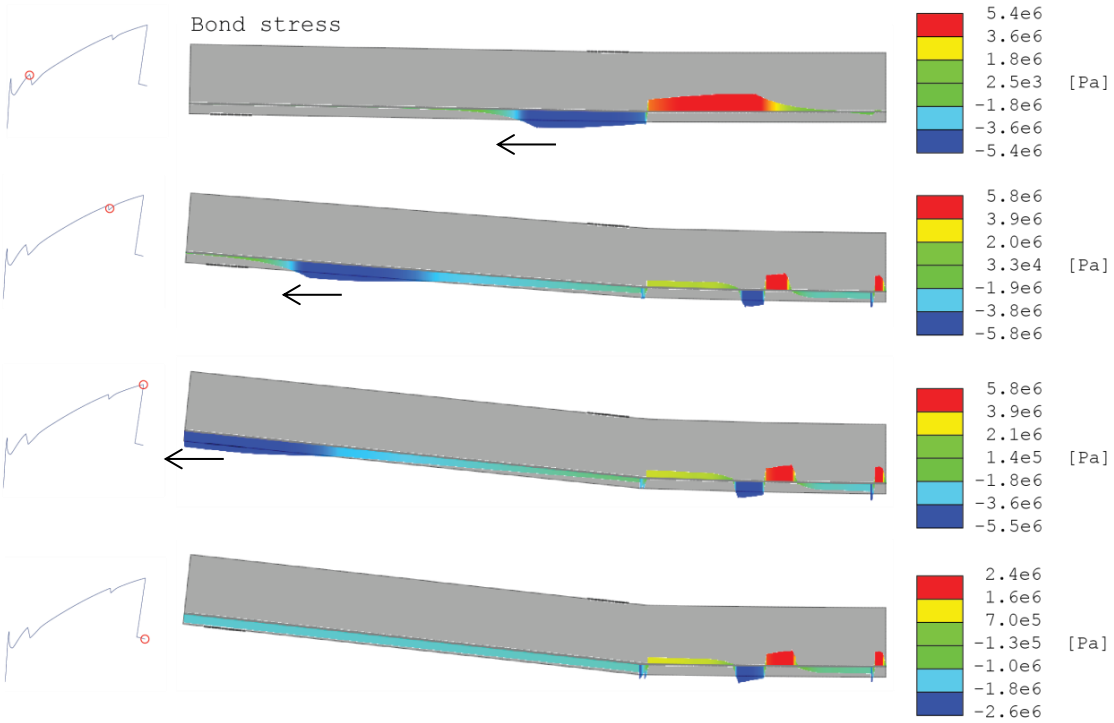

Figure 4-18 FE-results, development of bond stress

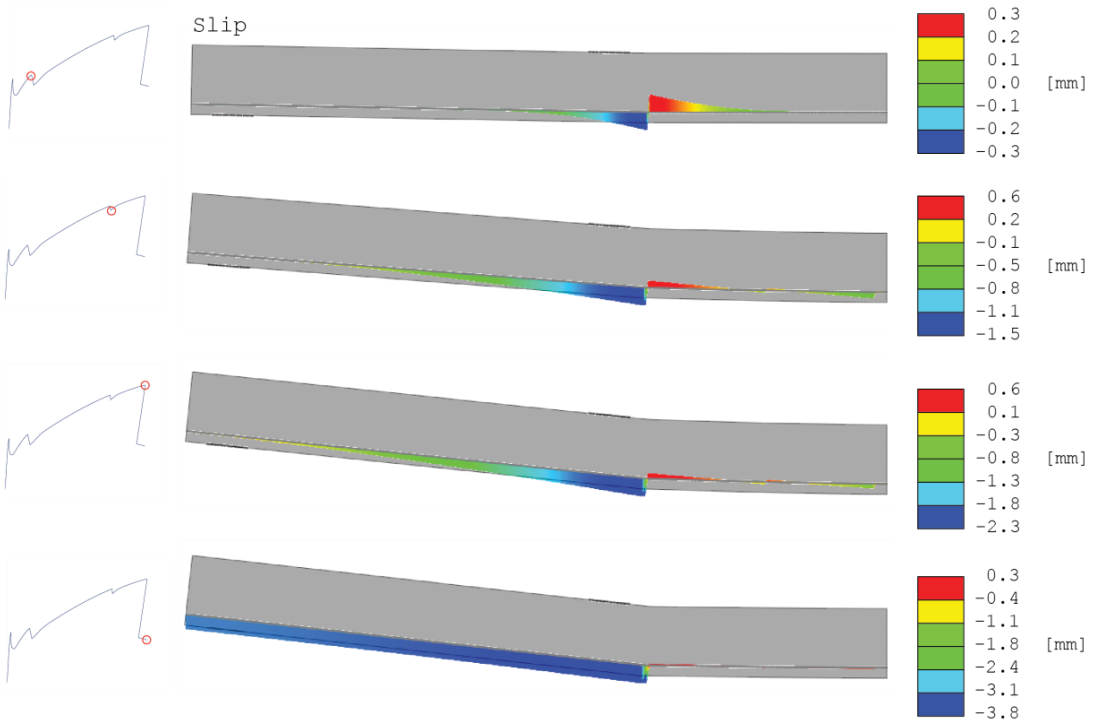

Figure 4-19 FE-results, development of slip

4.2.6 Convergence Study

To ensure that the analysis is sufficiently accurate, convergence studies were performed, both regarding load step size and mesh density. When using smaller step sizes, the model seems to crack at a lower load and displacement. However, the step size of 0.001 mm seems to be sufficient since decreasing the step size to 0.0002 mm does not result in any significant difference (Figure 4-20).

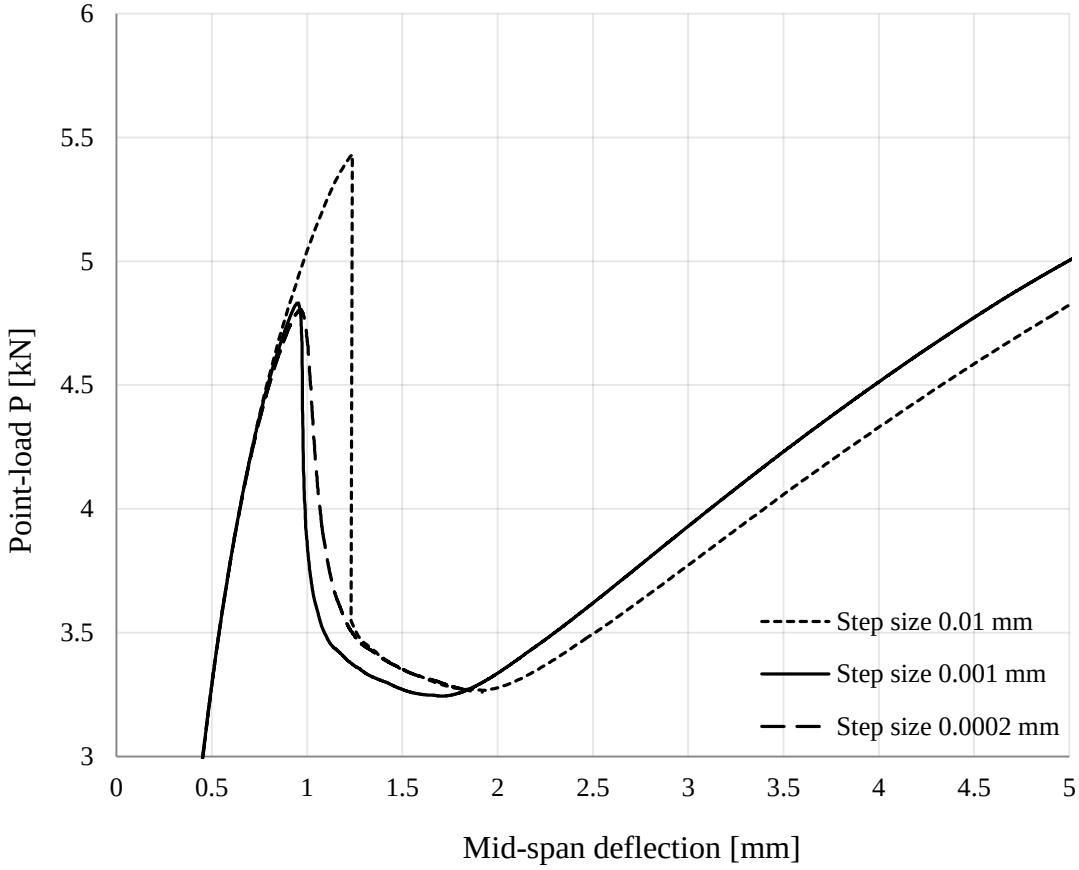

Figure 4-20 Convergence study, step size

As shown in Figure 4-21, when the mesh density increases, the first crack appears at a larger mid-span deflection. Regarding the number of cracks and crack load for the subsequent cracks, no pattern could be found. Overall, the mesh size of 2.5 mm seems to be accurate. The computational time, which is an important factor when choosing element and step size, is also presented in the figure.

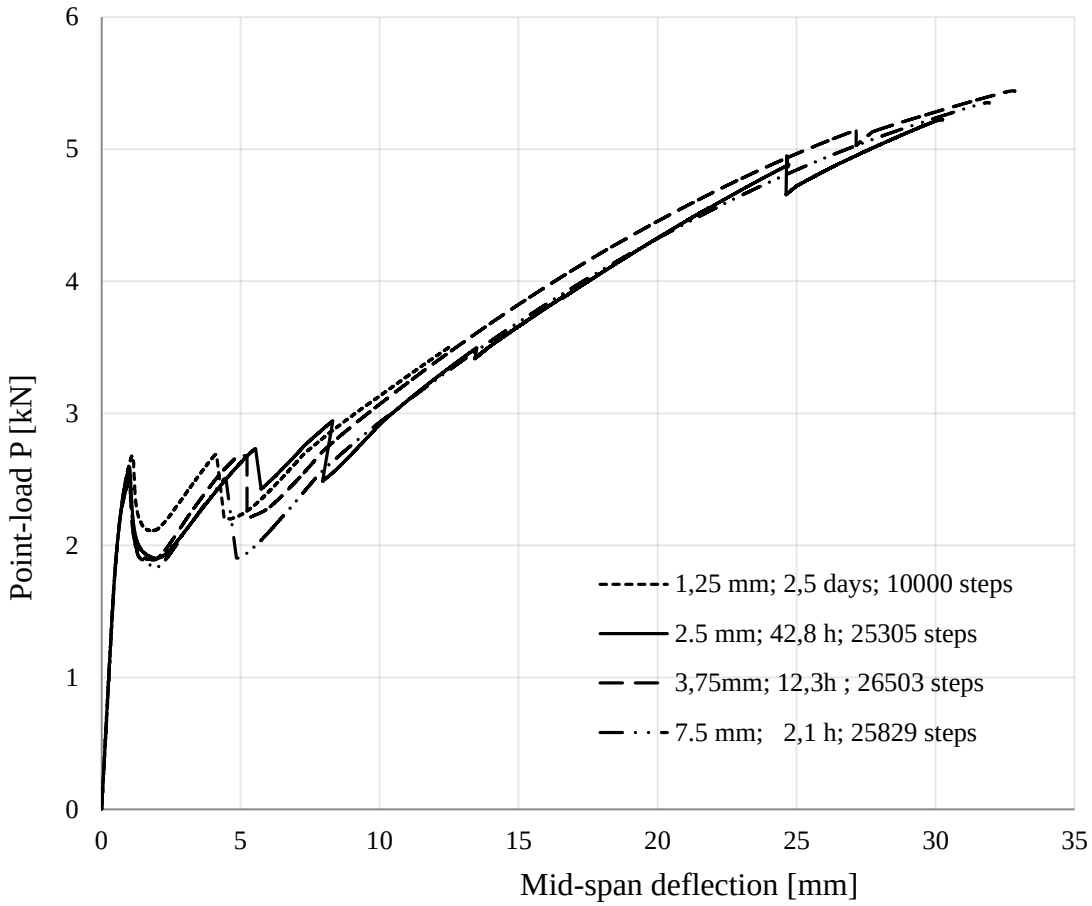

Figure 4-21 Convergence study, mesh size

4.3 Verification and Calibration

When comparing the results from the FE-model to the test results some differences are noticeable. After a similar initial state, the test specimens cracked at a lower load than that obtained from the FE-model. This behaviour seems to depend a lot on which step size that is used, but may also be an effect of stress concentrations. In the cracking phase, the test specimens develop more cracks with a shorter crack distance which may imply that inaccurate bond slip behaviour is used in the FE-model. After the cracking state the results show similar stiffness in all phases. The most obvious difference is that the FE-model can carry higher load.

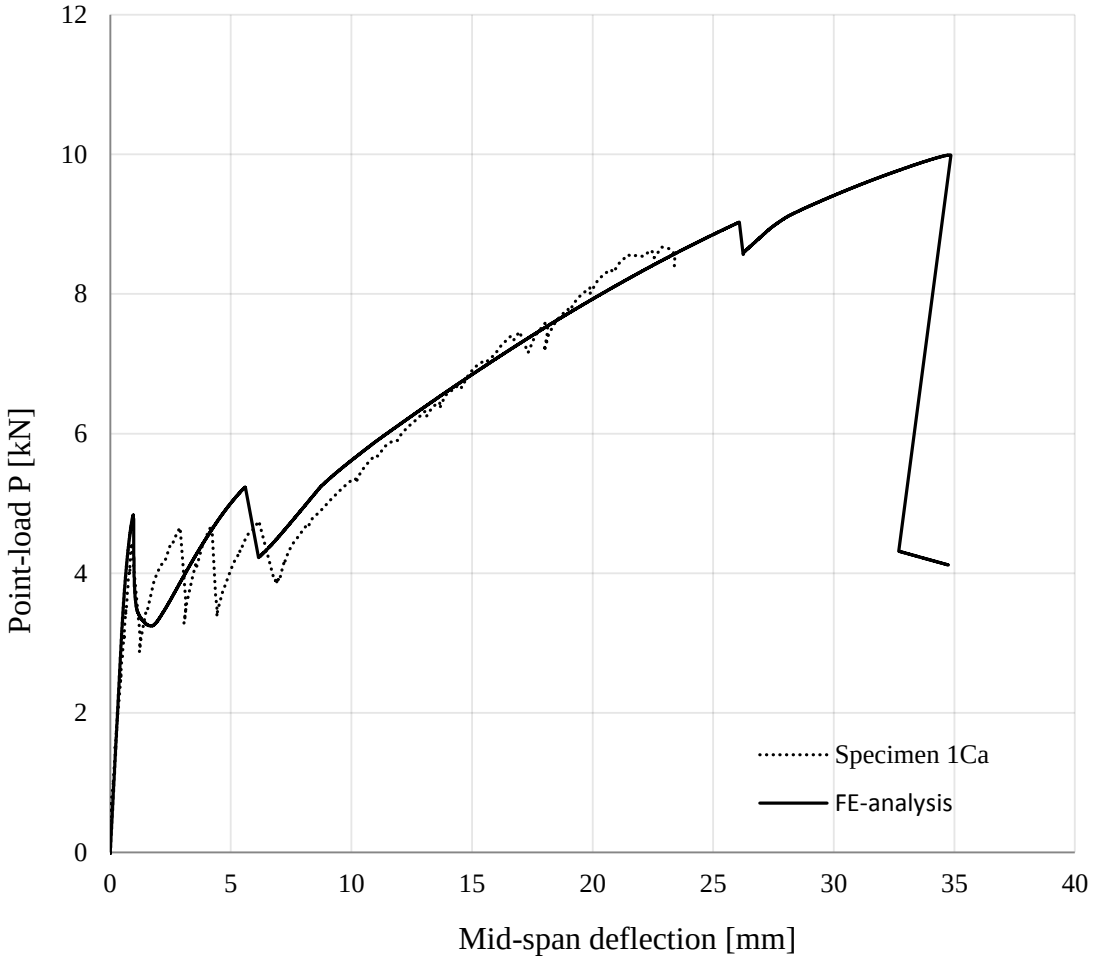

Figure 4-22 Comparison of mid-span deflection to load-curves

The material properties used in the FE-model are primarily retrieved from experiments conducted at DTI or from material producers. The properties typically correspond to the individual materials, i.e. single filament or yarn, textile reinforcement mesh, and unreinforced concrete. Accordingly, these material data do not regard the identical circumstances which exist in the textile reinforced concrete composite and, in turn, their implementation in the model will not necessarily depict the true composite behaviour. To compensate for this, some input data were calibrated based on hand calculations and literature.

4.3.1 Carbon Fibre Tensile Strength

It has been shown in studies that there is a difference between the strength of one filament and the strength of the fibres in a composite member (Brameshuber, 2006). The reason for this behaviour is hard to describe precisely, yet there are some possible reasons which could be discussed. Firstly, the damage of the filament can occur in many steps in the production such as at textile manufacturing, transport, composite manufacturing or by abrasion. Furthermore, as discussed in Chapter 2.3, the stress distribution may be uneven over the cross-section which means that locally the stress will grow higher than the mean stress.

Table 4-3 shows reduction factors for some different tested textile reinforcement meshes presented in Hegger and Voss (2008). Those factors are used to reduce the textile tensile strength no matter how the test specimen failed. It should be noted that these presented efficiency factors could be superior to date due to the rapid development of improved binders and coatings. Nevertheless, since the local bond behaviour is explicitly included in the FE-model, a similar factor was not applied. However, results where tensile stresses are above the maximum tensile stress in the test are regarded with certain caution. According to hand calculations, the test specimen fails with a textile tensile stress of approximately 2200 MPa, or 55 % of its capacity. The capacity above this reduced tensile strength is shown with a grey line in Figures 4-23, 4-24 and 4-27.

Table 4-3 Reduction factors

Fibre	Factor
Carbon	0.19
AR-glass 1, tricot	0.40
AR-glass 2, chain	0.25
AR-glass 3, chain	0.27
AR-glass 4, Epoxy impregnated	0.66

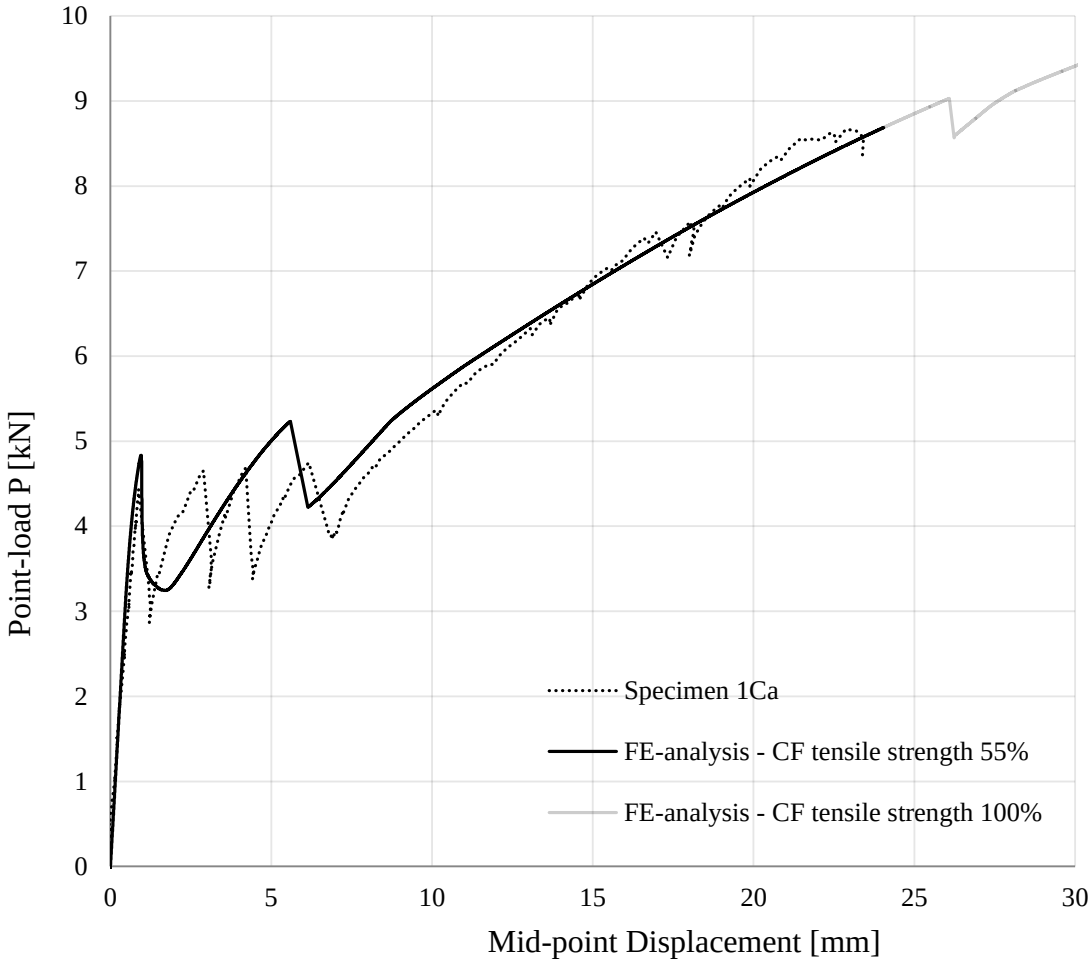

Figure 4-23 Comparison of mid-span deflection to load-curves, reduced textile tensile strength

4.3.2 Bond Slip Relation

The pull-out tests have been performed on a single yarn within a mesh in pure tension. As mentioned before, the bond-slip behaviour is very complex and many parameters can be changed particularly when a TRC member is exposed to bending. A TRC member in bending creates not only tension forces in the reinforcement but also transversal forces between the reinforcement and the concrete because of the developed curvature. Those forces enhance the frictional forces and also the bond especially between the inner filaments. This assertion has been used before to explain the fact that a higher amount of reinforcement increases the capacity of the carbon fibre when the member is subjected to bending. More reinforcement leads to shorter crack distances and more cracks. When this larger curvature is developed, it is followed by larger transversal forces and higher bond strength (Brameshuber, 2006).

Due to the method used to record the displacement measurements, the bond-slip curve (Figure 4-8) is inaccurate beyond the peak. If pure bond failure is assumed in the experimental tests, it indicates that this part of the curve is too flat. Accordingly, a steeper descending part of the curve would lead to a lower energy and an earlier failure.

To determine a sufficient and general bond-slip relation for members in bending, close investigation and testing is needed. Since that lies outside the scope of this thesis a factor is instead chosen to match the FE-results with the test results. A factor of 1.25 allows for a proper fit in terms of the crack number and position and is therefore used in the next steps.

Assuming that the failure was pure bond failure, the increase in bond means that the ultimate capacity will increase, and make the mismatch between experimental and numerical results even bigger. This, in turn, either means that the bond stress-slip relation is not accurate or that the bond mechanism is more complex than pure bond failure.

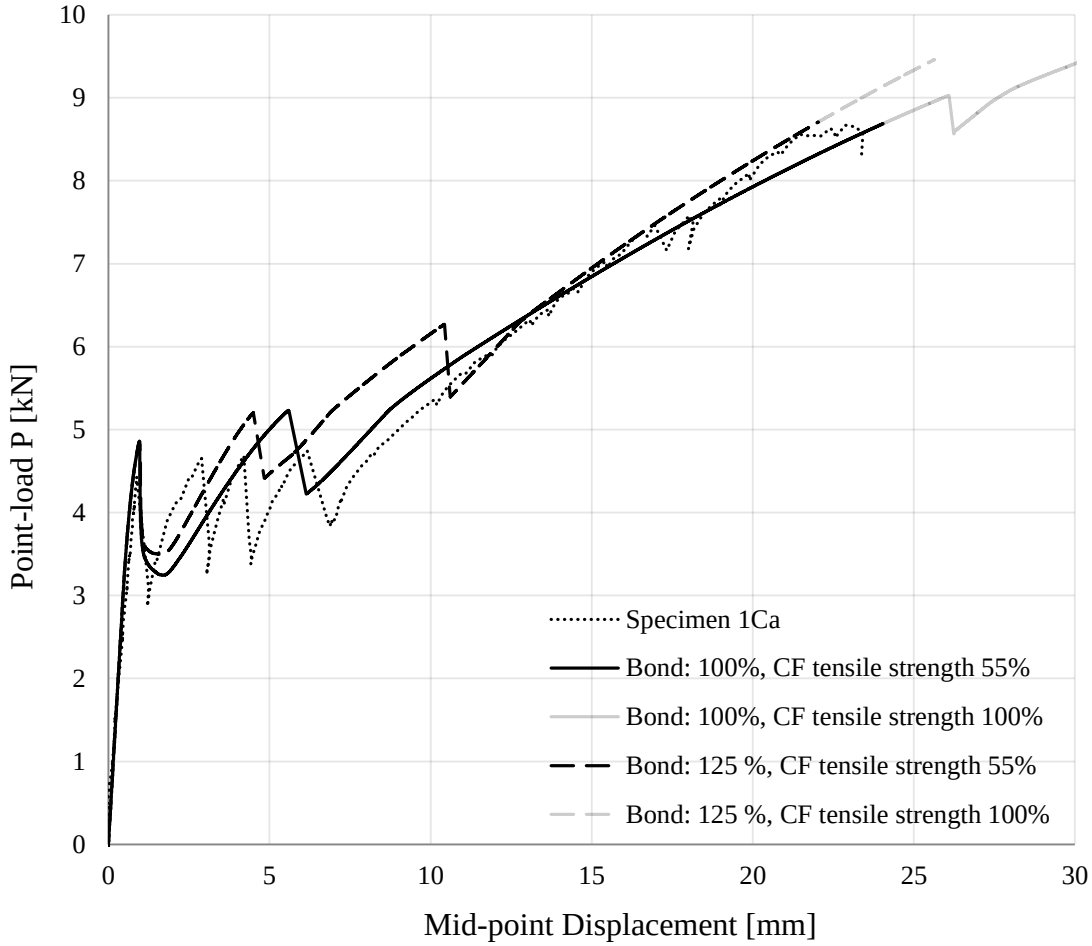

Figure 4-24 Comparison of mid-span deflection to load-curves, increased bond

4.3.3 Concrete Tensile Strength

As can be seen in Figure 4-22 the cracking load is somewhat higher in the FE-model, which can depend on some different parameters. Firstly, it is assumed that stress concentrations, shown in Figure 4-26, appear around the transversal yarns. In Figure 4-25, it is clearly presented for one of the test specimens how the first three cracks appeared right below the transversal yarns. These irregularities could either be modelled or considered as a reduction in concrete tensile strength. In addition, stresses from shrinkage were not considered in the model, which could affect the cracking

load. Lastly, the tensile splitting test may not be the most accurate way to test the tensile strength and may result in a overestimated capacity due to biaxial stresses (Domone and Illston, 2010). To compensate for those factors, the concrete tensile strength was reduced from 4.7 to 4.2 MPa (-10 %) in the FE-model.

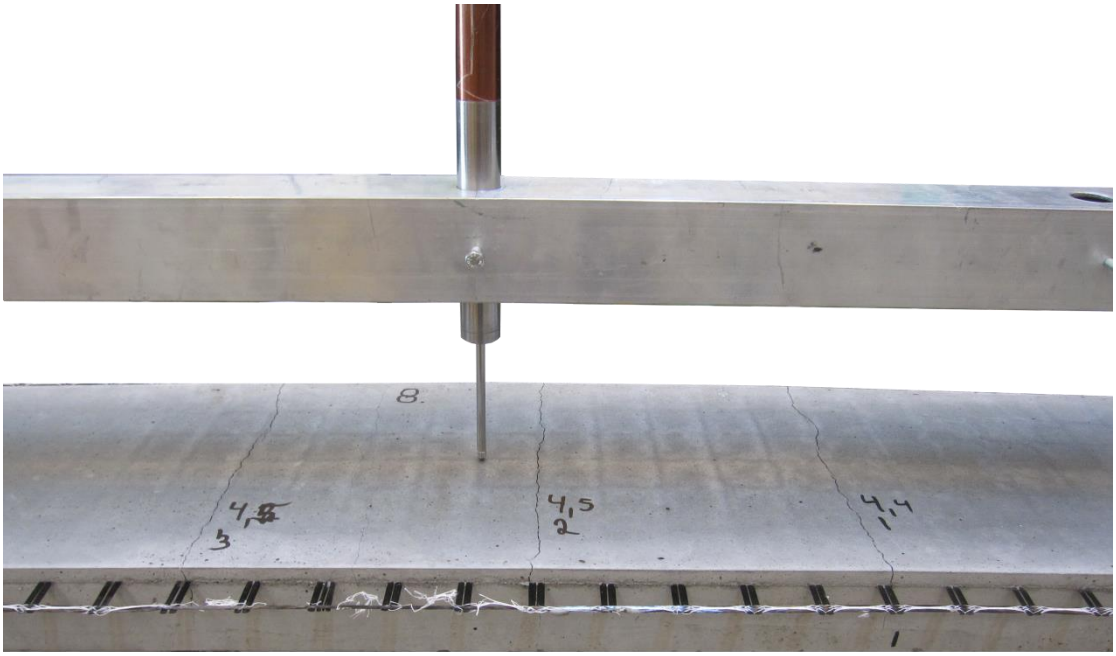

Figure 4-25 Crack positioning

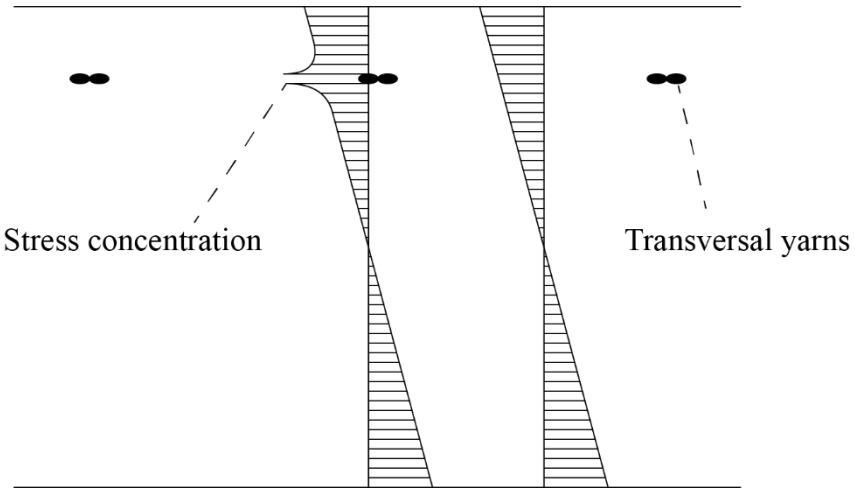

Figure 4-26 Stress concentration around transversal yarns

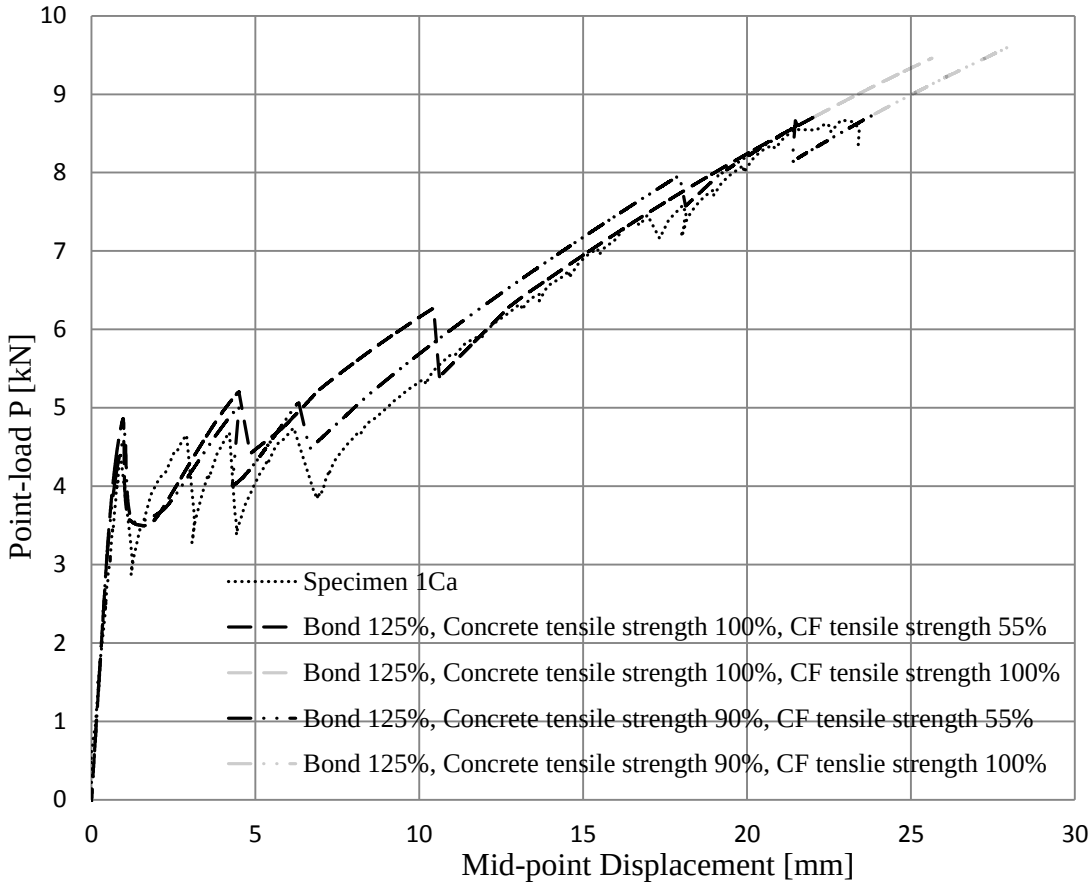

Figure 4-27 Comparison of mid-span deflection to load-curves, reduced concrete tensile strength

Table 4-4 Summary of crack load and ultimate load

Test specimen	Load at first crack [kN]	Ultimate load [kN]
Experimental work		
1Ca	4.4	8.6
1Cb	4.4	8.5
1Cc	4.2	8.4
FE-analysis		
Initial properties	4.8	10
Calibrated properties	4.6	10+

5 Design of Outer TRC-layer in Façade Element

Based on the benchmark model in Chapter 4, a FE-model was built to design an outer TRC layer in a façade element. Firstly, a 2D-model was created to ensure that the designed member reaches requirements regarding deflections and ultimate capacity and that it has sufficient capacity after cracking. Then, the member was analysed linearly in 3D to follow the linear behaviour in two-way action. Finally, stresses, strains, crack patterns and crack widths were evaluated in 2D for the most promising design in ultimate limit state.

5.1 Design Parameters

There exists numerous ways in which a façade element can be designed, TRC could be beneficial in many of these design solutions e.g. as layers of a prefabricated sandwich element or in an uninsulated glass/concrete façade. A sandwich element design was chosen with an inner, thick layer of steel reinforced concrete (200 mm), a mid-layer of EPS (200 mm) and a thin outer TRC layer (varying thickness). The inner concrete layer was assumed to carry the vertical loads and to be very stiff compared to the outer layer. The governing load case was assumed to be when no shear interaction between the materials occurs and that the outer layer is pinned along all edges to the inner layer. However, the 2D façade element model works, by definition, in one-way action which means that the element is solely supported on two edges only (i.e. top and bottom). The size of the element is 3000 x 7000 mm (H x B) as illustrated in Figure 5-1 which is demanded by producers.

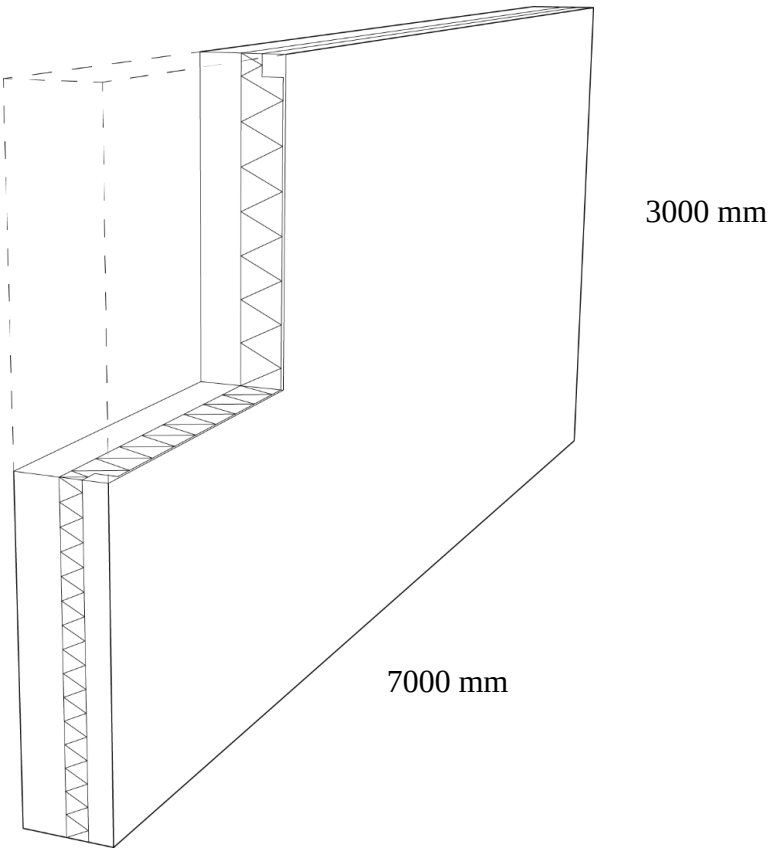

Figure 5-1 Design of façade element

Besides the end connections, the two concrete plates can be connected with intermediate fasteners casted into the structure. Those will shorten the span length and thus, make it possible to decrease the thickness of the outer concrete layer. In a first stage, a number of different thicknesses and four support conditions were analysed and evaluated regarding stiffness, cracking load and post cracking behaviour. For the most adequate solutions, further investigation of stresses and bond behaviour was performed. The different design variations are presented in Table 5-1.

Table 5-1 Design alternatives

Number of intermediate fasteners	Number of textile layers	Thickness of TRC layer			
0	2	40 mm	35 mm	30 mm	-
1	1	20 mm	18 mm	15 mm	-
2	1	15 mm	12 mm	10 mm	8 mm
3	1	10 mm	-	-	-

The stiffness of the intermediate fasteners depends on the materials and the design of the connection. In this case, the stiffness is analysed to give the lowest possible moment and a limit where the deflection of the element does not exceed L/250. Analyses performed in MATLAB (see Appendix B) showed that no real benefits could be achieved by searching for an optimal stiffness of the intermediate fasteners. However, the solutions that minimized deflections and span moments were both found when the stiffness was close to infinite such that the fasteners should therefore be made as stiff as possible.

In the cases with two or more intermediate fasteners, the optimal position was calculated linearly to minimize the deflection, span moment or support moment resulting from the applied wind load (Appendix C). This position was calculated with pinned end supports. In Figure 5-2 it is shown that the positioning for minimum deflection and minimum span moment matches while the positioning for optimized support moment differ. The three solutions were plotted together with a solution having evenly distributed fasteners. For this design, positioning is chosen to minimize the deflection and span moment.

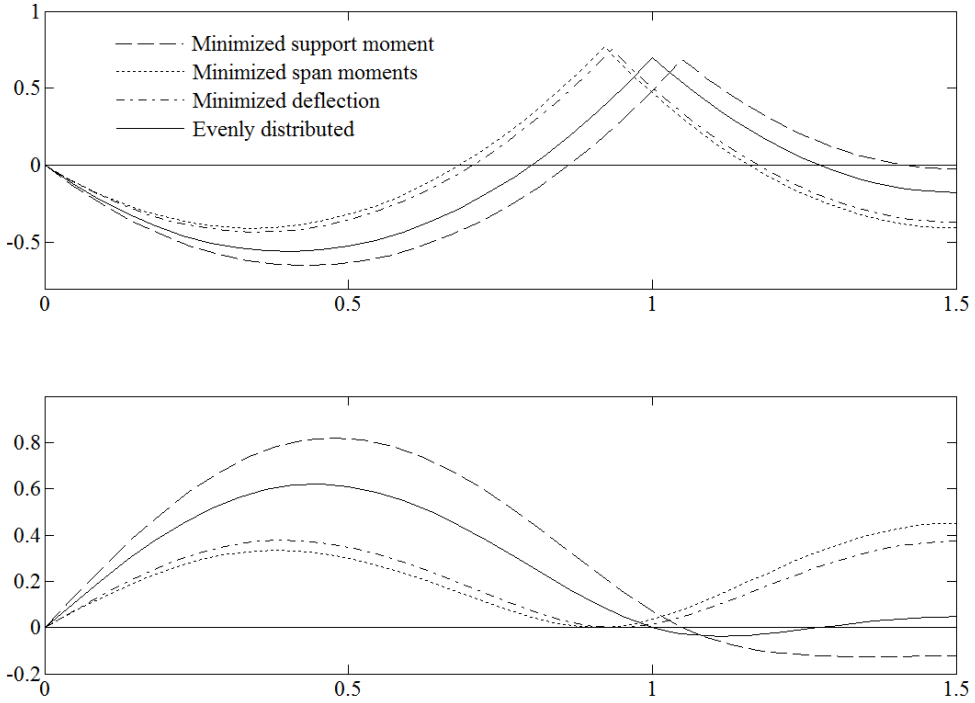

Figure 5-2 Optimization of intermediate fastener position

Furthermore, to determine the wind loads for the façade elements, a fictive building was considered. The chosen building is a rectangular, 10 story high, flat roofed residential house with dimensions 12 x 24 x 30 m (B x L x H) located at the seaside in Gothenburg, Sweden. As mentioned before, only wind loads were analysed in this thesis. The ULS load was determined as 1.70 kN/m^2 in pressure and 2.47 kN/m^2 in suction according to Eurocodes (Appendix D) which is referring to the worst case scenario as shown in Figure 5-3.

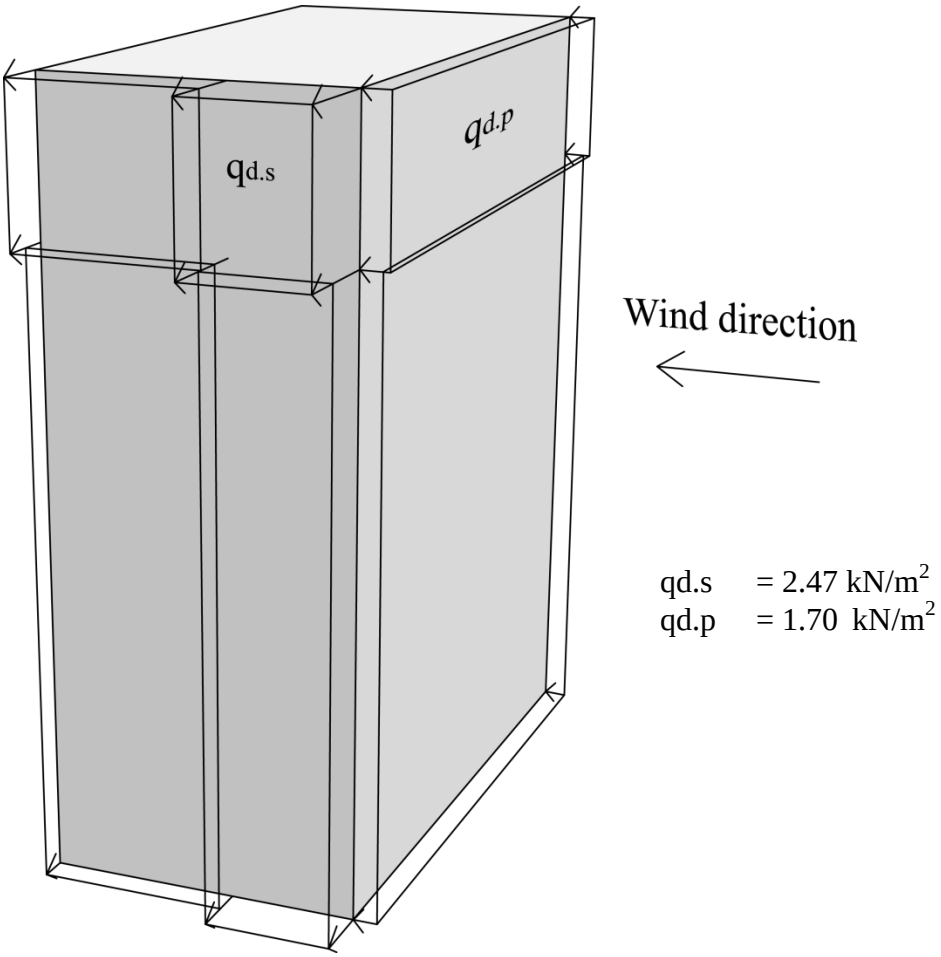

Figure 5-3 Wind load according to fictive building scenario

5.2 2D FE-model

In the 2D FE-model, a 1 m wide strip of the 3000 x 7000 mm element was analysed in one-way action. As the inner concrete layer is assumed to be much stiffer, the TRC layer is modelled with rigid supports. The way of modelling was overall very similar to the modelling described in Chapter 4.2. The element types, mesh size, the way of model cracking and the interaction between the two materials were unchanged while the material input was changed according to Chapter 4.3. The element size was chosen depending on the thickness of the plate with ten elements over the width of the plate. The boundary conditions were modelled in a similar way but the loads were modelled differently because of the altered loading situation.

5.2.1 Boundary Conditions

The support boundaries were modelled in the same manner as in Chapter 4. The support node was prevented in the x-direction and then tied to the neighbouring nodes. Again a dummy beam was used to add rotational DOF for the tying. Also the symmetry condition was modelled in almost the same way as in Chapter 4. The difference here was that the symmetry condition was dependent on the number of intermediate stiffeners. Illustrations of the different boundary conditions are shown in Figure 5-4.

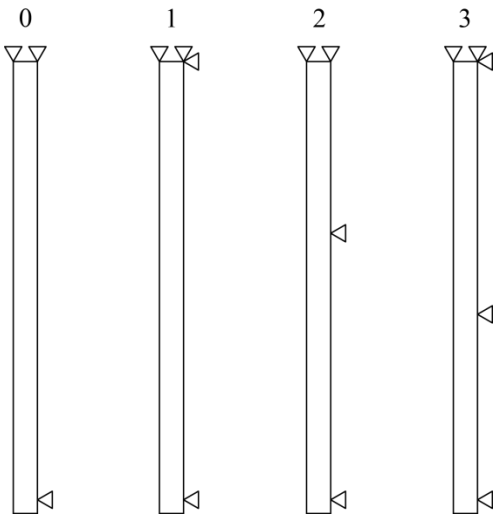

Figure 5-4 Prescribed boundary conditions

5.2.2 Loads and Analysis Method

Since the member is vertically positioned, the self-weight is not regarded and only wind load is acting on the façade element. Unlike in Chapter 4, the displacement pattern is unknown and the load needed to be applied as a force. The wind load was recalculated from a surface load to a line load of 2.47 kN/m and applied on the outer edges of the outer elements. To be able to follow the load-displacement behaviour the load was applied in steps and the solution was controlled by the arc length method.

5.2.3 Load to Mid-point Deflection

All design variations show similar trends regarding deflection versus load behaviour. To evaluate the results, the behaviour was plotted together with the ULS-load, SLS-load and the deflection requirement (L/250) in Figures 5-5 to 5-8.

The design without intermediate fasteners results in large deformations and the thickness, 40 mm, needed to reach the requirements is considered too large to be a competitive solution. Since the possibilities for thin members are the largest advantage for TRC, this design was not further investigated.

The design with one intermediate fastener and a thickness of 18 mm seems to have sufficient stiffness and load bearing capacity to reach the requirements as depicted in Figure 5-6. Since 18 mm is significantly thinner than a steel reinforced concrete plate according to Chapter 3.4, the design is considered reasonable. The thinner element with a thickness of 15 mm does not reach the deflection requirements.

With two intermediate fasteners, the thickness of 12 mm was observed to be most promising. Even a thickness of 10 mm meets the deflection requirement but with a very small margin. The latter solution is also thought to be problematic in terms of production to some extent. The same applies for the 10 mm thick layer with three supports, even though it easily reaches the requirement.

Accordingly, the alternative with 2 fasteners and a thickness of 12 mm is chosen for further analysis in Chapter 5.3 and 5.4.

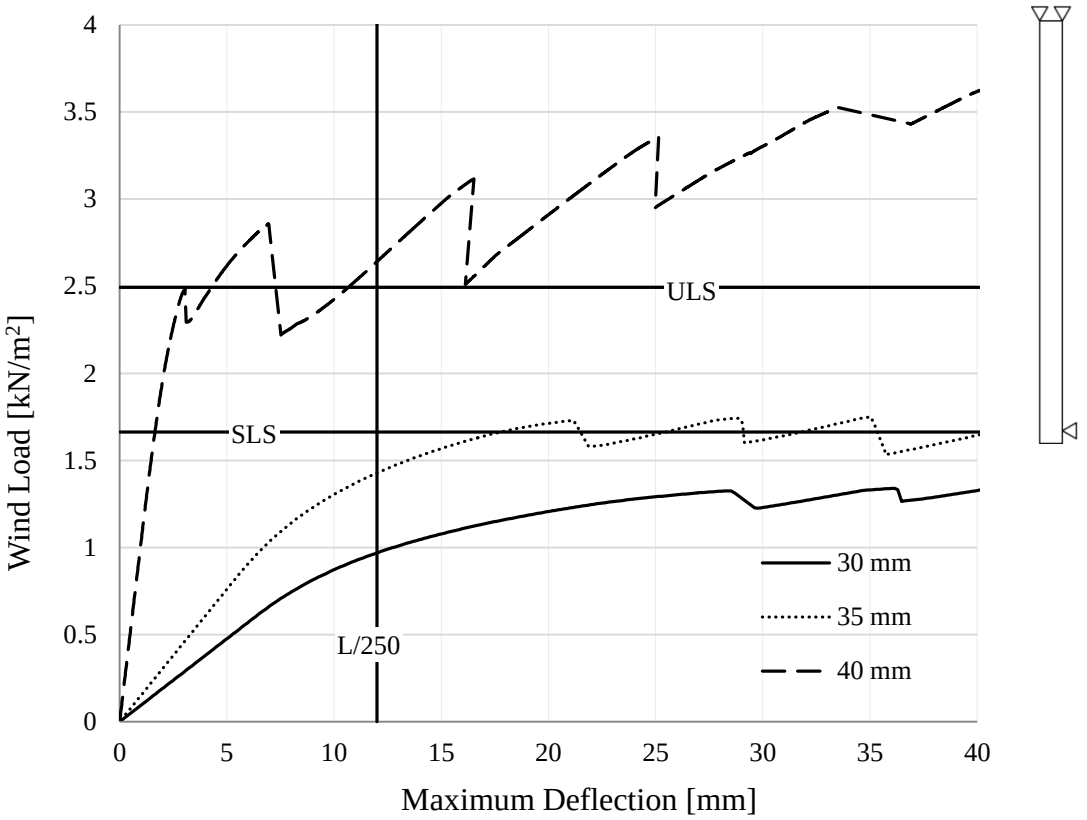

Figure 5-5 Maximum deflection to load-curves, no intermediate fasteners

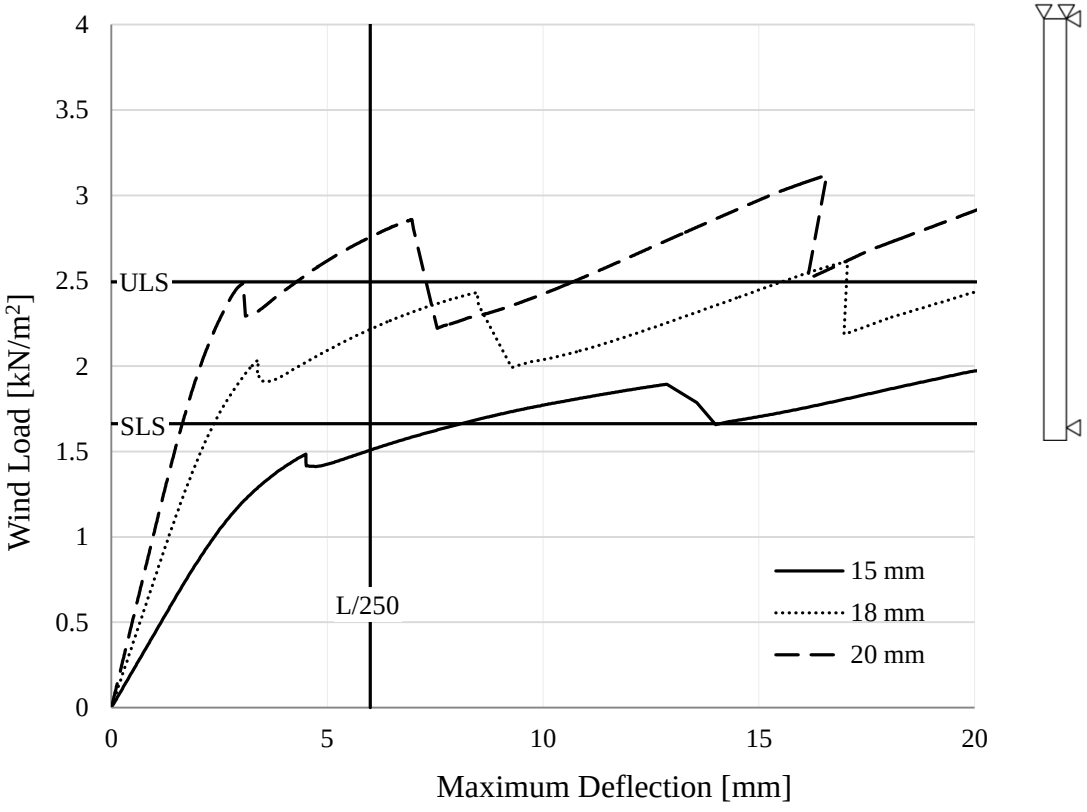

Figure 5-6 Maximum deflection to load-curves, one intermediate fastener

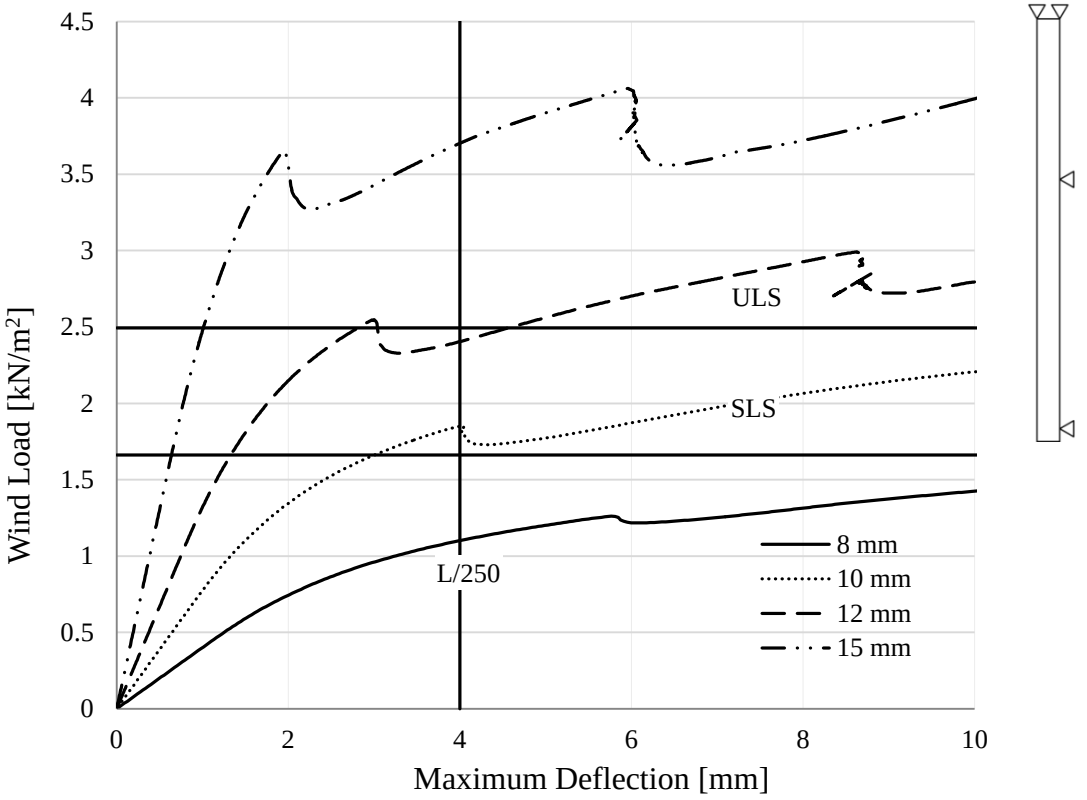

Figure 5-7 Maximum deflection to load-curves, two intermediate fasteners

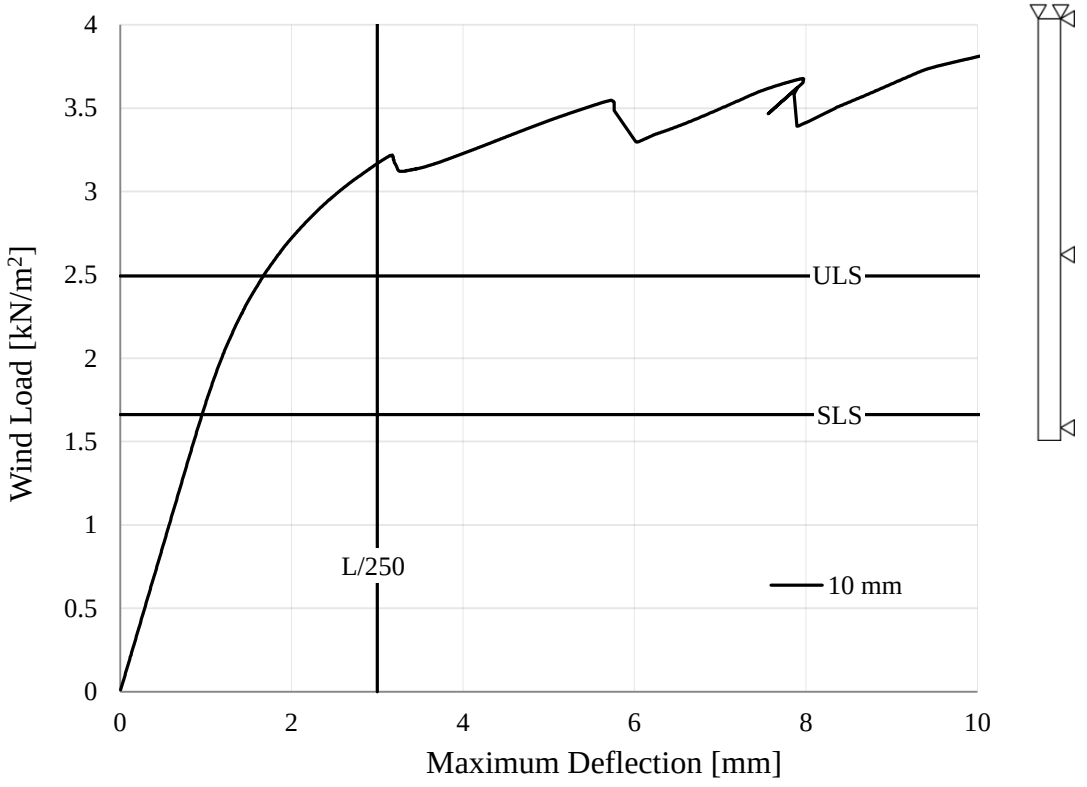

Figure 5-8Maximum deflection to load-curve, three intermediate fasteners

5.2.4 Behaviour at Reloading of a Cracked Element

Once a façade element is loaded until cracking, it loses stiffness and will behave according to this stiffness next time it is exposed to loads. Accordingly, the deflection will exceed the limit before the load reached SLS. Figure 5-9 shows the behaviour when one and two cracks have developed in the case with one intermediate fastener and a TRC panel thickness of 18 mm.

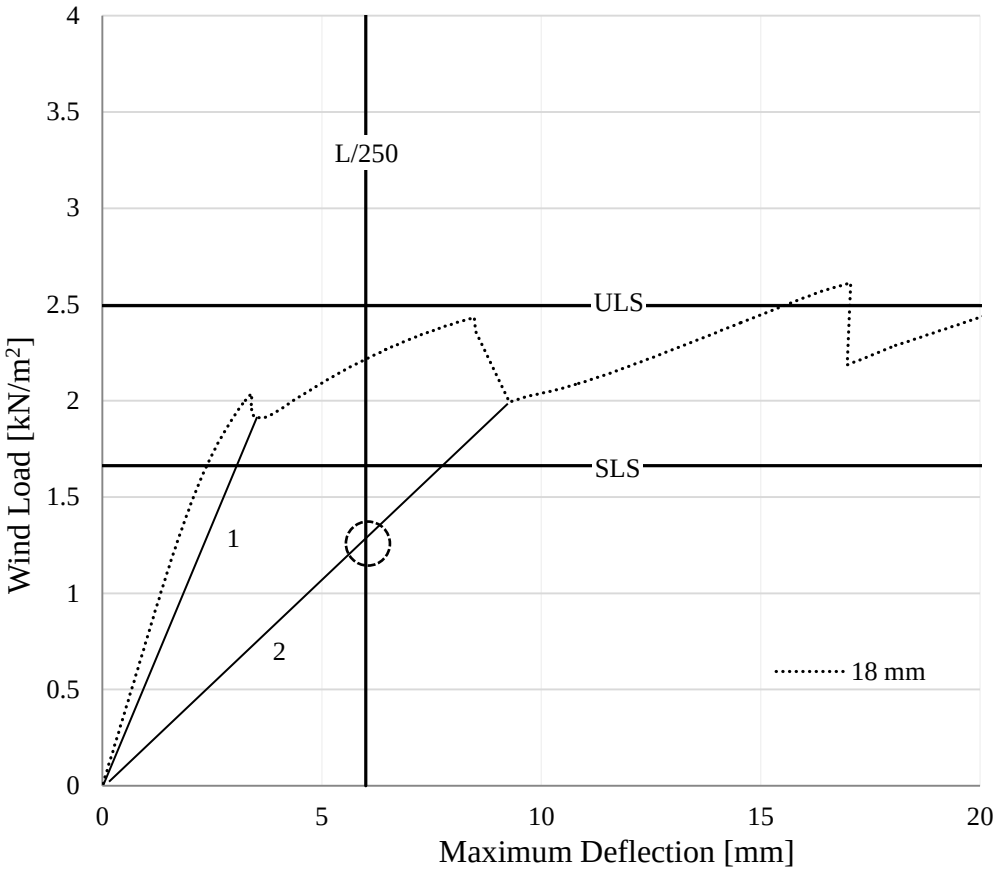

Figure 5-9 Behaviour at reloading

From Figure 5-9, the first unloading/reloading (curve 1) indicates the unloading behaviour of the element after the occurrence of one crack which is marked by a slight loss of stiffness. Subsequently, when the element is reloaded it follows curve 1 and will still fulfil the requirement. However, if the element is loaded until the second crack and then unloaded according to curve 2, the significant loss of stiffness does not allow the element to meet the requirements upon reloading. The fact that the structure reaches the requirements in an uncracked state but not in a cracked state is an issue that needs to be discussed with the client. The requirement can either apply for both uncracked and cracked members or different requirements can be set.

5.3 2D Versus 3D Modelling

From the 2D-analysis, the deflections are obtained by modelling the intermediate fastener as a constraint at a single point, like a continuous beam. When extruding to three dimensions, this point constraint becomes a line constraint. Instead of having fasteners along the whole line, it may be favourable, in terms of production and costs, to have only a few, like a flat slab. To analyse the behaviour when changing this line constraint to a couple of point constraints, a 3D-model was created for the design with two intermediate supports and a thickness of 12 mm. This was chosen as the most promising design because of its reasonable thickness and number of fasteners. Thinner elements were assumed to be problematic in production and the number of fasteners was kept as low as possible.

With the positioning of the intermediate stiffeners optimized to minimize the moment and constraints as in Figure 5-10, the moment distribution and deflection looks as in Figure 5-11.

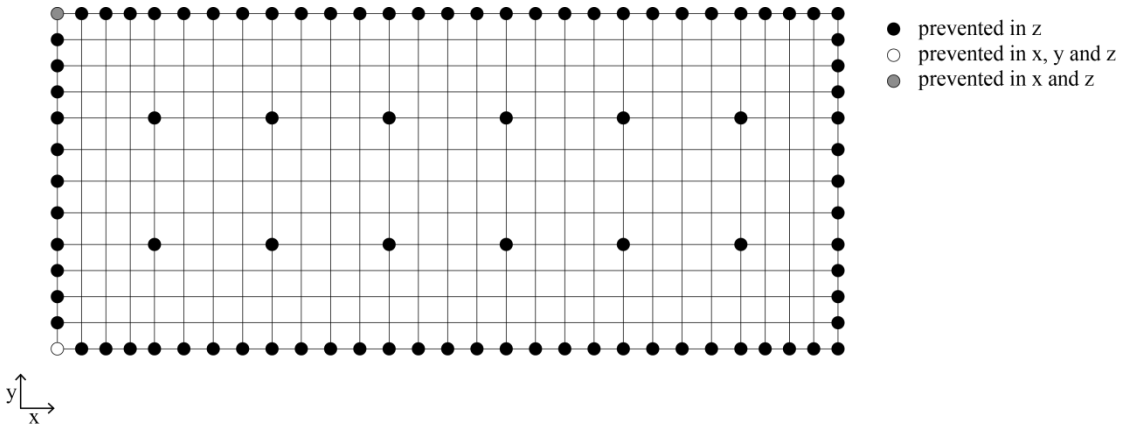

Figure 5-10 Boundary conditions

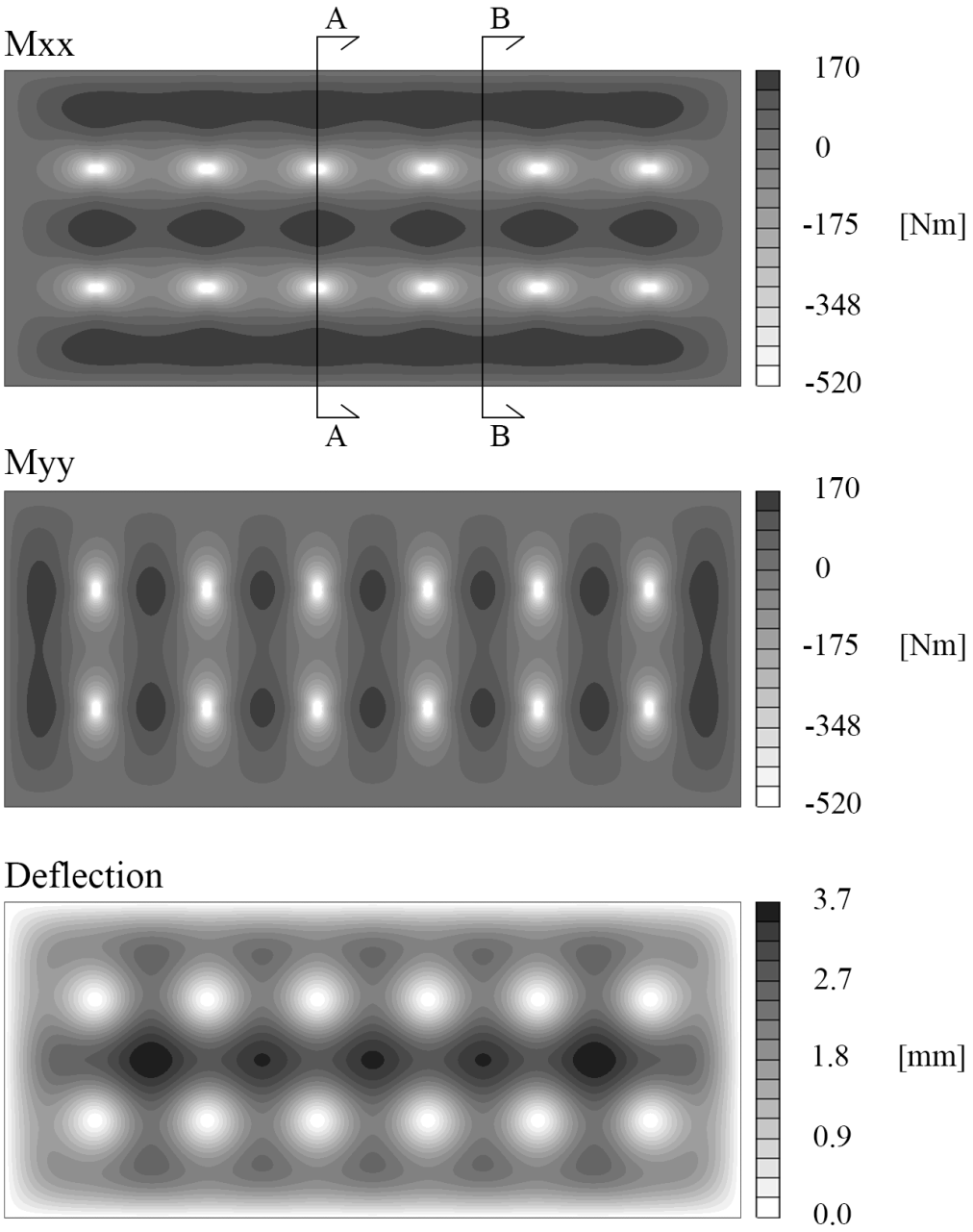

Figure 5-11 Moment and deflection from 3D-analysis

The 3D-model was analysed linearly with the ULS load. From this model, results in terms of moments and deflections were extracted for a section through a line of support points (section A-A) and a section between two lines of support points (section B-B). Those moments were then compared with the results obtained in the 2D-model. The results (Figure 5-12) show, as expected, that the 2D-results are a mean value of the results from the two sections in the 3D-model. Depending on possibilities for moment redistribution, this may not be regarded when checking the ultimate capacity.

When using FEM for analysis of continuous beams or slabs, singularities will appear over the supports. Smaller elements give a larger peak moment. To reduce this peak moment to a reasonable value, the moment at the edge of the support can be used as an estimated design value (Plos et al., 2012). This was implemented in the calculations with an assumed width of the intermediate fastener, see Figure 5-12.

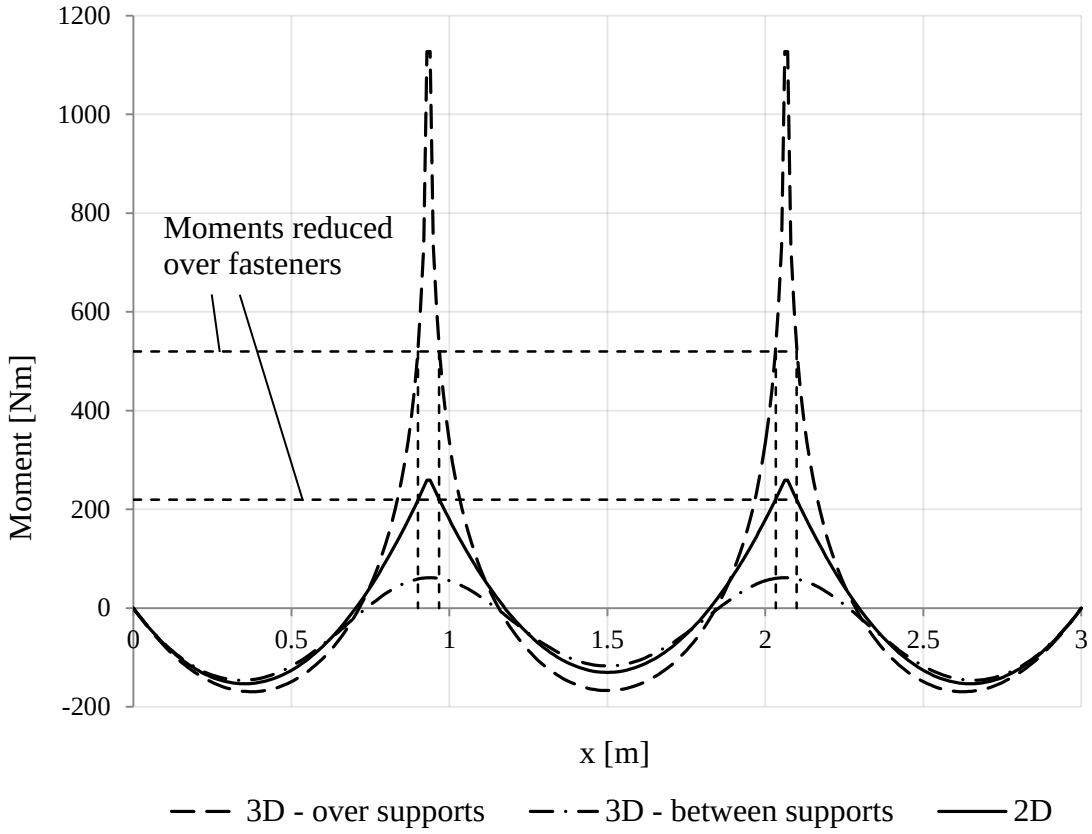

Figure 5-12 Comparison of moments in 2D and 3D

5.3.1 Moment Redistribution

The ability to redistribute forces is an important property of concrete structures. The needed amount of reinforcement decreases and the structure shows a more ductile behaviour. The redistribution occurs when a highly stressed section loses stiffness which, in steel reinforced members, happens when the steel is yielding. Since carbon fibre does not have the same yielding properties, the redistribution must occur in another way. Based on the results from the numerical analysis it is assumed that TRC can redistribute forces by the low bond stress capacity to tensile strength ratio. When the bond stress reaches the peak in the previously shown Figure 4-8, the section loses stiffness and the stresses redistribute to stiffer parts.

5.4 Stresses and Strains in ULS

It is depicted in Figure 5-12 that without any moment redistribution, the maximum moment is approximately 2.2 times higher in the linear 3D analysis. With the assumption that the difference will be similar in a non-linear analysis, the stresses are extracted both for the ULS load and for a load where the moment is 2.2 times larger than the ULS moment. Since the results from the 2D model indicate that the member has not yet cracked in ULS, the ULS moment is taken as the moment where the load crosses the ULS load after the crack. The two points are shown in Figure 5-13 and the corresponding results in Figures 5-14 to 5-18. If moment redistribution is possible, the true moment and stresses will lay between those results.

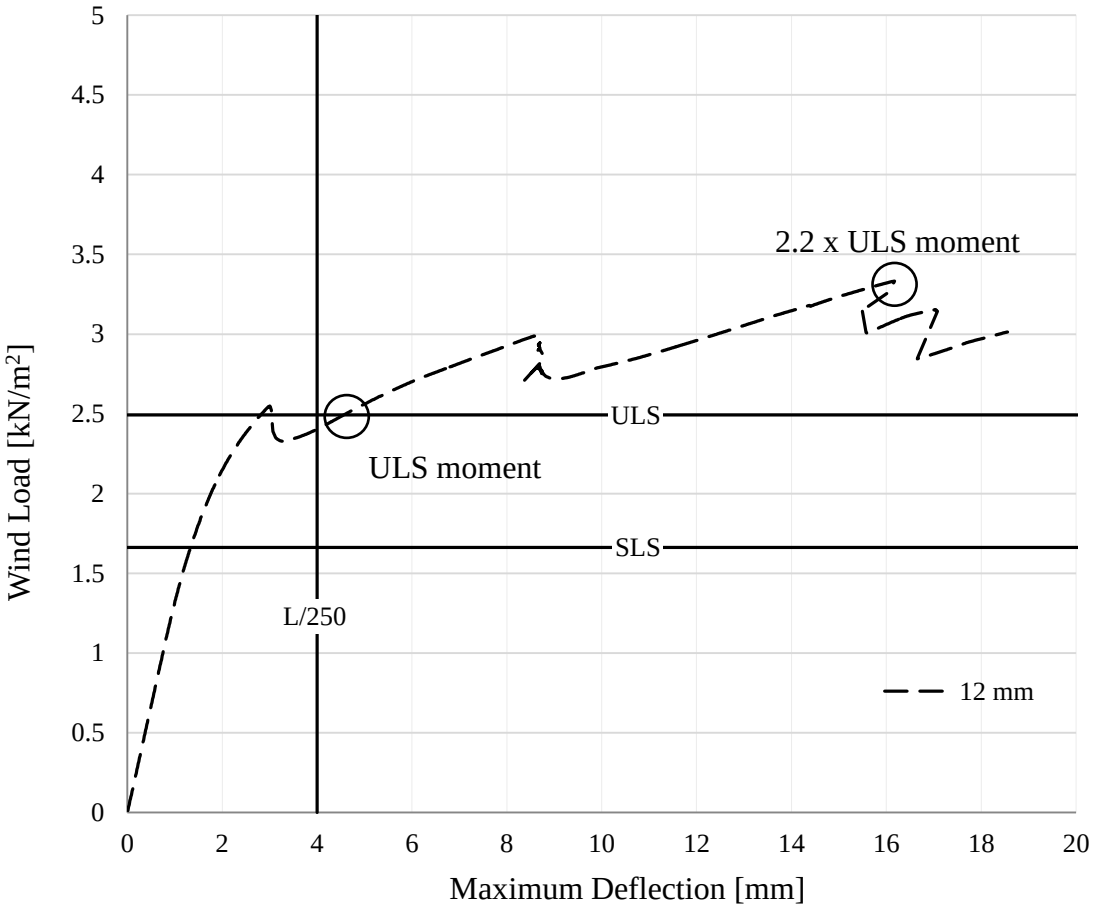

Figure 5-13 Points used when checking stresses and strains

The results show that the tensile force in the textile mesh lies between 359 and 775 MPa and the concrete compressive stress between 76 and 113 MPa. As described in Chapter 4.2.5, the compressive stress shown in Figure 5-16 is for one single node and the element mean stress is still below the capacity. However, the element size around the compressive zone is assumed to be too large to give a reliable result. To analyse the compressive zone closer, a finer FE-mesh is needed. Furthermore, the bond stress has reached its peak stress around the crack but has still sufficient bond. In Chapter 5.5.2 it is discussed what would happen if the crack appeared closer to the edge. The crack width is in the worst case calculated to approximately 0.25 mm. It should be noted that the deflections in Figures 5-14 to 5-18 are differently scaled (x 16 for ULS and x 4.5 for 2.2ULS, respectively).

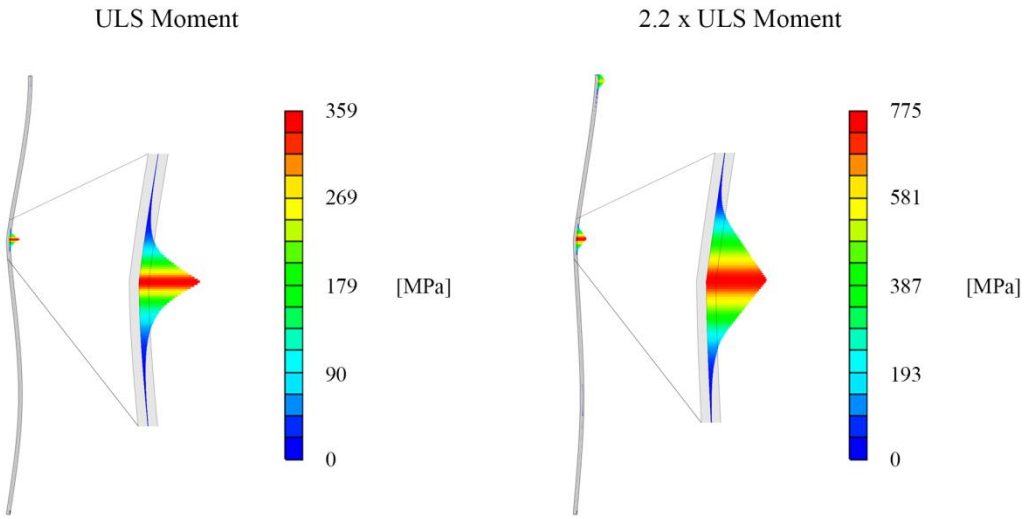

Figure 5-14 Reinforcement stress

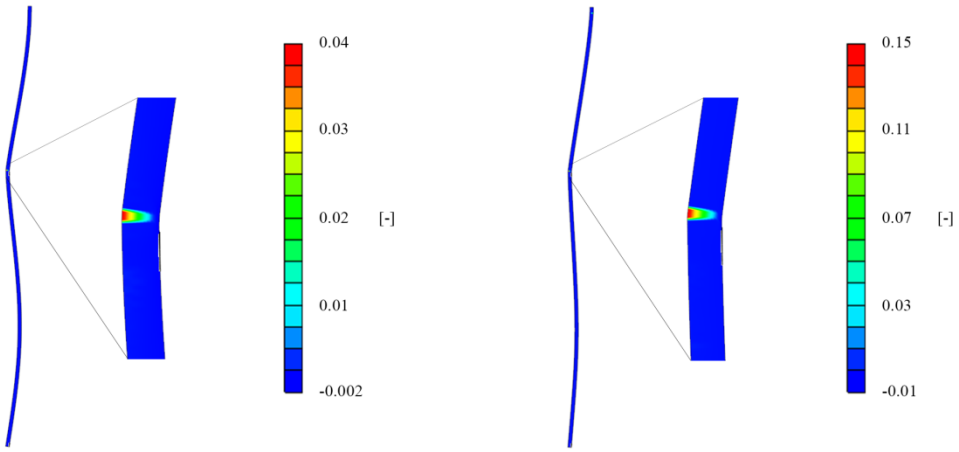

Figure 5-15 Concrete strain

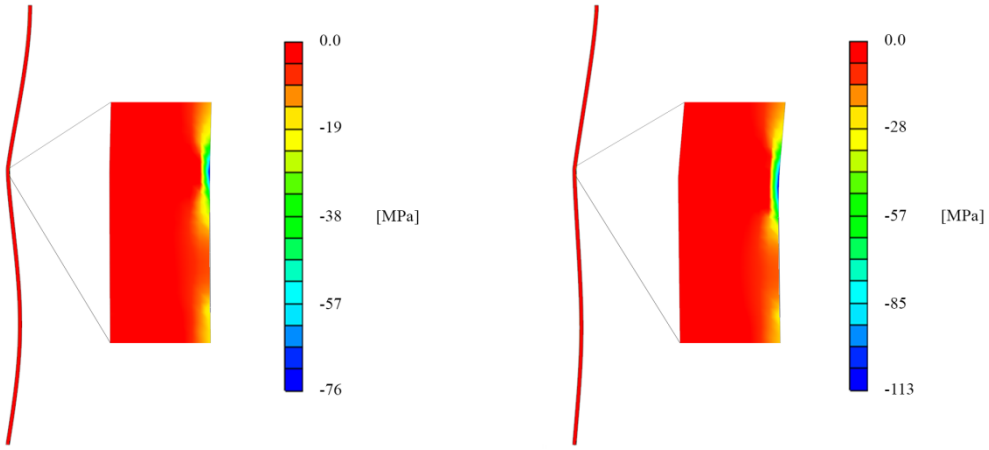

Figure 5-16 Concrete stress

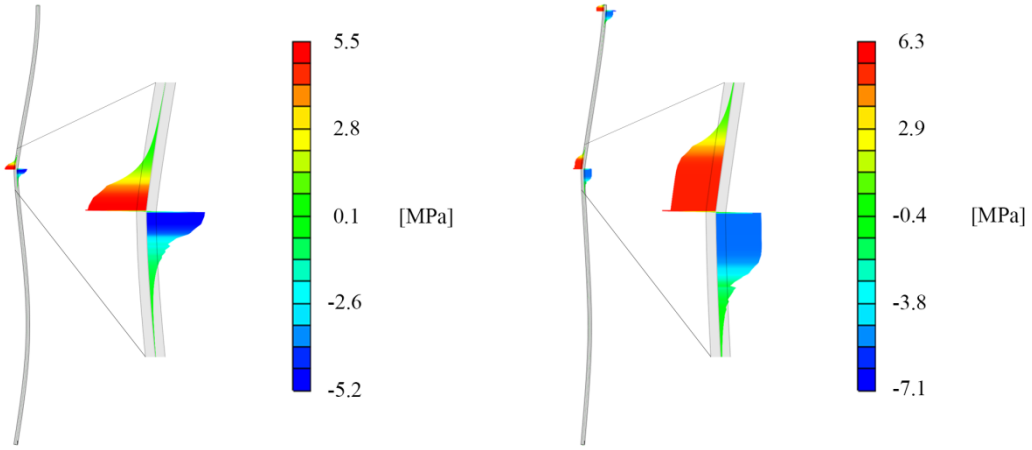

Figure 5-17 Bond stress

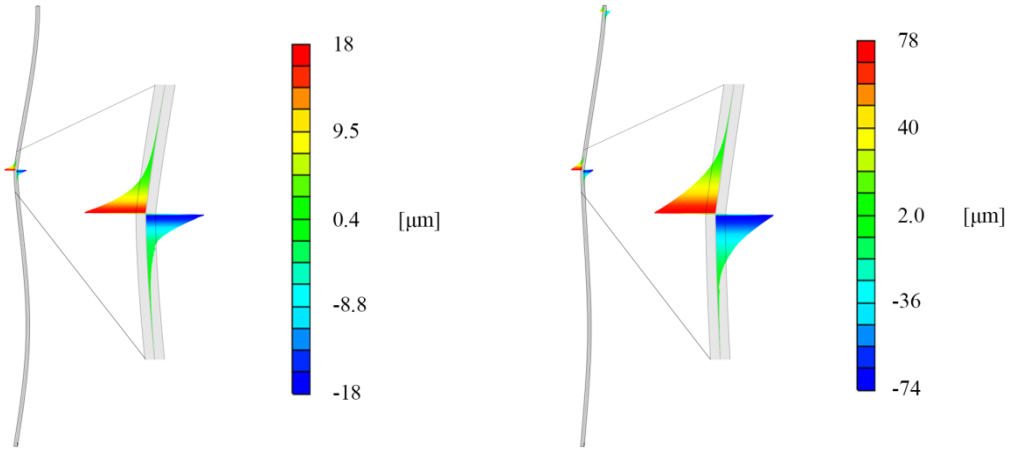

Figure 5-18 Slip

5.5 Critical details

Consideration has to be taken to details in the design of a façade panel. Usage of textile reinforced concrete may lead to a different behaviour than if the panel were to be reinforced using regular steel. Design of details lay outside of the scope of this thesis but an effort to identify the most critical details, based on the results from the numerical analyses, is made in this chapter.

5.5.1 Intermediate Fasteners

The intermediate fasteners could be faced by a number of different actions. The fastener will be exposed to a bending moment resulting from the wind load, as well as shear forces that need to be transferred to the supporting inner concrete layer. Depending on the thickness of the panel this section will be more or less critical. If the thickness of the TRC layer has to be significantly increased at the intermediate fasteners, the insulating performance may be reduced. The effects of these thermal bridges should be assessed and quantified.

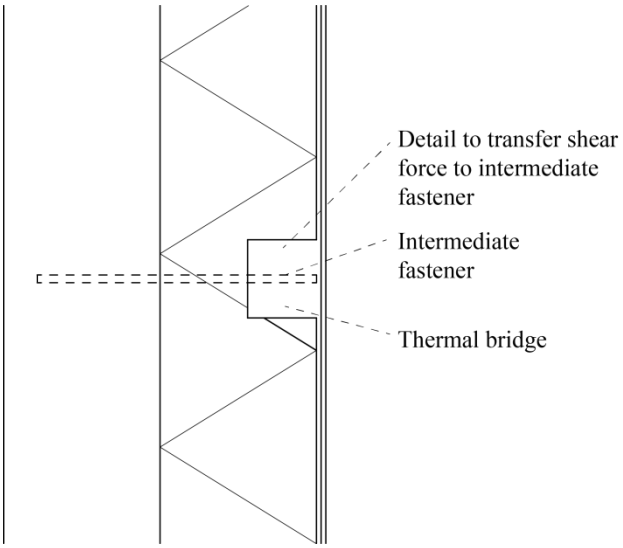

Figure 5-19 Intermediate fastener

5.5.2 End Supports

In the analysis performed, the end supports have been assumed as simply supported. However, depending on production and detailed design this could vary. If the rotation of the end supports is prohibited to some extent, a bending moment could cause the section to potentially crack. As such, the anchorage length could be insufficient and will need to be provided in a similar manner as suggested in Figure 5-20. Since the reinforcement must be bent around the corner to provide sufficient anchorage, the effect of bending carbon fibre yarns must be investigated regarding e.g. the tensile capacity. How the curvature of the yarn is to be controlled and limited to an acceptable value is a subject for further development.

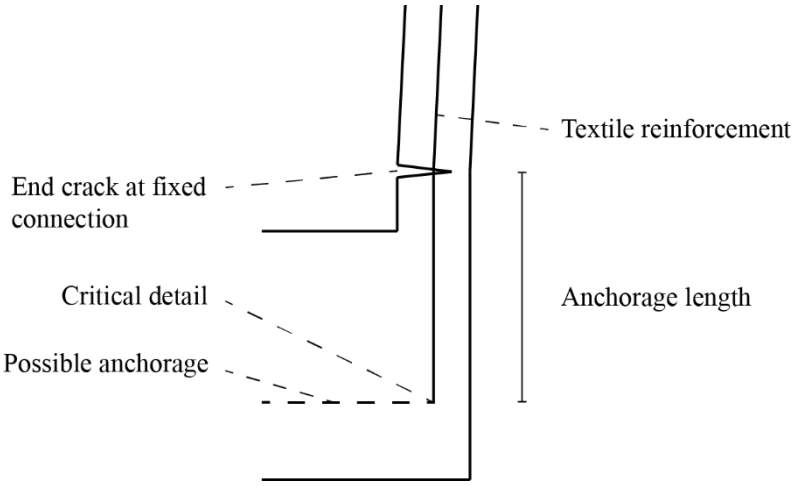

Figure 5-20 End support

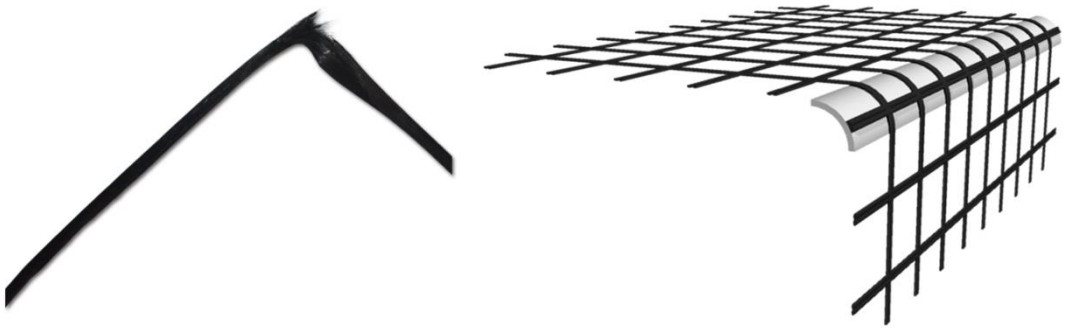

Figure 5-21 Bended carbon fibre yarn

5.5.3 Overlapping Textiles

Because of the low bond stress capacity to tensile strength ratio between textile and concrete, the splicing of two meshes is a critical detail. If the meshes are not in some way attached to each other, the important anchorage length is shortened and the ultimate capacity reduced. If cracks appear in the overlapping zone, the bond and hence the capacity is reduced even more.

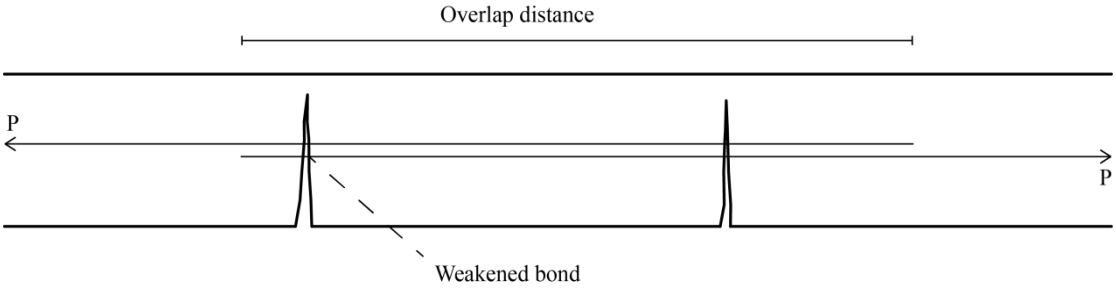

Figure 5-22 Overlapping textiles

6 Modelling of TRC-Sandwich Façade Element

This chapter should be viewed upon as a preliminary study of how a TRC-sandwich façade element can be modelled. The main aim was to show possibilities and identify difficulties in modelling using a specific sandwich façade element as an example. Results are presented to give an estimation of loadbearing capacity for one specific load case.

6.1 Geometry and Materials

The façade element is designed as a sandwich element where the two concrete layers interact and carry the load in bending and compression while shear forces are transferred by the middle layer of insulation or shear connectors. In this design both inner and outer layer are made out of TRC and foam concrete was chosen as insulation. This type of element can either be vertically load bearing or non-load bearing.

The sandwich element concept is a load bearing element with an inner TRC layer with a thickness of 50-80 mm, an insulating layer of foam concrete with a thickness of 150 mm and an outer TRC layer with a thickness of 15-25 mm. However, as a first step, only a non-load bearing element was regarded here and thus, both inner and outer concrete layers were chosen to 15 mm.

If full bond can be assured between concrete and foam concrete, the sandwich element will work in bending with full interaction. If the bond cannot be assured, shear connectors are required to transfer the shear forces. Since the chosen TRC layers are 15 mm, the connection of such parts may be problematic. The following analysis presented in this thesis is however limited to full interaction.

For the TRC layers the same material properties are used as in Chapter 5 which are the calibrated properties from Chapter 4. The foam concrete has the properties shown in Table 6-1. Compressive strength was received from a Swedish producer, Aercrete (see Appendix F) and the other properties were calculated according to EC2.

Table 6-1 Foam concrete properties

Compressive strength	f_{cm}	2 MPa
Tensile strength	f_{ctm}	0.39 MPa
E-modulus	E_{cm}	13.6 GPa
Fracture energy	G_F	82.7 N/m

6.2 FE-modelling

Two 2D-models were created with the same element types as in Chapter 4. Symmetry was used to reduce computational time as shown in Figure 6-1. In these analyses full bond was assumed between the TRC layers and foam concrete and the adjacent elements with different materials were therefore modelled with shared nodes. If partially bond is to be modelled, this could be implemented using interface elements in a similar manner as when bond stress-slip is modelled. The bond between the reinforcement and concrete is modelled with same bond stress-slip properties as in previous models.

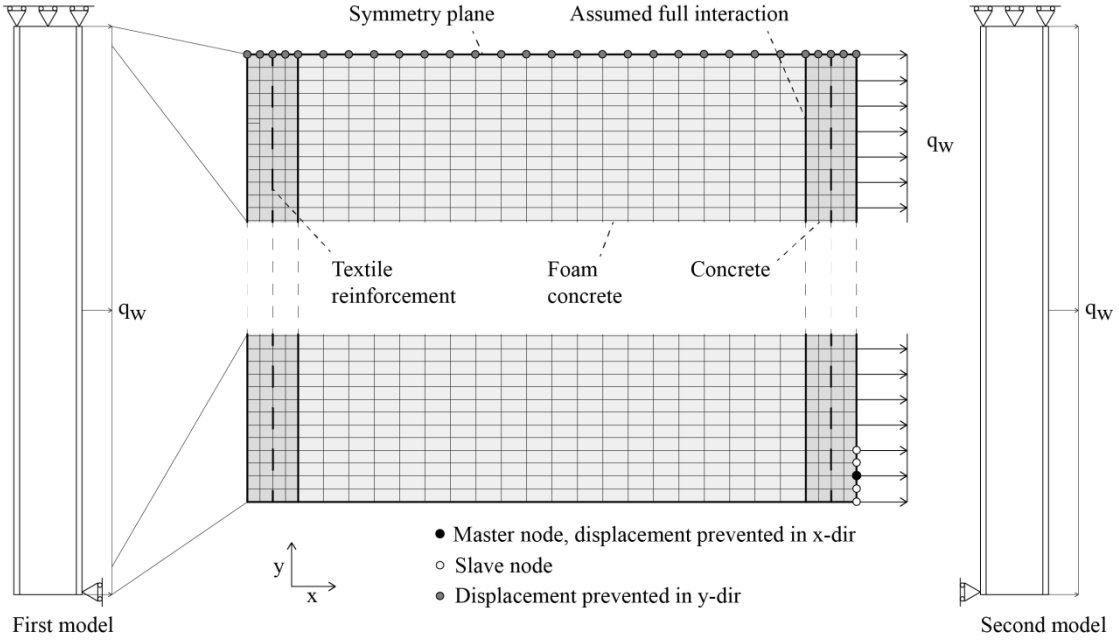

Figure 6-1 FE-modelling

Horizontal support was initially chosen at the outer edge of the element eliminating tensile cracks in the foam concrete near the support. To verify the need of tensile reinforcement in this section another analysis where the support was moved to the inside was also performed.

6.2.1 Results from First Model

According to the first model, the first crack appeared at a load level of 5.3 times the ULS wind load of 2.474kN/m^2. Thereafter the element continued to crack while the load was increased until reaching a load level of 10.2 times the ULS the analysis ended due to the prescribed limitation of load steps. At this stage it was assumed that no further information would be obtained and the analysis was terminated. The results pertaining to this first model are presented in Figures 6-2 and 6-3.

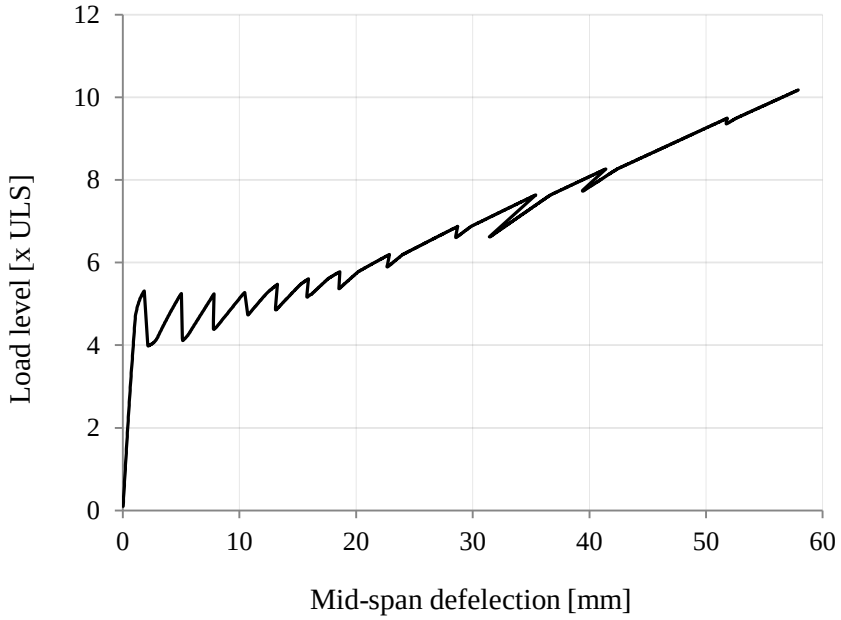

Figure 6-2 Mid-span deflection to load-curve, first model

Directly after the occurrence of the first crack at a load of 4.0 times ULS the tensile stress in the reinforcement was 610 MPa or about 15% of the tensile capacity of the reinforcement under ideal conditions. At the final load step (10.2 times the ULS) the tensile stress was 2600 MPa or 66% of the tensile capacity of the reinforcement under ideal conditions. It should be noted that the limit of 55% tensile stress was reached at a load level of 8.6 times ULS and that results after this should be considered with caution due to reasons discussed in Chapter 4.3.1.

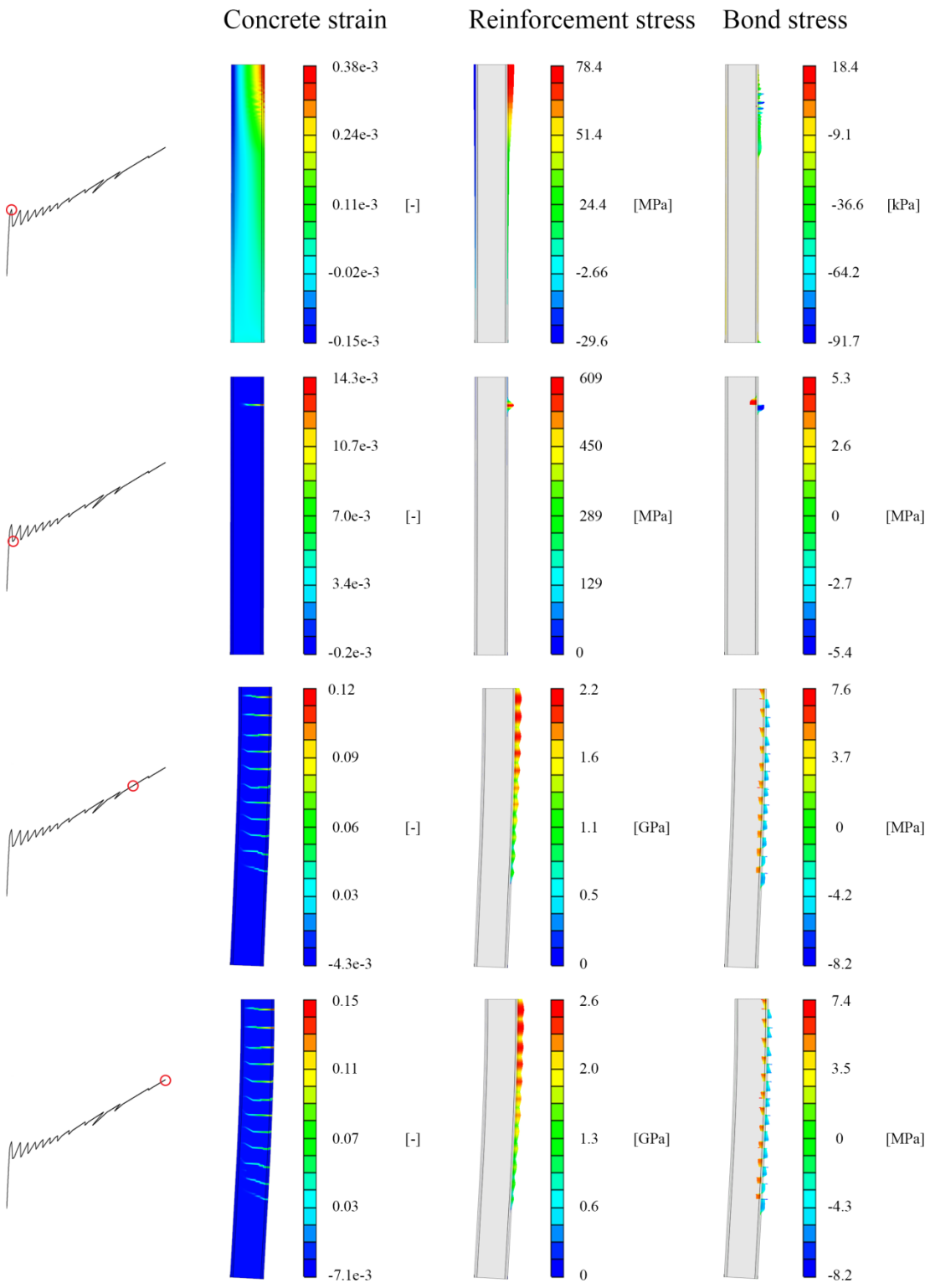

Figure 6-3 FE-results, first model

A critical section in this analysis was also found for the foam concrete near the TRC at the compressed side of the element. As mechanical properties of foam concrete were limited at the time of these analyses foam concrete was assumed to behave linear elastic up to compressive failure. Without ability to plasticise before failure compressive stresses higher than the compressive capacity of the foam concrete could occur at the interface between TRC and foam concrete, see Figure 6-4. Further investigations regarding this failure mode and the mechanical properties of foam concrete are required. It is important to note that this behaviour occurs when full interaction is assumed and could be avoided with partially interacting concrete layers.

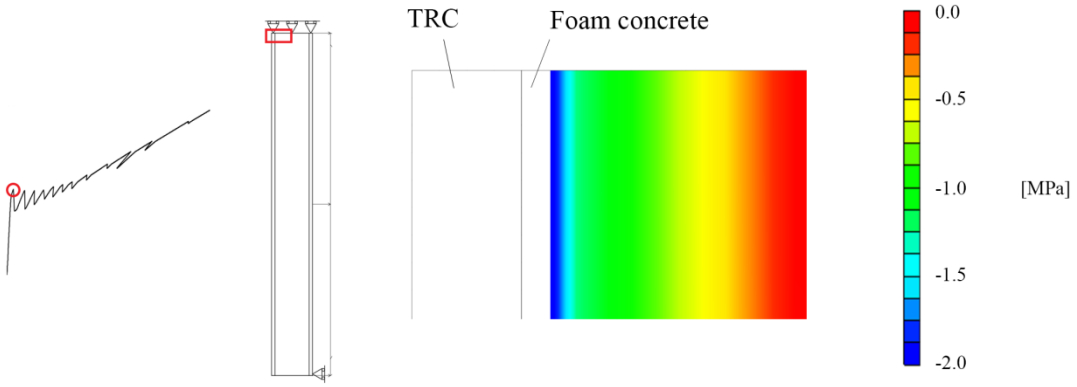

Figure 6-4 Crushing foam concrete

6.2.2 Results from Second Model

At a load level of 4,5 times the ULS load a crack was initiated in the foam-concrete layer near the horizontal support. After formation of this crack the load could no longer be increased and the crack propagated with a decreasing load. The model is allowing free vertical displacement of the horizontal support. In reality this would be slightly limited and this would induce tensile forces that would lead to bond failure of the reinforcement. This failure mode would result in a brittle behaviour and could be avoided by reinforcing the section or altering support conditions.

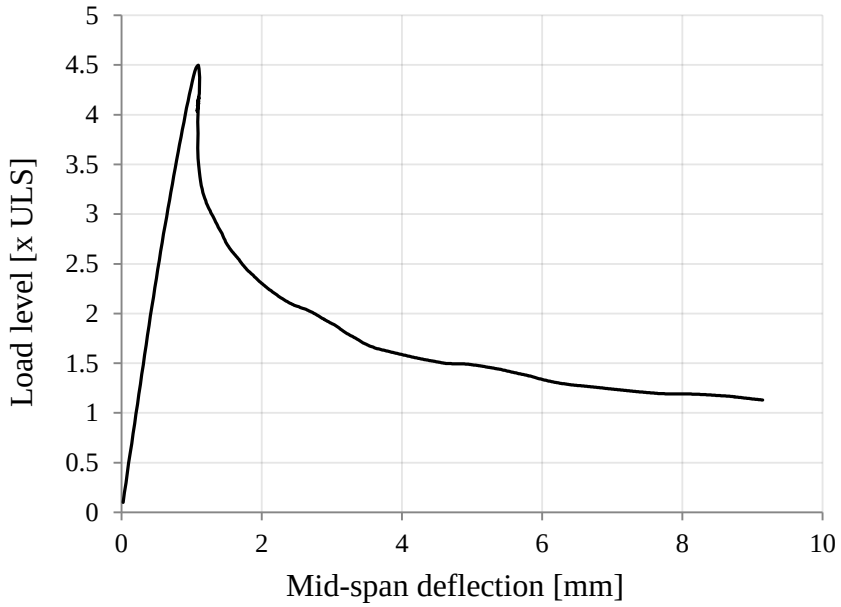

Figure 6-5 Mid-span deflection to load-curve, second model

6.2.3 Further Development of FE-model

To model a load bearing façade element, a point load should be applied to represent vertical loads from overlying floors. With high axial forces, risk of buckling exists and geometric non-linearity needs to be implemented. Limitations in DIANA-FEM using line-interface elements (L8IF) with a geometrically non-linear analysis rendered the analysis of load bearing façade elements impossible at this time. Development of beam and shell elements with possibility to implement bond stress-slip properties of reinforcement may permit this type of analysis. Investigations to find other FEM-software providing possibilities to implement this type of analysis have not been made in this thesis.

7 Conclusions and Outlook

7.1 Conclusions

Through FE-modelling, the behaviour of a given TRC design was determined and verified in this thesis. Comparison of the results from the FE-analysis and experimental work indicated that the model describes certain mechanisms adequately while posing limitations.

Firstly, the failure mechanism of TRC was challenging to capture and characterize. As the measured bond stress-slip relationship used in the analyses was assumed to be uncertain after the peak stress, bond failure could occur at a lower load than for the FE-model. The latter is not an issue directly related to the modelling yet it concerns the method in which the input data was determined. To make the model more reliable, improvement of the testing method may be required.

In addition, only the bond stress-slip relation between the textile and the cementitious matrix was implemented. In the case of damage in the textile, because of e.g. initial damage or tensile failure due to uneven stress distribution, also the bond within the yarn could be crucial. Modelling at a more detailed scale could make it possible to capture this failure mode.

Furthermore, shear capacity of the textile is not implemented. Since the shear capacity is assumed to be very low, the model is not accurate if the cracked section needs to transfer shear loads.

In the stages up to failure, before the bond stress has reached its peak and the textile tensile stress is lower than its capacity in all filaments, the developed model yielded accurate results. For structures such as the TRC façade elements analysed in this work, where the deflection is a tougher requirement than the ultimate capacity, the developed model could be useful tool for design.

It was shown that the bond between the textile and the concrete is a very important parameter which affects both crack development, deflections, and ultimate capacity. Because of the low bond stress capacity to tensile strength ratio, it is difficult to utilize the full tensile capacity of the carbon textile without improving the anchorage. To anchor the textile particularly at corner details in a façade element could prove to be difficult without incurring damage to the reinforcement. A further critical detail which was discussed in this work is the splicing of two mesh sections. To transfer the load between the two mesh sections, sufficient anchorage length is needed in the overlap zone.

For a material such as carbon fibre which is assumed to show an almost linear elastic behaviour up to failure, stress concentrations were found to be very crucial in determining the ultimate capacity of a structure. In this regard, the low bond stress capacity to tensile strength ratio could lead to a favourable possibility for the structure to redistribute loads and thus increase the utilisation of the tensile capacity of a textile mesh. Overall, TRC was shown in this thesis to be a promising composite for façade elements if adequate bond and anchorage is assured. Detailed design is however crucial and unforeseen cracks could jeopardize the structure.

7.2 Suggestions for Further Research

During the project, certain information and properties were missing to create a fully reliable model. Data related to the tensile strength of the textile embedded in concrete was uncertain, as tensile failure was not achieved in the pull-out tests performed prior to this work.

Accordingly, development of a reliable and standardized method to determine bond stress-slip properties would improve analyses of TRC elements and structures. Valuable data for improvement of bond stress-slip testing could be obtained by measuring the slip at the end of a yarn in pull-out tests.

When experimental bending tests are performed, measurement of crack widths during loading could provide valuable data for verification of FE-analyses.

It could also be possible to gain information about the condition of yarns embedded in concrete by measuring electrical conductivity of carbon-fibre during tensile and bending tests.

Factors such as area to perimeter ratio, cross-section geometry, textile material, coating or impregnating technique and concrete type all affect the behaviour of textile reinforced structures. To allow simplified analyses without extensive FE-modelling general relationships needs to be developed.

Since the anchorage of textile is important to reach full tensile capacity, different anchorage methods need to be evaluated. Special consideration to production, costs and tensile strength reduction should be taken.

Fibrous materials such as carbon-fibre textiles are assumed to show poor capacity when loaded out of the axial direction. Determining how strength is affected when the fibres are bent at a crack and the ability to transfer shear loads could be of interest.

8 References

ACI Committee 533 (1993): *Guide for Precast Concrete Wall Panels*, American Concrete Institute, Detroit, Michigan, 1993

Aercrete latest update 13/1 2014 www.earcrete.se/eng/foam6.html

Brameshuber, W. 2006. *Textile Reinforced Concrete, State-of-the-Art Report of RILEM Technical Committee 201-TRC, RILEM Report 36.* Bagneux, France, RILEM Publication.

Domone, P. and Illston, J. (2010): *Construction Materials, Their Nature and Behaviour*. Spon Press, New York, USA, 2010.

Graham, P. (2002): *Building Ecology: First Principals for a Sustainable Built Environment.* Wiley-Blackwell, 2002

Hegger, J. and Voss, S. (2008): "Investigations on the Bearing Behaviour and Application potential of textile reinforced concrete." *Engineering Structures* no. 30 (7):2050-2056. doi: 10.1016/j.engstruct.2008.01.006

International Federation for Structural Concrete (fib). Fib bulletin 55:Model Code 2010, First complete draft2010.

Marsh, C, F. (1904): *Reinforced Concrete*. D. Van Nostrand Company, New York, USA, 1904

Mobasher, B. (2012): *Mechanics of fiber and textile reinforced cement composites*: CRC Press.

Naik, T. (2008): *Sustainability of Concrete Construction*. Practice Periodical on Structural Design and Construction, 13(2), 2008

Orlowsky, J. and Raupach, M. (2011): "Textile reinforced concrete – from research to application." *Cement Wapno Beton* no. 16 (6):323-331.

Plos, M., Pacoste, C., Johansson, M. (2012): *Recommendations for finite element analysis for the design of reinforced concrete slabs*. KTH Stockholm, TRITA-BKN Report 144, Stockholm, Sweden, 2012.

Swedish Standards Institute (2008): *SS-EN 1992-1-1:2005, Eurocode 2: Design of Concrete Structures- Part 1-1: General rules and rules for buildings*, Swedish Standards Institute, Stockholm, Sweden, 2008

TNO Diana. Finite Element Analysis User's Manual – release 9.4.4:TNO; 2011.

Williams Portal, N. (2013): *Sustainability and flexural Behaviour of Textile Reinforced Concrete*. Department of Structural Engineering, Chalmers University of Technology, Publication no. 13:9, Göteborg, Sweden, 2013

Williams Portal, N., Fernandez Perez, I., Nyholm Thrane, L., Lundgren, K. (2014), Pull-out of Textile Reinforcement in Concrete. Submitted to Elsevier Construction and Building Materials.

Zandi Hanjari, K. (2008): *Load-Carrying Capacity of Damaged Concrete Structures*. Department of Structural Engineering, Chalmers University of Technology, Publication no. 13:9, Göteborg, Sweden, 2013

Appendix A - Mean Concrete Compressive Stresses

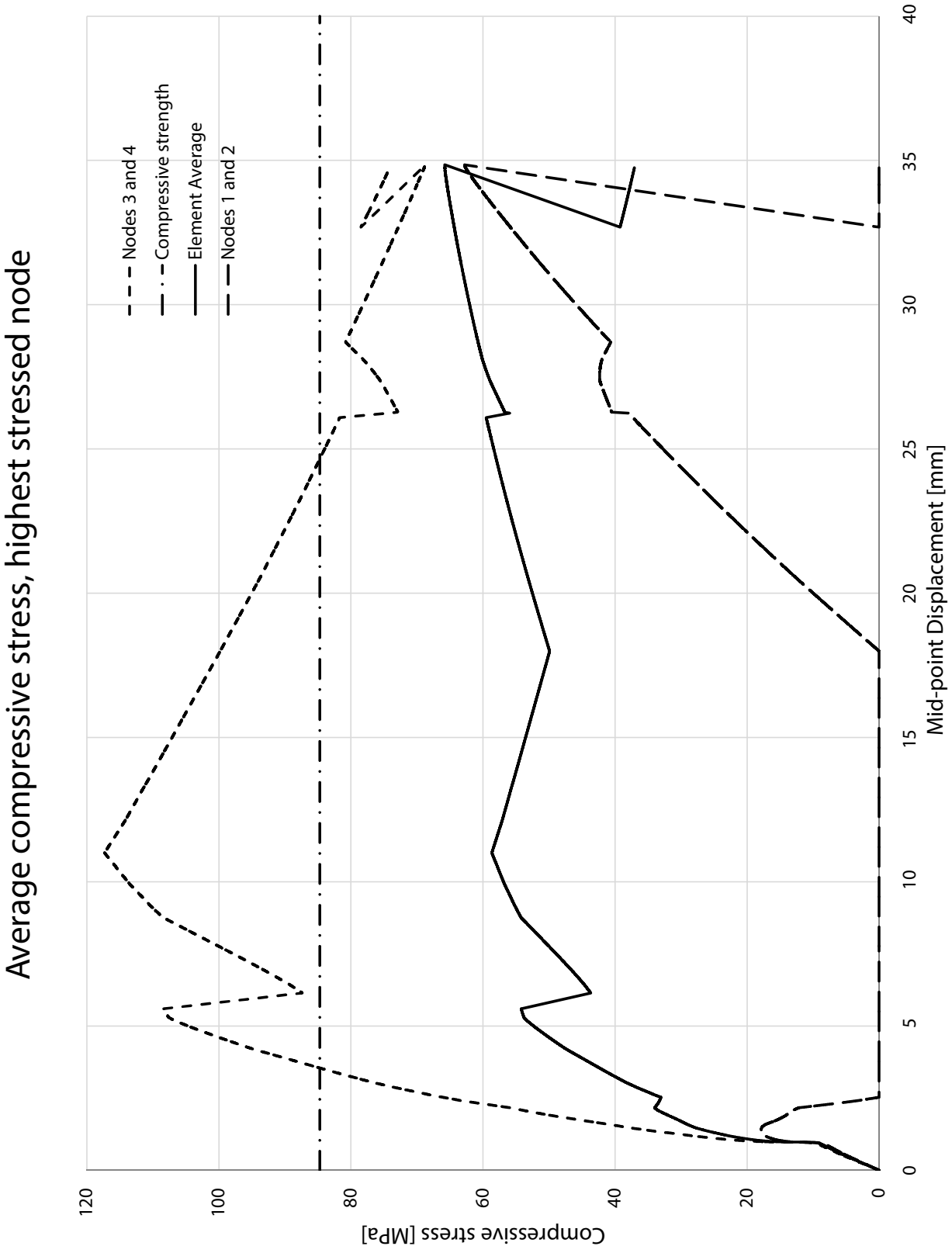

Appendix B - Stiffness of Intermediate Fasteners


```
% -------------------------------------- %
% This script was developed to esimate   %
% optimal stiffness for intemediate      %
% fasteners for facade elements.         %
% The CALFEM suite of subrutines was     %
% utilized to reduce code. The script can %
% only be used with those subrutines.    %
% -------------------------------------- %

clear all
close all
clc

W = 2.4;
L = 2.7;
t1 = 0.015;
t2 = 0.04;

E = 41.8e9;
A1 = W * t1;
I1 = W * t1^3 / 12;
A2 = W * t2;
I2 = W * t2^3 / 12;

q = 2.494e3 * W;

Edof1 = [1  1 2 3 4 5 6
         2  4 5 6 7 8 9
         3  10 11 12 13 14 15
         4  13 14 15 16 17 18];

Edof2 = [5 5 14];

bc = [1 0
      2 0
      8 0
      10 0
      11 0
      17 0];

[Ke1,fe1] = beam2e([0 L/2],[0 0],[E A1 I1],[0 q]);
[Ke2,fe2] = beam2e([L/2 L],[0 0],[E A1 I1],[0 q]);
Ke3 = beam2e([0 L/2],[0 0],[E A2 I2]);
Ke4 = beam2e([L/2 L],[0 0],[E A2 I2]);


n = 21;
x_vector = linspace(0,L/2,21);

qk = 1;
hej = 0;
```

```
for i=0:100

k = i^2*20000;
Ke5 = spring1e(k);

K = zeros(18);
f = zeros(18,1);

[K,f] = assem(Edof1(1,:),K,Ke1,f,fe1);
[K,f] = assem(Edof1(2,:),K,Ke2,f,fe2);
K = assem(Edof1(3,:),K,Ke3);
K = assem(Edof1(4,:),K,Ke4);
K = assem(Edof2,K,Ke5);

a = solveq(K,f,bc);

ed1 = extract(Edof1(1,:),a);
ed2 = extract(Edof1(2,:),a);

[es1,edi1,eci1] = beam2s([0 L/2],[0 0],[E A1 I1],ed1,[0 q],n);
[es2,edi2,eci2] = beam2s([L/2 L],[0 0],[E A1 I1],ed2,[0 q],n);

if abs(max(es1(:,3)))<abs(min(es1(:,3)))
    subplot(2,1,1)
    hold on
    plot(eci1,es1(:,3),'k')
    plot((eci2+L/2),es2(:,3),'k')

    subplot(2,1,2)
    plot(eci1,edi1(:,2),'k')
    hold on
    plot(eci2 + L/2,edi2(:,2),'k')

    Inner(i+1) = L/a(14);

    Global(i+1) = L/max(edi1(:,2));

    Local(i+1) = L/2/(max(edi1(:,2)-((2*eci1/L)*edi1(end,2))));
else
    if qk == 1;
        subplot(2,1,1)
        plot(eci1,es1(:,3),'r','LineWidth',2)
        plot((eci2+L/2),es2(:,3),'r','LineWidth',2)

        disp(['Spring stiffness for even moment distribution: ',num2str(k/1000),' kN/m'])
        qk = 0;

        Inner(i+1) = L/a(14);

        Global(i+1) = L/max(edi1(:,2));
```

```
        Local(i+1) = L/2/(max(edi1(:,2)-((2*eci1/L)*edi1(end,2))));

        subplot(2,1,2)
        plot(eci1,edi1(:,2),'r','LineWidth',1)
        plot(eci2 + L/2,edi2(:,2),'r','LineWidth',1)
    else
        subplot(2,1,1)
        plot(eci1,es1(:,3),'k')
        plot((eci2+L/2),es2(:,3),'k')

        subplot(2,1,2)
        plot(eci1,edi1(:,2),'k')
        plot(eci2 + L/2,edi2(:,2),'k')

        Inner(i+1) = L/a(14);

        Global(i+1) = L/max(edi1(:,2));

        Local(i+1) = L/2/(max(edi1(:,2)-((2*eci1/L)*edi1(end,2))));
    end
end

if Inner(i+1)>250 && Global(i+1)>250 && Local(i+1)>250 && hej==0
    hej = 1;
    disp(['Spring stiffness for u > L/250: ',num2str(k/1000),' kN/m'])
end

end

K = zeros(11);
f = zeros(11,1);

Edof1 = [1  1 2 3 4 5 6
         2  4 5 6 7 8 9
         3  1 2 10 4 5 6
         4  4 5 6 7 8 11];

[K,f] = assem(Edof1(1,:),K,Ke1,f,fe1);
[K,f] = assem(Edof1(2,:),K,Ke2,f,fe2);
K = assem(Edof1(3,:),K,Ke3);
K = assem(Edof1(4,:),K,Ke4);

bc = [1 0
      2 0
      8 0];

[a,r] = solveq(K,f,bc);

ed1 = extract(Edof1(1,:),a);
ed2 = extract(Edof1(2,:),a);
```

```
[es1,edi1,eci1] = beam2s([0 L/2],[0 0],[E A1 I1],ed1,[0 q],21);
[es2,edi2,eci2] = beam2s([L/2 L],[0 0],[E A1 I1],ed2,[0 q],21);

subplot(2,1,1)
plot(eci1,es1(:,3),'b','LineWidth',1)
hold on
plot(eci2 + L/2,es2(:,3),'b','LineWidth',1)
text(2,500,'Even moment distribution')
text(2,1200,'Minimized deflections')
plot([1.63 1.99],[-147 500],'k')
plot([1.6 1.99],[13 1200],'k')

subplot(2,1,2)
plot(eci1,edi1(:,2),'b','LineWidth',1)
hold on
plot(eci2 + L/2,edi2(:,2),'b','LineWidth',1)
text(2.4,.10,'Even moment distribution')
text(2.4,.08,'Minimized deflections')
plot([1.8 2.39],[0.01 .10],'k')
plot([2 2.39],[0.01 .08],'k')

%%

Inner2 = L/a(5);

Global2 = L/max(edi1(:,2));

Local2 = L/2/(max(edi1(:,2)-((2*eci1/L)*edi1(end,2))));
```

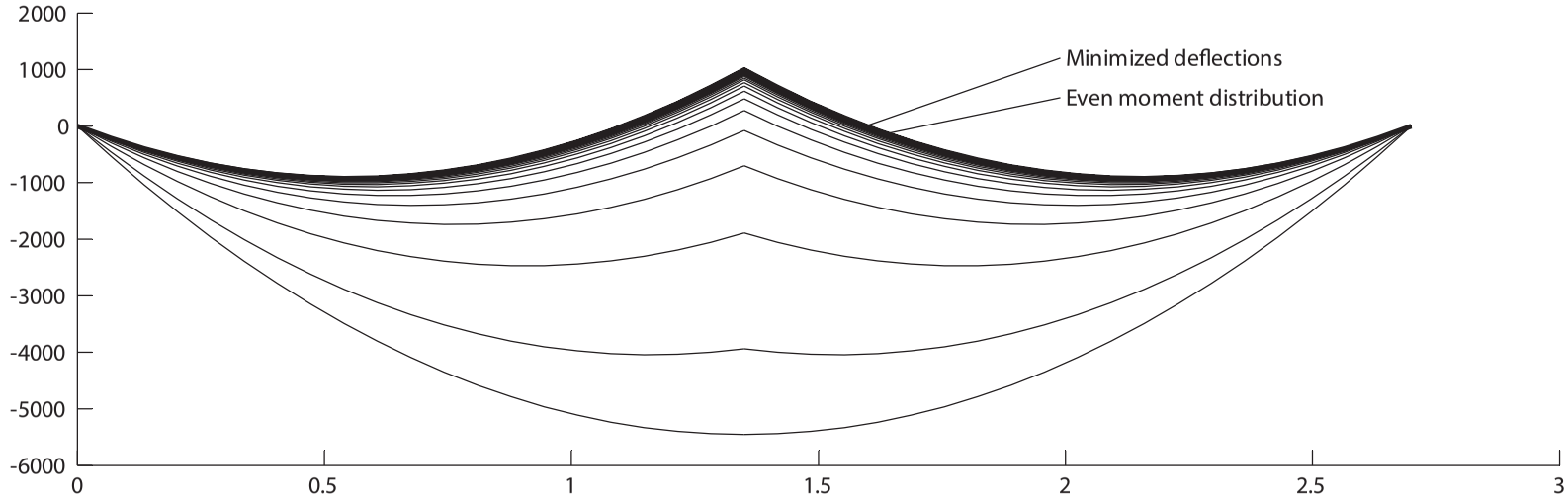
2000
1000
0
-1000
-2000
-3000
-4000
-5000
-6000
0
0.5
1
1.5
2
2.5
3
Minimized deflections
Even moment distribution

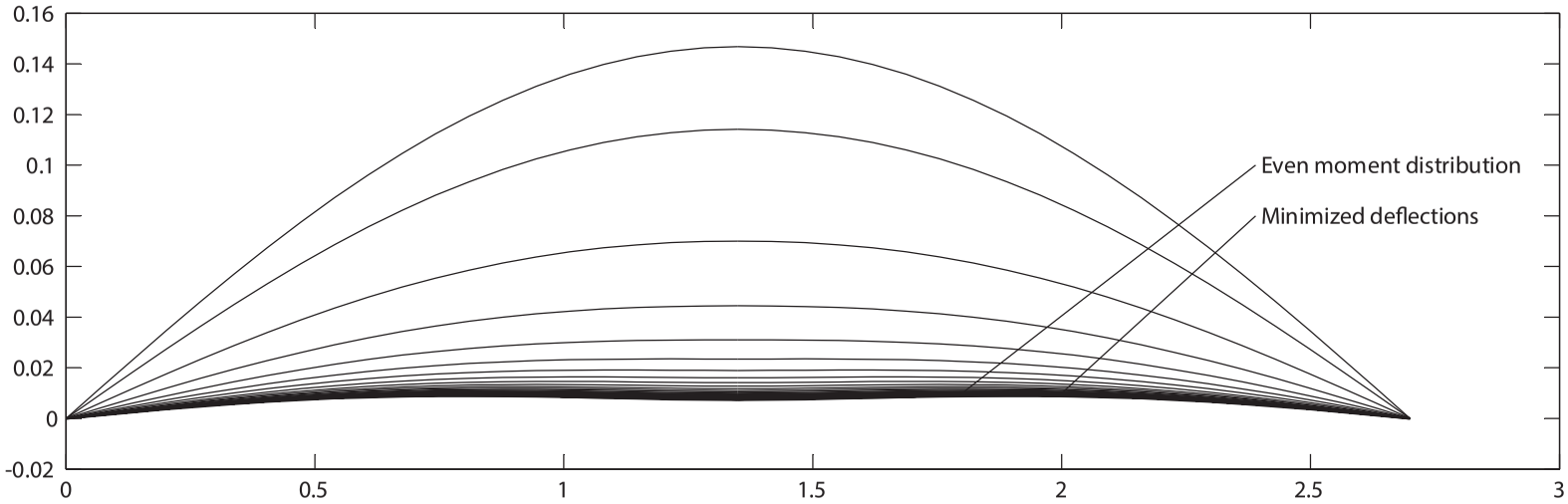
0.16
0.14
0.12
0.1
0.08
0.06
0.04
0.02
0
-0.02
0
0.5
1
1.5
2
2.5
3
Even moment distribution
Minimized deflections

Appendix C - Placement of Intermediate Fasteners

G:\Report\Calculations\Optim4supports\supports4.m Page 1

```
% ------------------------------------- %
% This script was developed to optimize  %
% placement of intemediate fasteners     %
% for facade elements.                   %
% The CALFEM suite of subrutines was     %
% utilized to reduce code. The script can %
% only be used with those subrutines.    %
% ------------------------------------- %

clear all
close all
clc

Ep = [1 1 1];

Eq = [0 1];

maxcheck = 1000;
maxcheckf = 1000;
y = 0;

val = 0;
val1 = 0;

Mscal = 7;
Zscal = .9e2;

for o = 1:1499
    x1 = o/1000;

    Ex = [ 0   x1
           x1  1.5];

    Ey = [0 0];

    Edof = [1   1  2  3  4  5  6
            2   4  5  6  7  8  9];

    K = zeros(9);
    f = zeros(9,1);

    for i = 1:2
        [Ke,fe] = beam2e(Ex(i,:),Ey,Ep,Eq);
        [K,f] = assem(Edof(i,:),K,Ke,f,fe);
    end

    bc = [1 0
          2 0
          5 0
          9 0];
```

```
    [a,r] = solveq(K,f,bc);

    ed = extract(Edof,a);

    n = 23;
    [es1,edi1,eci1] = beam2s(Ex(1,:),Ey,Ep,ed(1,:),Eq,n);
    [es2,edi2,eci2] = beam2s(Ex(2,:),Ey,Ep,ed(2,:),Eq,n);

    maxm = max([abs(es1(:,3))' abs(es2(:,3))']);
    maxmf = max([-(es1(:,3))' -(es2(:,3))']);

    if x1 == 0.934
        Eddef = [edi1' edi2'];
        Esdef = [es1(:,3)' es2(:,3)'];
        Ecidef = [eci1' eci2'+x1];
        val = 1;
    end
    if x1 == 1
        Eddef1 = [edi1' edi2'];
        Esdef1 = [es1(:,3)' es2(:,3)'];
        Ecidef1 = [eci1' eci2'+x1];
        val1 = 1;
    end
    if maxm < maxcheck
        maxcheck = maxm;
        Edmax = [edi1' edi2'];
        Esmax = [es1(:,3)' es2(:,3)'];
        Ecimax = [eci1' eci2'+x1];
        xopt = x1;
    end
    if maxmf < maxcheckf
        maxcheckf = maxmf;
        Edmaxf = [edi1' edi2'];
        Esmaxf = [es1(:,3)' es2(:,3)'];
        Ecimaxf = [eci1' eci2'+x1];
        xoptf = x1;
    end
    Ed = [edi1' edi2'];
    Es = [es1(:,3)' es2(:,3)'];
    Eci = [eci1' eci2'+x1];
%    figure(1)
if o == 1499
    figure('Position',[20 20 1500 1000])
    subplot(2,1,1)
    plot(Ecimax,Mscal*Esmax,'--g')
    hold on
    plot(Ecimaxf,Mscal*Esmaxf,'b')
    plot(Eci,Mscal*Es,'k')
    if val == 1
        plot(Ecidef,Mscal*Esdef,'--r')
    end
```

```
    if val1 == 1
        plot(Ecidef1,Mscal*Esdef1,'g')
    end
    plot([0 1.5],[0 0],'k')
    text(1.2,-.75,'Minimized support moment')
    plot([0.8 1.19],[-0.18 -.75],'--g')
    text(1.2,-1,'Evenly distributed')
    plot([0.7 1.19],[-0.24 -1],'g')
    text(1.2,-1.25,'Minimized deflection')
    plot([0.6 1.19],[-0.22 -1.25],'--r')
    text(1.2,-1.5,'Minimized span moments')
    plot([0.5 1.19],[-0.32 -1.5],'b')
    axis([0 1.5 -2 2])

    hold off
    subplot(2,1,2)
    plot(Ecimax,Zscal*Edmax,'--g')
    hold on
    plot(Ecimaxf,Zscal*Edmaxf,'b')
    plot(Eci,Zscal*Ed,'k')
    if val == 1
        plot(Ecidef,Zscal*Eddef,'--r')
    end
    if val1 == 1
        plot(Ecidef1,Zscal*Eddef1,'g')
    end
    plot([0 1.5],[0 0],'k')
    text(1.2,2.25,'Minimized support moment')
    plot([0.5 1.19],[0.82 2.25],'--g')
    text(1.2,2,'Evenly distributed')
    plot([0.6 1.19],[0.54 2],'g')
    text(1.2,1.75,'Minimized deflection')
    plot([0.7 1.19],[0.175 1.75],'--r')
    text(1.2,1.5,'Minimized span moments')
    plot([0.8 1.19],[0.046 1.5],'b')
    axis([0 1.5 -.5 3])
%    print('-dpng',num2str(o+10000))
    hold off
    pause(0.0001)
end
%    close all
end
%
% text(xopt-0.05,0.05,num2str(xopt))
% text(xoptf-0.05,0.05,num2str(xoptf))
```

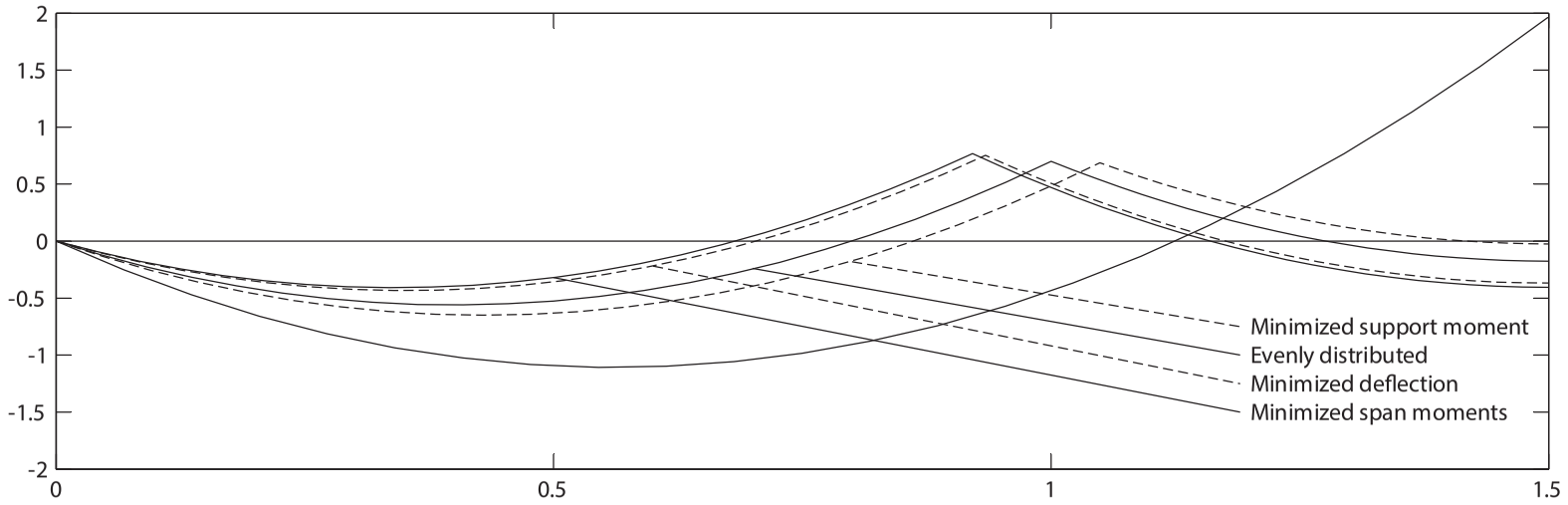
2
1.5
1
0.5
0
-0.5
-1
-1.5
-2
0
0.5
1
1.5
Minimized support moment
Evenly distributed
Minimized deflection
Minimized span moments

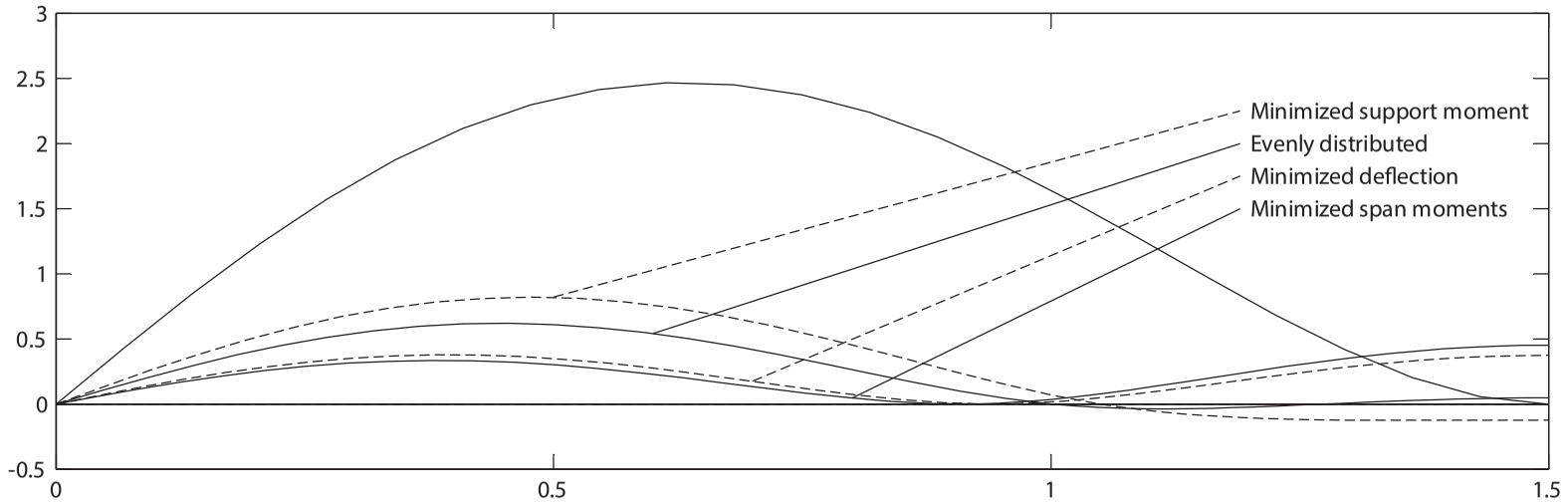
3
2.5
2
1.5
1
0.5
0
-0.5
0
0.5
1
1.5
Minimized support moment
Evenly distributed
Minimized deflection
Minimized span moments

Appendix D - Wind Load

Choosen geometry

$h := 30m$ Height of building

$d := 12m$ Width of building

$b := 24m$ Length of building

$h_{el} := 2.7m$ Height of facade element

$w_{el} := 2.4m$ Width of facade element

$A_{el} := h_{el} \cdot w_{el} = 6.48\,m^2$ Area of facade element

Basic wind velocity

$v_b := 25\frac{m}{s}$ (For Gothenburg according to National Annex, figure C-4 and table C-10)

Probobility factor

$K := 0.2$ SS-EN 1991-1-4:2005, Section 4.2

$n := 0.5$ SS-EN 1991-1-4:2005, Section 4.2

$p := 0.02$

$c_{prob} := \left(\frac{1 - K\cdot\ln(-\ln(1-p))}{1 - K\cdot\ln(-\ln(0.98))}\right)^n = 1$ SS-EN 1991-1-4:2005, Equation 4.2

$v_{b.d} := v_b\cdot\left(c_{prob}\right) = 25\frac{m}{s}$

Mean wind

$v_m := c_r\cdot c_o\cdot v_b$ SS-EN 1991-1-4:2005, Equation 4.3

Terrain roughness

$$c_r := k_r \cdot \ln\left(\frac{z}{z_0}\right)^{\blacksquare} \quad \text{for} \quad z_{min} \le z \le z_{max}$$

$$c_r := c_r(z_{min}) = \blacksquare \cdot k_r \cdot \ln\left(\frac{z_{min}}{z_0}\right)^{\blacksquare} \quad \text{for} \quad z \le z_{min}$$

$z_{0.II} := 0.05\text{m}$ SS-EN 1991-1-4:2005, Section 4.3.2

$z_{max} := 200\text{m}$ SS-EN 1991-1-4:2005, Section 4.3.2

Terrain category 0: Sea or costal area exposed to the open sea

$z_0 := 0.003\text{m}$ SS-EN 1991-1-4:2005, Table 4.1

$z_{min} := 1\text{m}$ SS-EN 1991-1-4:2005, Table 4.1

$k_r := 0.19\left(\frac{z_0}{z_{0.II}}\right)^{0.07} = 0.156$ SS-EN 1991-1-4:2005, Equation 4.5

Terrain orography

$c_o := 1$ for $\Phi < 0.05$ SS-EN 1991-1-4:2005, A.3

Choosen height of building

$z := 30\text{m}$

$c_r := k_r \cdot \ln\left(\frac{z}{z_0}\right) = 1.437$ SS-EN 1991-1-4:2005, Equation 4.4

$v_m := c_r \cdot c_o \cdot v_{b.d} = 35.929\,\frac{\text{m}}{\text{s}}$ SS-EN 1991-1-4:2005, Equation 4.3

Wind turbulence

$k_I := 1.0$ SS-EN 1991-1-4:2005, Section 4.4

$\sigma_v := k_r \cdot v_b \cdot k_I = 3.901\,\frac{\text{m}}{\text{s}}$ SS-EN 1991-1-4:2005, Equation 4.6

$I_v := \frac{\sigma_v}{v_m} = 0.109$ SS-EN 1991-1-4:2005, Equation 4.7

Peak velocity pressure

$\rho := 1.25 \frac{kg}{m^3}$ SS-EN 1991-1-4:2005, Section 4.5

$q_b := \frac{1}{2} \cdot \rho \cdot v_b^2 = 390.625\,Pa$ SS-EN 1991-1-4:2005, Equation 4.10

$q_p := \left(1 + 6I_v\right) \cdot \left(k_r \cdot \ln\left(\frac{z}{z_0}\right)\right)^2 \cdot q_b = 1.332 \cdot kPa$ National Annex, 4.5(1) Note1, 7 §

Wind pressure

$\frac{h}{d} = 2.5$ Height/Width ratio

The worst exposed areas: Zone A and D

$c_{pe.1} := \begin{pmatrix} -1.4 \\ 1 \end{pmatrix}$ $c_{pe.10} := \begin{pmatrix} -1.2 \\ 0.8 \end{pmatrix}$ $Zone := \begin{pmatrix} A \\ D \end{pmatrix}$

$c_{pe} := c_{pe.1} - \left(c_{pe.1} - c_{pe.10}\right) \log\left(\frac{A_{el}}{m^2}\right)$ SS-EN 1991-1-4:2005, Section 7.2.1

$w_e := q_p \cdot c_{pe} = \begin{pmatrix} -1.649 \\ 1.116 \end{pmatrix} \cdot kPa$ SS-EN 1991-1-4:2005, Equation 5.1

Design loads

$\gamma_{Q.1} := 1.5$ SS-EN 1990, Table A1.2(B)

$q_d := \gamma_{Q.1} \cdot w_e = \begin{pmatrix} -2.474 \\ 1.674 \end{pmatrix} \cdot kPa$ Design wind load

Appendix E - Foam Concrete Properties

AERCRETE™

Foam concrete

Data

Recipe for 1m³ of Aercrete FC

Density (kg)	Concrete			Foam			Wet weight (kg)
	Cement (kg)	Sand (kg)	Water (l)	Aercell (l)	Water (l)	Air (l)	
400	320	0	140	0,94	35,2	716	498
600	360	150	160	0,83	31,0	630	703
800	360	350	160	0,74	27,4	559	899
1000	360	550	140	0,67	24,9	506	1077
1200	360	750	140	0,57	21,3	434	1273
1400	400	900	160	0,46	17,1	349	1478
1600	400	1100	160	0,36	13,6	277	1675
1800	400	1300	160	0,27	10,1	205	1871

These preprogrammed recipes in the Aercrete 625 have been tested to give a good balance between strenght and material cost. Custom recipes can be programmed by operator.

Recipe for 1ft³ of Aercrete FC

Density (lbs)	Concrete			Foam			Wet weight (lbs)
	Cement (lbs)	Sand (lbs)	Water (gal)	Aercell (oz)	Water (oz)	Air (gal)	
25	19.7	0.0	1.05	0.90	35.2	5.36	30.8
35	22.5	7.0	1.20	0.81	31.6	4.81	41.6
45	22.5	17.2	1.20	0.74	28.7	4.37	51.6
55	22.5	27.4	1.20	0.66	25.8	3.93	61.6
65	22.5	37.5	1.05	0.61	23.9	3.64	70.4
75	22.5	47.7	1.05	0.54	21.0	3.20	80.4
85	25.0	55.1	1.20	0.45	17.4	2.65	91.3
95	25.0	65.3	1.20	0.37	14.5	2.21	101.3
105	25.0	75.5	1.20	0.30	11.6	1.77	111.3
115	25.0	85.7	1.20	0.23	8.8	1.34	121.3

Attainable Compressive strength*

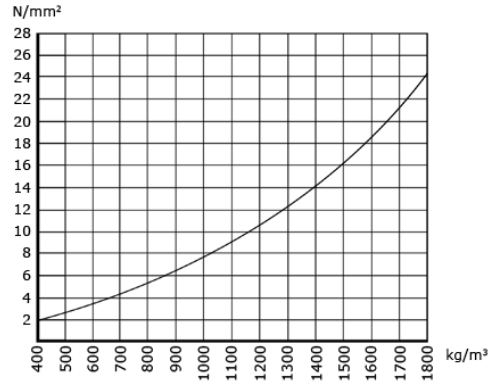

Attainable Compressive strength*

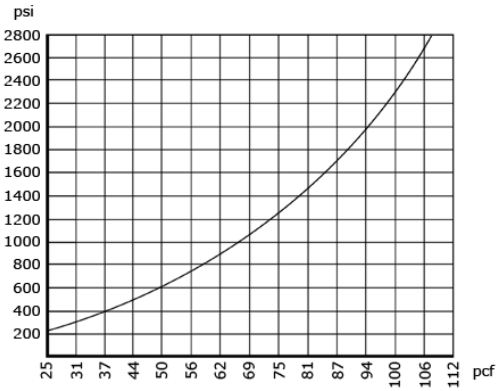

* The above curves are meant to give an idication of what is possible with Foam Concrete. It is based on tests made in cooperation with TPD (Technisch Physiche Dienst) in The Netherlands and reflects the results with specific materials, add agents and optimized recipes.

Aercrete can not guarantee that actual customer results meet the test results indicated in the chart.

The machine owner is responsible for actual results.

Test are recommended before delivering Foam Concrete to meet specific customer requirements.

Thermal conductivity

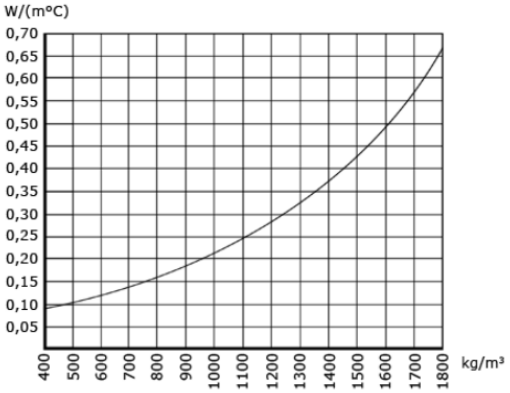

Thermal conductivity

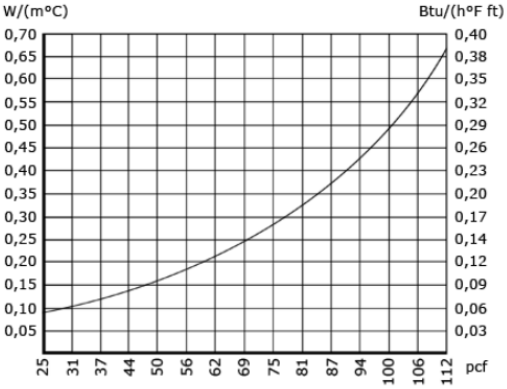

Appendix F - DIANA Files


```
% ---------------------------------------- %
% Dat-file for the analysis with original   %
% input data to compare with experiments.   %
% Also note the 2nd dat-file for phase 2.   %
% All comments following "%" sign is our    %
% comments and must be deleted when running %
% analysis in DIANA.                        %
% ---------------------------------------- %

Translated from FX+ for DIANA neutral file (version 1.2.0).
'DIRECTIONS'
   1  1.00000E+000  0.00000E+000  0.00000E+000
   2  0.00000E+000  1.00000E+000  0.00000E+000
   3  0.00000E+000  0.00000E+000  1.00000E+000
'COORDINATES'
   7  3.00000E-002  0.00000E+000  0.00000E+000
 151  3.00000E-001  5.00000E-002  0.00000E+000
1112  0.00000E+000  7.50000E-003  0.00000E+000
... (rows deleted)
    (rows deleted) ...
5533  4.97500E-001  7.50000E-003  0.00000E+000
'MATERI'
   1 NAME   CONCRETE
     YOUNG   4.18000E+010
     POISON  2.00000E-001
     DENSIT  2.13000E+003
     TOTCRK ROTATE               % Rotating crack model was chosen
     CRACKB  2.50000E-003        % Crack band with = element size
     COMCRV MULTLN               % Modified Thorenfeldt-curve, 2.5mm
     COMPAR -0.00E+00 -0.00E+00
            -7.04E+07 -1.73E-03
            -7.29E+07 -1.81E-03
            -8.14E+07 -2.13E-03
            -8.37E+07 -2.28E-03
            -8.44E+07 -2.35E-03
            -8.47E+07 -2.43E-03
            -8.47E+07 -2.45E-03
            -8.47E+07 -2.45E-03
            -8.37E+07 -8.74E-03
            -7.99E+07 -3.08E-02
            -7.06E+07 -7.77E-02
            -3.04E+07 -2.67E-01
            -1.54E+07 -3.48E-01
            -8.77E+06 -3.94E-01
            -7.10E+06 -4.09E-01
            -4.09E+06 -4.43E-01
            -2.40E+06 -4.73E-01
            -1.43E+06 -5.00E-01
            -8.77E+05 -5.26E-01
            -5.47E+05 -5.50E-01
            -2.38E+05 -5.96E-01
            -0.00E+00 -8.82E-01
     TENCRV HORDYK
     TENSTR  4.70000E+006
     GF1     1.62000E+002        % Fracture Energy
     COMSTR  8.47000E+007
```

```
   2 NAME   CARBONFIBER
     YOUNG   2.30000E+011
     POISON  2.00000E-001
     TENSTR  3.800E+009
     TENCRV LINEAR
     DENSIT  1.80000E+003
   3 NAME   TYINGBEAMS
     YOUNG   1.00000E+000
     POISON  0.00000E+000
     DENSIT  0.00000E+000
   4 NAME   INTERFACE
     DSTIF   1.00000E+010  7.44000E+010
     BONDSL 3                          % 3 = Bond Stress-Slip
     SLPVAL  0.00000E+000  0.00000E+000 % Bond Stress-Slip curve
             7.45000E+006  3.00000E-005
             7.45000E+006  8.00000E-005
             4.20000E+006  3.80000E-004
             2.00000E+006  2.00000E-003
             0.00000E+000  1.10000E-002
'GEOMET'
   1 NAME   "Interface"
     THICK   2.340000E-002             % Perimeter, only valid with this
     CONFIG  BONDSL                    % specific Bond Stress-Slip curve
   2 NAME   "CFTruss"
     CROSSE  1.285000E-005
   3 NAME   "Tyingbeams"               % Dummy beams to add rotational dofs
     RECTAN  1.00000E-001  1.00000E-001
     ECCENT  0.00000E+000  0.00000E+000  0.00000E+000  0.00000E+000
     ZAXIS   0.00000E+000  0.00000E+000  1.00000E+000
   4 NAME   "Concrete"
     THICK   2.00000E-001
'DATA'
   4 NAME   "Tyingbeams"
   1 NAME   "Concrete"
   5 NAME   "CFTruss"
   6 NAME   "Interface"
'ELEMENTS'
CONNECT
5004 L8IF   5533 5333 5316 1113
... (rows deleted)
    (rows deleted) ...
5203 L8IF   5334 5335 1112 1554
5204 L2TRU  5334 5335
... (rows deleted)
    (rows deleted) ...
5403 L2TRU  5533 5333
5404 L6BEN  1122 1123
... (rows deleted)
    (rows deleted) ...
5427 L6BEN  1409 1408
1004 Q8MEM  1116 1117 1552 1551
... (rows deleted)
    (rows deleted) ...
5003 Q8MEM  5332 1333 1334 1335
```

```
MATERI
/ 1004-5003 / 1
/ 5204-5403 / 2
/ 5404-5427 / 3
/ 5004-5203 / 4
DATA
/ 5404-5427 / 4
/ 1004-5003 / 1
/ 5204-5403 / 5
/ 5004-5203 / 6
GEOMET
/ 5004-5203 / 1
/ 5204-5403 / 2
/ 5404-5427 / 3
/ 1004-5003 / 4
'LOADS'
CASE 1
WEIGHT
2 9.81
'GROUPS'
ELEMEN
  18 "Concrete" / 1004-5003 /
  25 "Interface" / 5004-5203 /
  26 "Reinforcement" / 5204-5403 /
  27 "TyingSupport" / 5404-5415 /
  28 "TyingLoad" / 5416-5427 /
'SUPPOR'
/ 7 / TR 2
/ 1113 5333 1315-1334 / TR 1
'TYINGS'                    % Tying rotation and displacement
ECCENT TR 2 RO 3            % of nodes 1122-1133 to node 7
/ 1122-1133 / 7
'UNITS'
FORCE N
LENGTH M
'END'
```

```
% ---------------------------------------- %
% Dat-file for the analysis with original   %
% input data to compare with experiments.   %
% Note that this is the 2nd dat-file only   %
% concerning phase 2. Also see dat-file 1   %
% All comments following "%" sign is our    %
% comments and must be deleted when running %
% analysis in DIANA.                        %
% ---------------------------------------- %

PHASE 2

'LOADS'
CASE 1
WEIGHT
2 9.81
CASE 2
DEFORM             % Deformation controlled loading
151  TR 2 -0.001   % The only addition in phase 2
'SUPPOR'
/ 7 151 / TR 2
/ 1113 5333 1315-1334 / TR 1
'TYINGS'
ECCENT TR 2 RO 3
/ 1122-1133 / 7
/ 1408-1419 / 151
```

```
% ---------------------------------------- %
% Dcf-file for the analysis with original   %
% input data to compare with experiments.   %
% Also note the 2nd dcf-file for phase 2.   %
% All comments following "%" sign is our    %
% comments and must be deleted when running %
% analysis in DIANA.                        %
% ---------------------------------------- %

*FILOS
 INITIA
*INPUT
*PHASE

*NONLIN

 BEGIN EXECUT
   BEGIN LOAD
     LOADNR 1
     STEPS  EXPLIC  SIZES 1(1)      % Self-weight applied in one step
   END LOAD
   BEGIN ITERAT
     BEGIN CONVER
       DISPLA CONTIN TOLCON 0.001   % Convergence criteria
       ENERGY CONTIN TOLCON 0.0001
       FORCE CONTIN TOLCON 0.01
       SIMULT
     END CONVER
     MAXITE 1000                    % Maximum number of iterations
     METHOD  SECANT  TANGEN
   END ITERAT
 END EXECUT

 BEGIN OUTPUT
   FXPLUS
   FILE FP
 END OUTPUT

*END
```

```
% ---------------------------------------- %
% Dcf-file for the analysis with original   %
% input data to compare with experiments.   %
% Note that this is the 2nd dcf-file only   %
% concerning phase 2. Also see dcf-file 1   %
% All comments following "%" sign is our    %
% comments and must be deleted when running %
% analysis in DIANA.                        %
% ---------------------------------------- %

*INPUT
READ TABLE LOADS      % Read from filos-file from phase 1
READ TABLE SUPPORTS
READ TABLE TYINGS
*PHASE

*NONLIN

 BEGIN EXECUT
   BEGIN LOAD
     LOADNR 2
     STEPS  EXPLIC  SIZES 0.001(20000) % Load applied in steps
   END LOAD
   BEGIN ITERAT
     BEGIN CONVER
       DISPLA CONTIN TOLCON 0.001
       ENERGY CONTIN TOLCON 0.0001
       FORCE CONTIN TOLCON 0.01
       SIMULT
     END CONVER
     MAXITE 500
     METHOD  SECANT  TANGEN
   END ITERAT
 END EXECUT

 BEGIN OUTPUT
   FXPLUS
   FILE SP
 END OUTPUT

*END
```